

1993

# Multiple Fluxes Influencing Amazonian River Chemistry

Kurt O. Konhauser

Follow this and additional works at: <https://ir.lib.uwo.ca/digitizedtheses>

---

## Recommended Citation

Konhauser, Kurt O., "Multiple Fluxes Influencing Amazonian River Chemistry" (1993). *Digitized Theses*. 2230.  
<https://ir.lib.uwo.ca/digitizedtheses/2230>

This Dissertation is brought to you for free and open access by the Digitized Special Collections at Scholarship@Western. It has been accepted for inclusion in Digitized Theses by an authorized administrator of Scholarship@Western. For more information, please contact [tadam@uwo.ca](mailto:tadam@uwo.ca), [wlsadmin@uwo.ca](mailto:wlsadmin@uwo.ca).

**MULTIPLE FLUXES INFLUENCING  
AMAZONIAN RIVER CHEMISTRY**

by

**Kurt O Konhauser**

**Department of Geology**

**Submitted in partial fulfillment of the  
requirements for the degree of  
Doctor of Philosophy**

**Faculty of Graduate Studies  
The University of Western Ontario  
London, Ontario  
January, 1993**

**© Kurt O Konhauser 1993**



National Library  
of Canada

Acquisitions and  
Bibliographic Services Branch

395 Wellington Street  
Ottawa, Ontario  
K1A 0N4

Bibliothèque nationale  
du Canada

Direction des acquisitions et  
des services bibliographiques

395, rue Wellington  
Ottawa (Ontario)  
K1A 0N4

Library of Congress

Library of Congress

**The author has granted an irrevocable non-exclusive licence allowing the National Library of Canada to reproduce, loan, distribute or sell copies of his/her thesis by any means and in any form or format, making this thesis available to interested persons.**

**L'auteur a accordé une licence irrévocable et non exclusive permettant à la Bibliothèque nationale du Canada de reproduire, prêter, distribuer ou vendre des copies de sa thèse de quelque manière et sous quelque forme que ce soit pour mettre des exemplaires de cette thèse à la disposition des personnes intéressées.**

**The author retains ownership of the copyright in his/her thesis. Neither the thesis nor substantial extracts from it may be printed or otherwise reproduced without his/her permission.**

**L'auteur conserve la propriété du droit d'auteur qui protège sa thèse. Ni la thèse ni des extraits substantiels de celle-ci ne doivent être imprimés ou autrement reproduits sans son autorisation.**

ISBN 0-315-81320-2

**Canada**



### **FRONTISPIECE**

**Aerial photo of the confluence of the "whitewaters" of the Rio Solimões  
with the "blackwaters" of the Rio Negro, in central Amazonia, Brazil.**

## ABSTRACT

The rivers flowing through the Amazon Basin are both physically and chemically heterogeneous. Through detailed geochemical analyses, this study indicates that variability is primarily controlled by substrate lithology in the source region and the erosional regime. The solute-rich waters of the Rio Solimões reflect drainage from the Andes Mountains and the fertility of the varzea. In contrast, the solute-deficient waters of the Rio Negro reflect the infertility of the lateritic and podsolitic terrains of the Central Amazon. Rivers flowing through the Precambrian Shields have an intermediate composition. Such observations suggest that it is possible to classify the chemical composition of Amazonian rivers according to the geochemistry of the soils in their catchment regions and vice versa. These findings have profound implications for using water chemistry as an indicator of the agricultural and mineral potential of a region.

While weathering has proven to be of fundamental importance in the supply of solutes to the river system, this research suggests that the chemistry of these rivers also locally reflect the influence of microorganisms, the concentration of dissolved organic materials, and the input of land-derived aerosols from forest burning.

The ability of microorganisms to undergo chemical exchanges with their aqueous environment, involving both the uptake and excretion of various elements, has been overlooked as an important factor in determining the chemistry of Amazonian rivers. Silicon extracted and precipitated by diatoms indicate that the dissolved silicon levels of the Rio Negro are in part controlled by biological activity. In the Rio Solimões, both filamentous algae and bacteria were shown to bind and accumulate significant amounts of dissolved metals at the surfaces of their anionic cell walls. In a solute-rich river system, the metal-loaded microorganisms play an important role in the transfer of metals from the hydrosphere to the sediment. Given a constant rain of algae and bacteria throughout a

natural body of water, it is not difficult to imagine that they could effectively cleanse the water of dissolved metals and partition them into the sediments

In the Amazon Basin, many of the rivers are characterized by their high organic content and their solute-deficiency. In the Rio Negro, major cations such as Fe, Al, and Si are significantly bound into organo-metallic complexes, contributing largely to the mobilization and transport of these metals in the river. The high organic-inorganic matter ratio of this river also seems to provide sufficient reactive sites for the adsorption of trace metals. As a whole, this process may cause significant changes in the overall chemical composition of rivers draining highly leached and low relief, podsolitic terrains.

Lastly, as human settlement into the Amazon Basin has expanded over the past 30 years, it has become apparent that anthropogenic forces now influence the nutrient dynamics of the forest system. As population pressures increase, large tracts of undisturbed forest are converted to agricultural and pastoral lands through slash-and-burn methods of forest clearing. Biomass burning has been recognized as a significant source of elements to the natural aerosol content. Results from this study indicate that numerous metals are released as aerosols through the combustion of vegetation. In addition, an entire suite of metals are concentrated in the residual ash, which potentially can be dispersed into the atmosphere. Analyses of radiogenic isotopes (Sr, Pb) in rainfall suggest that these emissions may provide nuclei for the condensation of water vapor, with the net result being a high concentration of dissolved metals in the precipitation. In solute-deficient river systems such as the Rio Negro, this process may have enormous impact on chemical composition.

This thesis presents some of the most detailed, multi-element, geochemistry of Amazonian waters today. These systems are extremely complicated and will require constant monitoring as humans invade the entire Amazon system.

## ACKNOWLEDGMENTS

Thanks Bill!!! Your willingness to take me on as a graduate student and your continued and unconditional support made everything possible

I would like to thank Darci and Zara Lindermeier and Augusta Kishida from DOCEGEO for making the sampling in Carajás possible. Also, thanks to Barbara Kronberg and Michael Bird for their assistance in sampling and all their ideas, and to Henrietta Mann for her help on how to collect microbial samples.

My various analyses would never have been completed without the assistance of Charlie Wu on the XRF, John Forth for thin sectioning, Jennifer McKay on soil separations and XRD, Ross Davidson on the SEM, Bob Harris on the TEM, and Cindy Swiney for help with the Radiogenic work. Special thanks go out to Fred Longstaffe, Kurt Kyser, and Terry Beveridge for all of their cooperation and allowing me the use of their labs, to the entire B17 lab at Guelph for their assistance, to Charlie Trick for identifying the diatoms, and to Mike Powell for his continued help with everything.

I would also like to thank Dolors Planas, Neil MacRae, Grant Ferris, and Steve Hicock with all their assistance on various manuscripts, and Ian Craig for the outstanding photography work.

Last but not least, none of this work would ever have been accomplished without the support of my parents.

THANKS!

## TABLE OF CONTENTS

	<b>Page</b>
<b>CERTIFICATE OF EXAMINATION</b>	ii
<b>ABSTRACT</b>	iii
<b>ACKNOWLEDGMENTS</b>	v
<b>TABLE OF CONTENTS</b>	vi
<b>LIST OF TABLES</b>	viii
<b>LIST OF FIGURES</b>	x
<b>LIST OF APPENDICES</b>	xi
<b>CHAPTER 1. Introduction</b>	<b>1</b>
1.1 Characteristics of the Amazon Basin	1
1.2 Amazonian River Chemistry	4
1.3 Purpose of Study	5
<b>CHAPTER 2. Multi-Element Chemistry of Some Amazonian Rivers: Guide to the Nature of Source Rocks and Soils and their Agricultural and Mineral Potential</b>	<b>6</b>
2.1 Introduction	6
2.2 Study Area	9
2.3 Sampling and Analytical Methodology	12
2.4 Results	14
2.4.1 Soil and Sediment Chemistry and Mineralogy	14
2.4.2 Surface Water Chemistry	23
2.5 Discussion	33
<b>CHAPTER 3. The Impact of Microbial Metal Sorption and Biom mineralization on Amazonian River Chemistry</b>	<b>36</b>
3.1 Introduction	36
3.2 Sampling and Analytical Methodology	40
3.3 Results	42
3.3.1 Metal Sorption and Biom mineralization by Bacteria	42
3.3.2 Metal Sorption by Filamentous Aigae	60
3.3.3 Silica Precipitation by Diatoms	69



	<b>Page</b>
3 4 Discussion	88
3 4 1 The Role of Bacteria	88
3 4 2 The Role of Algae	91
<b>CHAPTER 4. METAL COMPLEXATION BY ORGANIC MATERIAL</b>	<b>97</b>
4 1 Introduction	97
4 2 Sampling and Analytical Methodology	98
4 3 Results	99
4 4 Discussion	99
<b>CHAPTER 5. THE IMPACT OF BIOMASS BURNING ON AMAZONIAN RIVER CHEMISTRY</b>	<b>105</b>
5 1 Introduction	105
5 2 Sampling and Analytical Methodology	109
5 3 Results	110
5 3 1 Chemical Composition of Aerosols and Residual Ash	110
5 3 2 Chemical Composition of Rainfall	111
5 3 3 Determination of Isotopic Ratios	114
5 3 3 1 Sr Ratios	114
5 3 3 2 Pb Ratios	115
5 4 Discussion	118
<b>CHAPTER 6. Summary and Conclusions</b>	<b>124</b>
<b>APPENDICES</b>	<b>126</b>
<b>REFERENCES</b>	<b>139</b>
<b>VITA</b>	<b>149</b>

## LIST OF TABLES

<b>Table</b>	<b>Description</b>	<b>Page</b>
2.1	Major oxide composition of soils in the Central Amazon	16
2.2	Major oxide composition of soils in the Precambrian Shield	16
2.3	Major oxide composition of soils in the varzea	16
2.4	Comparison of major oxide composition of soils in study areas with crustal abundance	17
2.5	Mineralogy of soils and sediments in study areas	18
2.6	Trace element composition of soils in the Central Amazon	20
2.7	Trace element composition of soils in the Precambrian Shield	20
2.8	Trace element composition of soils in the varzea	20
2.9	Comparison of trace element composition of soils in study areas with crustal abundance	21
2.10	Trace element composition of soil size fractions in soils of the varzea	22
2.11	Chemical analyses of waters from the Rio Negro	25
2.12	Chemical analyses of waters from the Rio Solimões	26
2.13	Chemical analyses of waters from forested areas, Carajás	27
2.14	Comparison of dissolved metal concentrations in Amazonian rivers with world river average	28
2.15	Average enrichment status of Amazonian rivers to world river average	32
2.16	Comparison of dissolved solutes in principle world rivers	34
3.1	Concentration of metals in algae from the Rio Negro	61
3.2	Concentration of metals in algae from the Rio Solimões	62
3.3	Concentration of metals in algae from forested terrains	65
3.4	Concentration of metals in algae from deforested terrains	66
3.5	Inorganic elements required by algae	92

<b>Table</b>	<b>Description</b>	<b>Page</b>
3 6	Comparison of dissolved solutes in the Rio Negro with average Shield and lateritic soils	94
5 1	Inorganic composition of aerosols released during biomass burning and residual ash	112
5 2	Chemical composition of precipitation in study area.	113
5 3	Sr isotopic ratios of water, rainfall, soils, and ash	116
5 4	Pb isotopic ratios of water, rainfall, soils, and ash	117

## LIST OF FIGURES

Figure	Description	Page
1.1	Dimensions of the Amazon Basin with its principle rivers	3
2.1	The major geochemical provinces of the Amazon Basin	8
2.2	Location of study areas and sample sites	11
2.3	Comparison of dissolved metal concentrations in Amazonian rivers with world river average	30
3.1	EDS spectra of mineralized and unmineralized capsules	44
3.2	Distribution of Fe, Al, and Si in bacterial mineral precipitates	47
3.3	Concentration factor plot for algae in the Rio Negro and Rio Solimões	64
3.4	Concentration factor plot for algae in forested and deforested terrains	68
3.5	EDS spectra of siliceous gels	75
4.1	EDS spectra of dissolved and particulate organic material	103
5.1	Movement of burn plumes across the Amazon Basin	107
5.2	$^{87}\text{Sr}/^{86}\text{Sr}$ and $^{206}\text{Pb}/^{204}\text{Pb}$ isotopic ratios for ocean water, and river water, soils, vegetation, and rainfall collected in Carajás	121

## LIST OF APPENDICES

Appendix	Page
<b>APPENDIX 1. Geochemical Data for Standards: Soil Samples</b>	
A1 1 XRF data for major oxide composition in soil standards SY-2 and MRCI-1 and comparison with accepted values	127
A1 2 XRF data for trace element composition in soil standards G-2 and BHVO-1 and comparison with accepted values	128
A1 3 Precision calculations for major oxides	129
A1 4 Precision calculations for trace elements	130
<b>APPENDIX 2. Geochemical Data for Standards: Water Samples</b>	
A2 1 ICP-MS data for water standards ERI CN1 and ERI CN2 and comparison with accepted values	132
A2 2 Precision calculations	133
<b>APPENDIX 3. Geochemical Data for Standards: Organic Samples</b>	
A3 1 ICP-MS data for biological standards TORT-1, NOAA BT2, and PACS-1 and comparison with accepted values	135
A3 2 Precision calculations	136
<b>APPENDIX 4. Geochemical Analyses of Water, Soils, and Algae (see disk)</b>	138

The author of this thesis has granted The University of Western Ontario a non-exclusive license to reproduce and distribute copies of this thesis to users of Western Libraries. Copyright remains with the author.

Electronic theses and dissertations available in The University of Western Ontario's institutional repository (Scholarship@Western) are solely for the purpose of private study and research. They may not be copied or reproduced, except as permitted by copyright laws, without written authority of the copyright owner. Any commercial use or publication is strictly prohibited.

The original copyright license attesting to these terms and signed by the author of this thesis may be found in the original print version of the thesis, held by Western Libraries.

The thesis approval page signed by the examining committee may also be found in the original print version of the thesis held in Western Libraries.

Please contact Western Libraries for further information:

E-mail: [libadmin@uwo.ca](mailto:libadmin@uwo.ca)

Telephone: (519) 661-2111 Ext. 84796

Web site: <http://www.lib.uwo.ca/>

# CHAPTER 1

## INTRODUCTION

### 1.1 Characteristics of the Amazon Basin

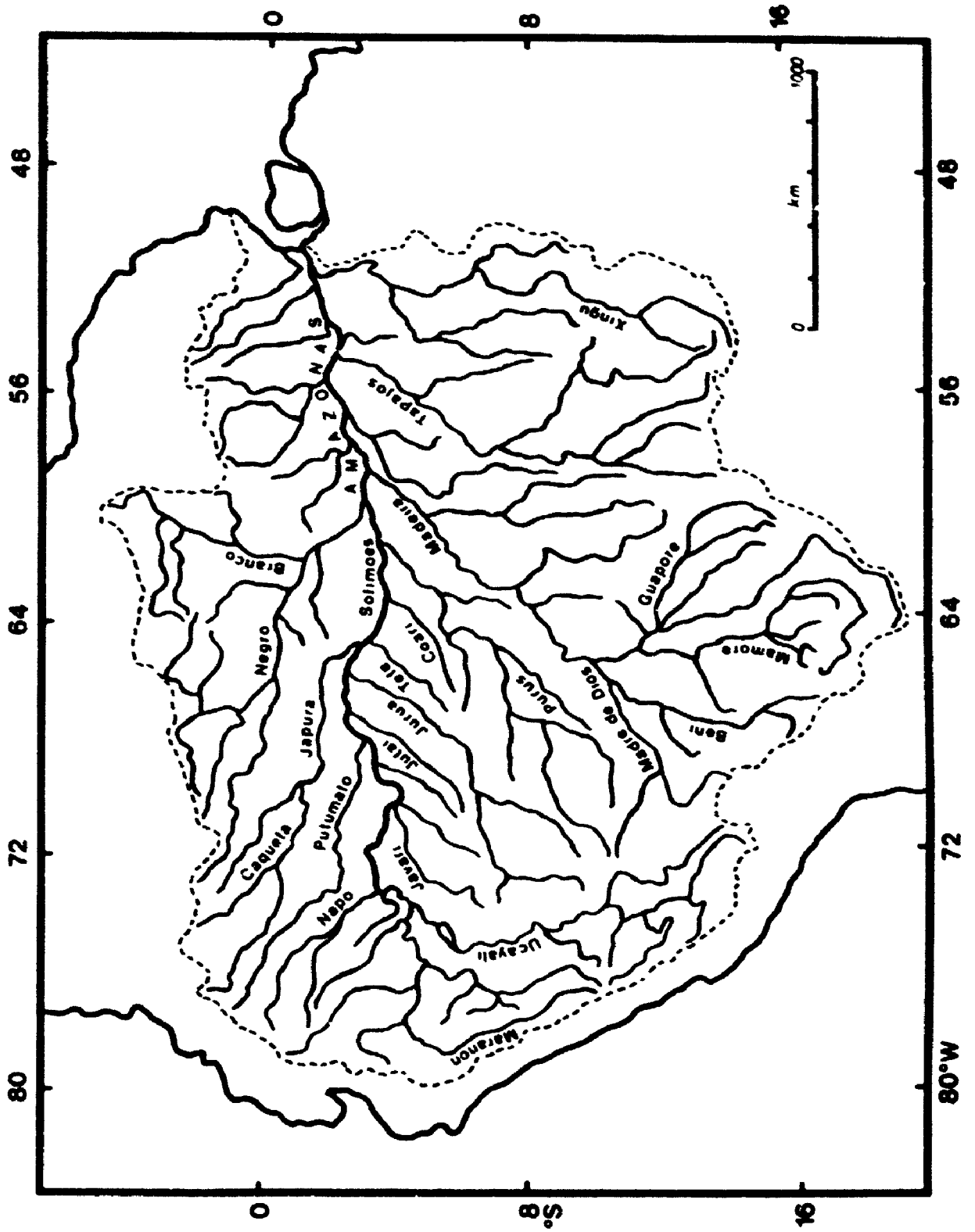
The Amazon Basin is composed of the world's largest tropical forest ecosystem, covering an area over 7 million km<sup>2</sup>. The basin extends from 5°N to 17°S and from 46°W to 79°W (Sioli, 1984) -- almost the entire continental width (Figure 1.1). Structurally, the eastern two thirds of the basin is situated in a subsiding trough between Precambrian shields to the north and south, and is terminated in the West by the Andes Mountains (Stallard and Edmond, 1983).

The climatic zones of the Amazon Basin range from tropical rainforests in the East to high alpine conditions in the western Andes Mountains, and form one of the widest ranges found in any single river basin in the world (Gibbs, 1967). Mean temperatures range from a low of <15°C in the high Andes to a constant 29 ± 1°C all year round in the lowland rainforests. Mean annual precipitation for the basin is approximately 2300 mm/yr (Sioli, 1984) with the precipitation cycle being composed of a rainy season from January to June and a drier period for the remainder of the year (Guerra, 1959).

The Amazon Basin is drained by the 6,518 km long Amazon River, which is fed by more than 1000 tributaries (Salati and Vose, 1984). The Amazon's average annual discharge of 175,000 m<sup>3</sup>/s is 4.6 times that of the Congo River and 11 times that of the Mississippi River (Oltman, 1965). In both drainage area and volume of discharge the Amazon is the world's largest river (Gibbs, 1967). The Amazon also ranks third in sediment output to the ocean at 9 × 10<sup>8</sup> tonnes/yr (Meade et al., 1979) and perhaps first in output of dissolved material, transporting about 2.9 × 10<sup>8</sup> tonnes/year (Gibbs, 1972).

**Figure 1.1** Dimensions of the Amazon Basin with its principal rivers





## **1.2 Amazonian River Chemistry**

Early studies in the Amazon Basin showed that the waters were chemically and physically very heterogeneous. The first classification of Amazonian rivers was based on their physical appearance (Sioli, 1950). Whitewater rivers are rich in dissolved solutes and are extremely turbid owing to their high concentrations of suspended sediment.

Blackwater rivers are relatively infertile rivers characterized by low sediment yields and their "tea-colored" (Hedges et al., 1986, p. 719) acidic waters that are rich in dissolved humic material (Ertel et al., 1986). Finally, clearwater rivers are relatively transparent, green-colored rivers that are neither turbid with detrital materials or colored by humic compounds (Sioli, 1984).

The chemistry of Amazonian rivers have long been attributed both to the variability of the geological source and to the erosional regime through which the rivers flow. Early studies by Raimondi (1884) and Katzer (1897) observed that the low dissolved inorganic concentrations in some lowland rivers contrasted with those of rivers draining the Andes Mountains. It was later shown that the rivers flowing through the central lowlands were typically blackwater in composition, whitewater streams were distinctive of the waters draining the Andes, while clearwater types were characteristic of rivers originating in the Precambrian shields (Sioli, 1968, 1975, Stallard and Edmond, 1983).

More recently, several papers have begun to deal specifically with the elemental composition of Amazonian rivers (Gibbs, 1970, 1972, 1973, 1977, Boyle, 1978, Stallard, 1978; Stallard and Edmond, 1983, Furch et al., 1982; and Furch, 1984). Studies such as Stallard and Edmond (1983) have indicated that the distribution of major cations and anions in the dissolved load were controlled by substrate lithology in the source regions. This relationship was later extended to several trace elements (Furch, 1984).

The chemistry of rivers in the Amazon Basin have also been attributed to the atmospheric precipitation of cyclic salts (Gibbs, 1970). According to Gibbs, the low total dissolved solids and the ratios of major dissolved ions (which are similar to sea salt) in

lowland rivers indicate that their chemical compositions are controlled mainly by the amount of dissolved salts added through atmospheric precipitation. Further, some of these Amazon tributaries are thousands of kilometers from the sea, indicating that the supply of dissolved salts to the freshwater systems is not limited to waters near the coast (Gibbs, 1970)

### **1.3 Purpose of Study**

Despite the compilation of published work on the chemistry of Amazonian waters, most studies have dealt specifically with

- a) a limited number of major elements and trace metals, and
- b) the impact of geologic, geochemical, and petrographic properties of the source regions on the chemical composition of surface waters.

While weathering is of fundamental importance in the supply of solutes to a river system, I believe that other factors also have impact. It is, therefore, the purpose of this thesis to discuss the multiple fluxes which influence Amazonian river chemistry through the most detailed geochemical analyses to date

## **CHAPTER 2**

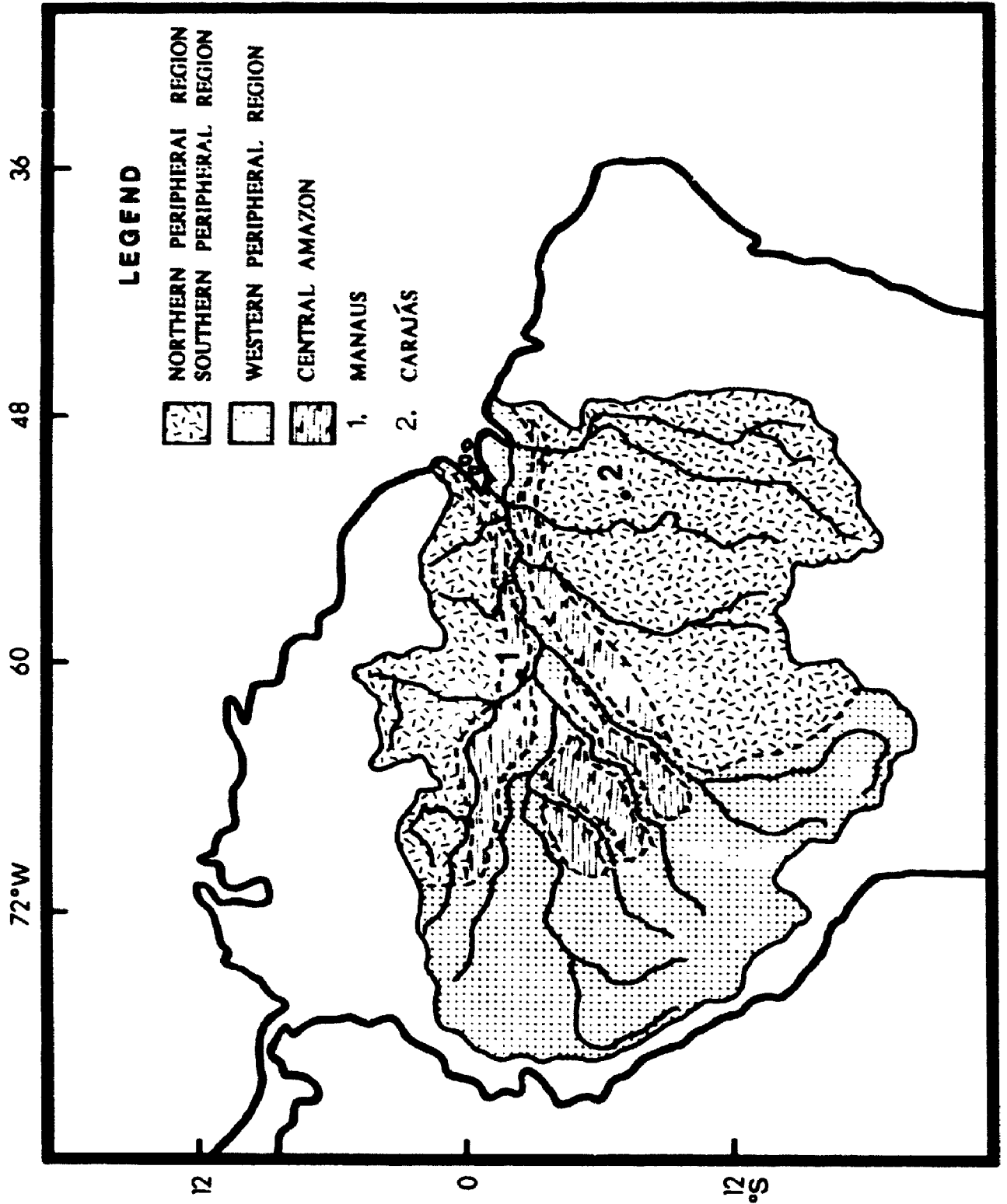
### **MULTI-ELEMENT CHEMISTRY OF SOME AMAZONIAN WATERS: GUIDE TO THE NATURE OF SOURCE ROCKS AND SOILS AND THEIR AGRICULTURAL AND MINERAL POTENTIAL**

#### **2.1 Introduction**




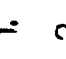
Since the earliest studies on Amazonian river chemistry, it has become apparent that the chemical and physical variability exhibited by surface waters were largely attributed to geologic heterogeneity of the Amazon Basin. On the basis of distinct differences in geology, soil types, and vegetation, Fittkau et al., (1975) have divided the Amazon Basin into three major geochemical provinces (Figure 2.1) the western peripheral region, where soils and waters are fertile, the Central Amazon, an area where the soils and waters are deficient in nutrients; and the northern and southern peripheral regions with intermediate compositions (Furch, 1984)

In the western peripheral region, the soils are directly influenced by erosion of the different lithologies (acid to intermediate volcanics, shales, limestones, and arenitic sandstones) in the headwater regions of the Andes Mountains (Stallard and Edmond, 1983). In these geologically active sites, the addition of new volcanic materials and substantial weathering along the steep slopes, result in enormous quantities of fresh detrital material being carried downstream. The whitewater rivers are estimated to carry about 85% of the total suspended solids discharged by the Amazon River at its mouth (Gibbs, 1967). This sediment is systematically deposited over the entire catchment area from the broad valleys at the foot of the Andes to the central Amazonian lowlands, and along the banks and floodplains of the river systems (Sioli, 1975). The resulting alluvial soils, known as the varzea, represent the only naturally fertile terrains throughout the Amazon (Klinge et al., 1981). The constant fertility of these soils are sustained by the annual deposition of new sediments during seasonal floods (Sioli, 1975)

**Figure 2 i: The major geochemical provinces of the Amazon Basin, after Fittkau et al. (1975) Location of the study areas in Manaus and Carajás are shown**



**LEGEND**

-  NORTHERN PERIPHERAL REGION
-  SOUTHERN PERIPHERAL REGION
-  WESTERN PERIPHERAL REGION
-  CENTRAL AMAZON
- 1. MANAUS
- 2. CARAJÁS

In contrast, the Central Amazon is composed of highly weathered Tertiary and Pleistocene sediments of fluvial and lacustrine origin (Fittkau et al., 1975). In these lowlands, lack of exposed rock and intense chemical weathering of the humid tropics over millions of years has resulted in the development of thick, lateritic soils (Kronberg et al., 1979) with low erosional rates (Stallard and Edmond, 1983). In the Rio Negro Basin, open caatinga forests and igapo forests (a forest type that is adapted to partial or complete inundation) allow the heavy rains to wash away the fine clay particles, leaving behind sandy, podsolitic soils that are characterized by a bleached quartz A horizon and an underlying clay layer cemented with humic materials derived from decaying surface vegetation (Klinge, 1965; Leenheer, 1980). Rivers originating in these extremely infertile soils contain low levels of dissolved solids and suspended matter (Sioli, 1984), and are frequently colored black due to leaching of humic materials (Ertel et al., 1986).

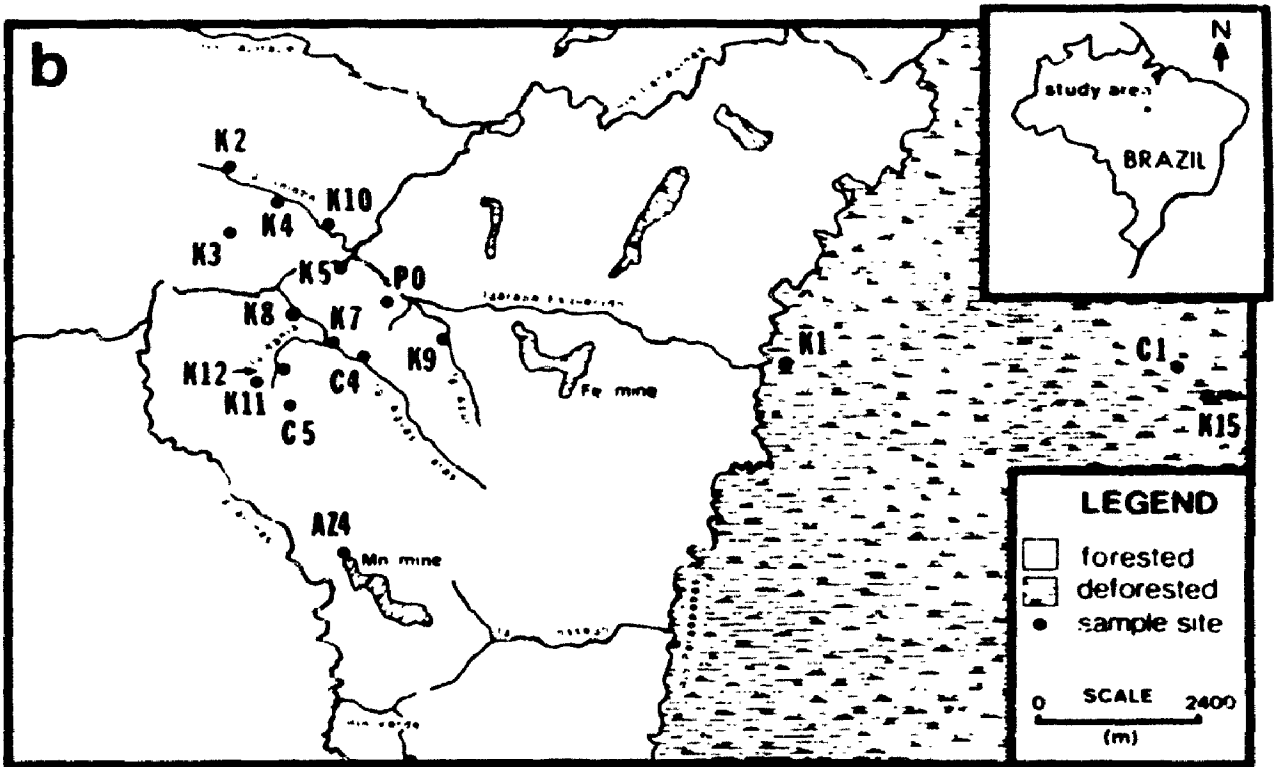
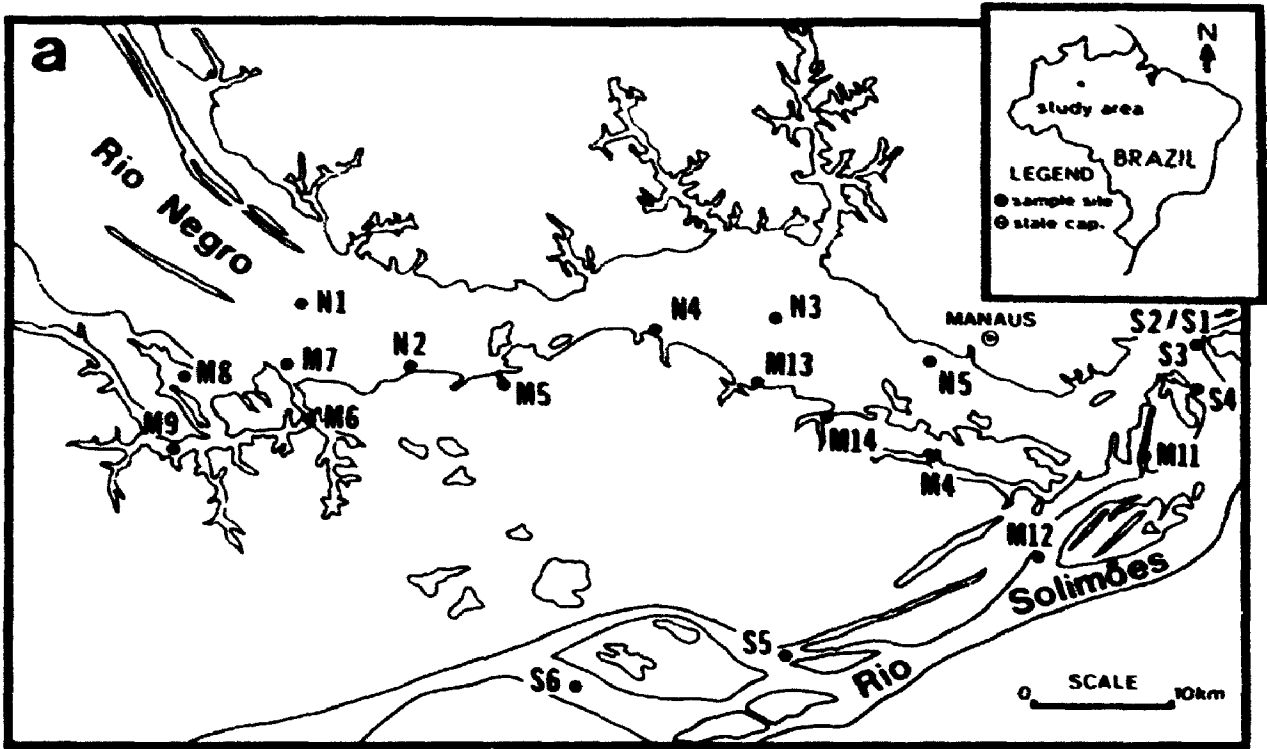
The areas in the northern and southern peripheral regions are dominated by low-lying crystalline platforms of the Precambrian Shield (Klammer 1984), comprised of granites, gneisses, acid and basic volcanics, and metasediments (Putzer, 1984). In these stable cratonic regions the soils tend to be deficient in nutrients (Fyfe et al., 1983), giving rise to the poor soils of the Amazonian high grounds -- the so-called terra firme. The closed terra firme forest canopy (which protects the soils against direct impact of rainfall, thereby reducing surface erosion) generally is characterized by clearwater rivers (Sioli, 1984). Due to local conditions and seasonal fluctuations these rivers may assume black or whitewater characteristics, locally or for short time periods (Sioli, 1967).

## 2.2 Study Area

Studies were conducted in both the Manaus area, in the state of Amazonia (Figure 2.2a), and the Carajás mining area in the state of Pará (Figure 2.2b). The sampling area in Manaus provided the opportunity to sample the water, soils, and sediment of both the varzea (which serves as a projection of the western peripheral region) and the Central

**Figure 2 2** Location of study areas and sample sites in (a) Manaus and (b) Carajás.





Amazon lowlands, while Carajás allowed sampling to be undertaken in the southern peripheral area (shield)

The city of Manaus is built at the confluence of the Rio Solimões and the Rio Negro in central Amazonia, 1600 km from the Atlantic coast. The Rio Solimões, also known as the Upper Amazon, is a typical whitewater river that drains the Andes Mountains and the western peripheral region of the Amazon Basin. The Rio Negro, volumetrically the largest tributary of the Amazon, is a blackwater river that drains the Central Amazon. The frequently flooded area between the two Amazon tributaries is partly influenced by both water types. It consists of the varzea forest that borders the Rio Solimões and a mixture of caatinga forests and the less dense igapo forest, which is annually flooded by the Rio Negro (Hedges et al., 1986)

The Carajás Range is located within the central Brazilian Shield, approximately 550 km south of Belém in the state of Pará. The area is almost completely covered by an equatorial rainforest, broken only by clearings of sparse vegetation. Most of the Carajás area is served by the Itacaiunas River which flows into the Tocantins River at Marabá. The main tributary of the Itacaiunas River, the Paraopebas River, marks both the eastern boundary of the Carajás area, and an abrupt transition from a forested to deforested landscape. More recently, large areas of Pará's forests are being destroyed as raw material for charcoal to be used in smelting pig iron (Fearnside, 1989)

### **2.3 Sampling and Analytical Methodology**

Water samples were collected upstream of Manaus on the Rio Negro (and some of its tributaries) and on the Rio Solimões on two consecutive sampling periods in mid-July/90 and early June/91, following the annual rainy season in the Amazon. Soil and sediment samples were also collected from several locations along both rivers. Soil samples M8, M11, S4A, S4B and S5 were collected within 50 m of the river bank from the upper 10 cm of the soil profile, while samples M7, M13A, and N2B were collected

randomly at greater depths from the soil profiles exposed along the embankments of the Rio Negro. All stream sediment samples (except sample M14) were collected from the river bottom by diving to depths of approximately 5 m below the water surface. Sample M14 was collected at a greater depth (approximately 15 m) by a dredging device operating during our sampling period.

In Carajás, sampling occurred during three consecutive summers in late July/89, middle July/90, and late June/91. Water and sediment samples were collected from several small streams draining completely forested regions, while soil samples were collected throughout the area. Soil samples K3C and K7A were collected in close proximity to the river embankments, while both samples C5D and P0 were taken several kilometers from any water systems.

Approximately 1 L samples of water were collected for multi-element analysis. The water samples were placed in two 500 mL Nalgene bottles and then acidified on site with 5 mL analytical grade  $\text{HNO}_3$ . Prior to multi-element analysis, materials in suspension were removed in the laboratory by pressure filtration through 0.2  $\mu\text{m}$  Nuclepore membranes (Costar Corp.) To determine the dissolved metal content, the water samples were then analyzed by inductively coupled plasma - mass spectroscopy. An ICPMS Model PQ1 by Elemental Ltd. was used.

All bulk soil and sediment samples were analyzed for major and minor elements ( $\text{SiO}_2$ ,  $\text{Al}_2\text{O}_3$ , total Fe as  $\text{Fe}_2\text{O}_3$ ,  $\text{K}_2\text{O}$ ,  $\text{CaO}$ ,  $\text{MgO}$ ,  $\text{MnO}$ ,  $\text{P}_2\text{O}_5$ ,  $\text{Na}_2\text{O}$ , and  $\text{TiO}_2$ ) and trace elements (Nb, Zr, Y, Sr, Rb, Pb, Zn, Cu, Ni, Co, Cr, Ba, V, As, Ga, U, and Th) by X-Ray Fluorescence Spectrometry (XRF) on a Philips PW-1450 automatic sequential spectrometer. Prior to analysis, samples were air dried for one week and subsequently ground for 50 seconds in a tungsten carbide mill. The percentage of major and minor elements were determined from the preparation of fusion disks, while the concentration of trace elements were determined using pressed powder pellets (Wu, 1986).

To analyze the different varzea soil size fractions, unmilled samples were disaggregated with an agate mortar and pestle, and dispersed in distilled water using an ultrasonic probe. The resulting supernatant was decanted into a settling column and the residual  $>20 \mu\text{m}$  fraction was removed. The  $2\text{--}20 \mu\text{m}$  and  $<2 \mu\text{m}$  size fractions were removed by settling according to Stokes Law, and subsequently dried in a pre-heated oven. All size fractions were analyzed by XRF.

Mineralogies for all soil and sediment samples were determined by X-ray diffraction (XRD) on a Rigaku rotating anode diffractometer (Co  $K\alpha$ ). The scans were carried out at 160 kV and 45 mA, from  $2\text{--}82^\circ$  two-theta at a rate of  $10^\circ/\text{min}$ . Sample preparation involved packing the milled soil and sediments into Al sample holders, so as to retain a random orientation. From the  $<2 \mu\text{m}$  size fractions, approximately 2 mL subsamples were pipetted to a glass slide and analyzed by XRD under the following conditions: untreated, 54 percent relative humidity, and glycol solvated.

The Nuclepore membranes which contained the suspended sediments were allowed to air dry and subsequently were mounted on glass slides with double-sided tape. To determine the mineralogy of the suspended sediments the samples were similarly analyzed by XRD.

In conjunction with the XRD work, thin sections of several soil samples were made and studied with a transmitting light microscope. This proved useful in determining the presence of minerals found in only trace amounts.

## **2.4 Results**

### **2.4.1 Soil and Sediment Chemistry and Mineralogy**

Soils in the Amazon Basin are collectively some of the poorest soils in the world. This nutrient deficiency is typified by the soils in the Central Amazon. These highly leached soils have had most of their base cations reduced to very low levels with some samples having levels below those detectable by XRF (Table 2.1). In these soils, over 95%

of the macrochemical components are accounted for by a  $\text{SiO}_2$  -  $\text{Al}_2\text{O}_3$  -  $\text{Fe}_2\text{O}_3$  assemblage. Compared to crustal abundances (Table 2.4), these soils are more siliceous and aluminous, with considerably lower levels of major cations. At this advanced stage of weathering the soils have a rather simple mineralogy dominated by quartz, Fe+Al-oxides, and kaolinite, with a few refractory minerals such as anatase and zircon (Table 2.5).

Soils from the shield areas are also highly leached, however, not nearly to the degree as those from the Central Amazon (Table 2.2). These soils show an extreme variability in their  $\text{SiO}_2$  -  $\text{Al}_2\text{O}_3$  -  $\text{Fe}_2\text{O}_3$  ratios, with some samples being very siliceous (K7A) and others very ferruginous (C5D). The major cation levels show slight enrichments which are probably due to the presence of trace amounts of illite and smectite, in addition to quartz, kaolinite, and Fe+Al+Ti-oxides (Table 2.5). These levels, however, are still lower than crustal abundance (Table 2.4).

The only fertile soils in the Amazon are those of the varzea. These soils show higher cation to silica ratios with consistently higher concentration of the oxides of Ti, Mn, Mg, Ca, K, P, and Na (Table 2.3). This in turn is reflected by a more diverse mineralogy (Table 2.5). The most noticeable difference is the presence of primary minerals such as feldspars and micas and a high proportion of diverse clay minerals (approximately 11% of sample) such as kaolinite, illite, chlorite, and smectite.

The geochemistry of the river sediment samples from all three geochemical provinces closely reflect those of the soils. Due to the limited number of mineral phases in Central Amazon soils, the suspended sediment load (as determined by analysis of the filter paper) contains mainly kaolinite, with minor quartz. This leads to sediment samples dominated by  $\text{SiO}_2$  and  $\text{Al}_2\text{O}_3$ , with extremely low cation levels. Sample M14, collected from the middle reaches of an off-branch of the Rio Negro, also indicates high LOI (lost on ignition) values. This is expected due to the high concentration of organic material in solution (Ertel et al., 1986) and in suspension (Hedges et al., 1986).

TABLE 2.1 MAJOR OXIDE COMPOSITIONS IN THE CENTRAL AMAZON (in wt. %)

	SOIL				SEDIMENT			
	M7	M8	M13A	N2B	M4	M14	N2D	N4B
SiO <sub>2</sub>	74.30	72.95	53.32	80.32	90.33	46.17	85.46	75.18
TiO <sub>2</sub>	0.46	0.91	0.74	0.35	0.29	1.37	0.35	0.62
Al <sub>2</sub> O <sub>3</sub>	15.29	7.96	32.70	10.67	5.11	24.40	7.34	7.49
Fe <sub>2</sub> O <sub>3</sub>	2.58	5.63	1.18	1.78	0.75	2.60	1.33	7.68
MnO	0.02	0.02	0.01	0.01	0.01	0.02	0.01	0.02
MgO	0.00	0.39	0.03	0.29	0.06	0.35	0.55	0.46
CaO	0.00	0.00	0.00	0.00	0.00	0.13	0.00	0.00
K <sub>2</sub> O	0.06	0.02	0.08	0.01	0.00	0.57	0.00	0.00
P <sub>2</sub> O <sub>5</sub>	0.04	0.06	0.02	0.04	0.07	0.07	0.05	0.13
Na <sub>2</sub> O	0.00	0.00	0.00	0.00	0.00	0.00	0.00	0.00
LOI	6.00	6.81	12.60	4.74	2.39	23.58	3.47	7.69
TOTAL	98.76	98.74	100.67	98.22	99.01	99.25	98.57	99.28

TABLE 2.2 MAJOR OXIDE COMPOSITIONS IN THE PRECAMBRIAN SHIELD (in wt. %)

	SOIL				SEDIMENT			
	C5D	K3C	K7A	PO	K2D	K7C	K9	K12
SiO <sub>2</sub>	16.89	54.05	79.40	56.78	77.56	84.51	57.02	72.90
TiO <sub>2</sub>	3.06	0.65	0.30	0.65	1.28	1.00	1.46	1.33
Al <sub>2</sub> O <sub>3</sub>	30.87	9.84	4.69	23.21	8.14	4.13	12.18	5.72
Fe <sub>2</sub> O <sub>3</sub>	37.90	19.00	10.42	8.75	5.68	3.92	14.04	4.34
MnO	0.08	0.32	0.13	0.01	0.08	0.06	0.06	0.03
MgO	0.23	0.19	0.41	0.21	0.49	0.14	0.20	0.15
CaO	0.14	0.11	0.00	0.00	0.18	0.04	0.03	0.65
K <sub>2</sub> O	0.06	0.24	0.44	0.12	0.67	0.40	0.27	0.41
P <sub>2</sub> O <sub>5</sub>	0.13	0.14	0.11	0.03	0.08	0.06	0.15	0.09
Na <sub>2</sub> O	0.07	0.00	0.00	0.00	0.00	0.00	0.01	0.00
LOI	9.06	14.46	2.78	10.74	5.68	5.64	14.28	14.69
TOTAL	98.48	99.00	98.68	100.50	99.84	99.90	99.70	99.71

TABLE 2.3 MAJOR OXIDE COMPOSITIONS IN THE VARZEA (in wt. %)

	SOIL				SEDIMENT			
	M11	S4A	S4B	S5	A1A	A2A	S3	S6
SiO <sub>2</sub>	61.84	61.55	64.57	64.22	64.75	71.00	68.59	60.26
TiO <sub>2</sub>	0.90	0.89	0.88	0.83	0.86	0.70	0.75	0.90
Al <sub>2</sub> O <sub>3</sub>	16.36	16.30	14.73	14.49	15.08	12.59	13.55	16.68
Fe <sub>2</sub> O <sub>3</sub>	6.24	6.28	5.54	5.42	5.79	4.55	5.02	6.39
MnO	0.10	0.11	0.09	0.08	0.10	0.07	0.09	0.14
MgO	1.90	1.56	1.50	2.03	1.26	1.13	1.37	1.98
CaO	1.28	1.29	1.50	1.43	1.40	1.59	1.61	1.28
K <sub>2</sub> O	2.26	2.25	2.19	2.14	2.18	2.05	2.09	2.36
P <sub>2</sub> O <sub>5</sub>	0.18	0.15	0.16	0.22	0.14	0.09	0.13	0.20
Na <sub>2</sub> O	1.07	1.29	1.37	1.26	1.54	1.73	1.73	1.43
LOI	7.50	7.81	7.24	8.27	6.89	4.27	5.12	9.03
TOTAL	100.00	99.48	99.78	100.39	99.98	99.78	100.05	100.65

Note: values of "0.00" indicate concentrations below detection limit. LOI = lost on ignition

TABLE 2.4: COMPARISON OF MAJOR OXIDE COMPOSITIONS OF SOILS  
IN STUDY AREAS WITH CRUSTAL ABUNDANCE (in wt.%)

	CRUSTAL ABUNDANCE	CENTRAL AMAZON	SHIELD	VARZEA
SiO <sub>2</sub>	58.50	70.22	51.78	63.05
TiO <sub>2</sub>	1.05	0.62	1.17	0.88
Al <sub>2</sub> O <sub>3</sub>	15.80	16.66	17.15	15.47
Fe <sub>2</sub> O <sub>3</sub>	6.50	2.79	19.32	5.87
MnO	0.14	0.02	0.14	0.10
MgO	4.57	0.18	0.26	1.75
CaO	6.51	0.00	0.06	1.38
K <sub>2</sub> O	2.22	0.04	0.22	2.21
P <sub>2</sub> O <sub>5</sub>	0.25	0.04	0.10	0.18
Na <sub>2</sub> O	3.06	0.00	0.02	1.25
TOTAL	98.60	99.10	99.17	99.91

Note: crustal abundances are from: Fairbridge (1972).

TABLE 2.5: MINERALOGY OF SOILS AND SEDIMENTS IN STUDY AREAS

	AVERAGE SOIL			AVERAGE SEDIMENT		
	CENTRAL AMAZON	SHIELD	VARZEA	CENTRAL AMAZON	SHIELD	VARZEA
Quartz	m	m	m	m	m	m
Kaolinite	m	m	mn	mn	m	mn
Gibbsite	mn	mn				
Goethite		m			mn	
Hematite	mn	mn	mn	t	mn	mn
Anatase	mn	mn	mn	t	t	mn
Plagioclase			m			m
K-feldspar			mn			mn
Micas		t	mn		t	mn
Illite		t	mn		t	mn
Chlorite			t			t
Smectites		t	mn		t	mn
Zircon	t		t	t		t
Tourmaline			t			
Rutile	t					

m = major constituent    mn = minor constituent    t = trace constituent



Rivers that originate in the crystalline shields (in the Carajás area) carry little suspended sediment. The mineralogy includes quartz, kaolinite, and trace micas and illite, which reflect a more intermediate composition in both chemistry and mineralogy.

Finally, the presence of suspended feldspars and cation-rich clays (smectite, illite, and chlorite) in the Rio Solimões reflect drainage from the Andes Mountains and the varzea soils. The considerable load of enriched detritus in this whitewater river leads to the fertile sediments of the varzea. A comparison of the soil and sediment samples shows similarities in composition and mineralogy, indicating that the floodplains are formed almost exclusively by river sediment (Victoria et al., 1989).

The variability between the soils of all three geochemical provinces is also shown by their trace element composition (Tables 2.6-2.8). The infertile soils of the Central Amazon typically have the lowest abundances of trace elements with only Nb and Th having greater concentrations than the other soils. In addition, only Zr and Th are enriched relative to crustal abundance (Table 2.9).

In soils of the Shield, several elements - Cu, Cr, V, As, Ga, U, Th, and (Fe and Mn) - are enriched relative to both the other soils and crustal abundances (Table 2.9). These enrichments clearly reflect the mineral wealth (e.g. bauxite, copper, gold, iron ore, manganese, nickel, and tin deposits) discovered and exploited in the Carajás area (Shaw, 1990). The soils also show the highest levels of organic debris present, suggesting that some elements are exhibiting a form of biological affinity (Kronberg et al., 1979).

Although the level of organic material in the varzea soils appears lower than those of the Shield, these soils have the highest concentrations of Y, Sr, Rb, Pb, Zn, Ni, and Ba, with substantial enrichments (relative to the crust) of several elements, including Zr, Y, Rb, Pb, Zn, Ba, As, Ga, and Th (Table 2.9). The high trace element concentrations suggest that elemental enrichments may be associated with the presence of clay minerals (Kronberg et al., 1979; Larocque, 1989). Where primary minerals are present, the levels of most inorganic species in the soil solutions are sufficiently high for smectite.

TABLE 26. TRACE ELEMENT COMPOSITION IN THE CENTRAL AMAZON (in µg/g)

	SOIL				SEDIMENT			
	M7	M8	M13A	S2B	M4	M14	S2D	S4B
Nb	15.00	24.00	28.00	12.00	9.30	36.00	12.00	19.00
Zr	407.00	1141.00	403.00	450.00	582.00	557.00	399.00	500.00
Y	6.80	14.00	7.90	6.30	5.50	31.00	5.30	5.80
Sr	4.70	7.60	22.00	3.70	7.30	48.00	3.30	5.80
Rb	7.30	2.60	7.40	3.50	3.40	8.00	3.30	2.40
Pb	12.00	<5.00	30.00	7.00	7.50	47.00	<5.00	35.00
Zn	10.00	<5.00	19.00	<5.00	7.60	58.00	<5.00	13.00
Cu	8.30	<5.00	10.00	9.40	5.50	21.00	5.40	8.30
Ni	8.30	5.70	5.80	7.80	7.80	26.00	<5.00	13.00
Co	<5.00	<5.00	<5.00	<5.00	<5.00	5.80	<5.00	<5.00
Cr	244.00	56.00	142.00	12.00	359.00	80.00	11.00	12.00
Ba	40.00	86.00	43.00	36.00	18.00	207.00	35.00	36.00
V	31.00	33.00	42.00	22.00	27.00	108.00	23.00	23.00
As	<5.00	<5.00	5.00	<5.00	<5.00	<5.00	<5.00	5.40
Ga	17.00	5.40	27.00	7.60	4.60	34.00	3.00	<2.00
U	2.00	<5.00	2.00	<5.00	2.00	5.00	<5.00	<5.00
Th	12.00	17.00	20.00	8.00	5.00	20.00	7.00	15.00

TABLE 27. TRACE ELEMENT COMPOSITION IN THE PRE-CAMBRIAN SHIELD (in µg/g)

	SOIL				SEDIMENT			
	C5D	K7C	K7A	P0	K2D	K7C	K9	K12
Nb	36.00	13.00	10.00	19.00	24.00	8.00	16.00	12.00
Zr	508.00	328.00	221.00	389.00	1253.00	409.00	320.00	352.00
Y	26.00	15.00	51.00	11.00	54.00	15.00	27.00	21.00
Sr	21.00	35.00	23.00	9.50	32.00	24.00	5.60	24.00
Rb	3.80	14.00	36.00	10.00	24.00	15.00	9.30	11.00
Pb	14.00	15.00	15.00	9.80	16.00	11.00	<5.00	7.00
Zn	23.00	39.00	43.00	10.00	74.00	70.00	63.00	52.00
Cu	102.00	408.00	829.00	113.00	161.00	71.00	350.00	626.00
Ni	15.00	15.00	25.00	14.00	31.00	18.00	43.00	27.00
Co	10.00	36.00	31.00	5.00	21.00	15.00	17.00	14.00
Cr	376.00	99.00	139.00	32.00	108.00	97.00	445.00	129.00
Ba	19.00	22.00	174.00	51.00	173.00	135.00	131.00	91.00
V	545.00	175.00	142.00	65.00	226.00	231.00	172.00	246.00
As	23.00	21.00	6.00	15.00	<5.00	<5.00	<5.00	<5.00
Ga	54.00	16.00	6.00	22.00	13.00	<2.00	15.00	7.00
U	5.00	5.00	5.00	10.00	11.00	<5.00	5.00	<5.00
Th	<5.00	9.00	8.00	89.00	25.00	<5.00	15.00	<5.00

TABLE 28. TRACE ELEMENT COMPOSITION IN THE VARZEA (in µg/g)

	SOIL				SEDIMENT			
	M11	S4A	S4B	S5	A1A	A2A	S3	S6
Nb	17.00	19.00	13.00	16.00	18.00	12.00	18.00	20.00
Zr	273.00	279.00	441.00	327.00	307.00	354.00	279.00	275.00
Y	36.00	32.00	47.00	41.00	33.00	32.00	34.00	43.00
Sr	208.00	215.00	225.00	210.00	203.00	235.00	212.00	214.00
Rb	108.00	109.00	85.00	94.00	92.00	81.00	80.00	126.00
Pb	25.00	20.00	18.00	23.00	12.00	22.00	12.00	20.00
Zn	87.00	109.00	96.00	75.00	84.00	69.00	75.00	87.00
Cu	30.00	32.00	30.00	17.00	19.00	9.00	17.00	28.00
Ni	27.00	36.00	33.00	25.00	33.00	30.00	18.00	24.00
Co	17.00	18.00	14.00	18.00	15.00	15.00	16.00	19.00
Cr	63.00	56.00	61.00	54.00	50.00	51.00	50.00	57.00
Ba	480.00	474.00	455.00	456.00	524.00	507.00	479.00	478.00
V	98.00	107.00	102.00	96.00	102.00	91.00	89.00	114.00
As	9.60	10.00	8.30	<5.00	7.70	<5.00	<5.00	7.40
Ga	22.00	21.00	18.00	20.00	8.30	5.70	16.00	10.00
U	<5.00	<5.00	<5.00	<5.00	<5.00	<5.00	9.00	<5.00
Th	<5.00	5.00	11.00	15.00	9.00	8.00	5.00	39.00

Note: "<" indicate concentrations below detection limit

TABLE 2.9: COMPARISON OF TRACE ELEMENT COMPOSITION OF SOILS  
IN STUDY AREAS WITH CRUSTAL ABUNDANCE (in ug/g)

	CRUSTAL ABUNDANCE	CENTRAL AMAZON	SHIELD	VARZEA
Nb	20.00	19.75	19.50	16.00
Zr	162.00	600.25	361.50	330.00
Y	31.00	8.65	25.75	39.00
Sr	384.00	9.50	22.13	214.50
Rb	78.00	5.20	15.95	99.00
Pb	13.00	13.50	13.45	21.50
Zn	76.00	9.75	28.75	91.75
Cu	68.00	8.13	363.00	27.25
Ni	99.00	6.85	17.25	30.25
Co	29.00	<5.00	20.50	16.75
Cr	122.00	113.50	161.50	58.50
Ba	390.00	37.75	66.50	466.25
V	136.00	45.50	231.75	100.75
As	1.80	<5.00	16.25	8.20
Ga	19.00	14.25	24.50	20.25
U	2.30	<3.50	6.25	<5.00
Th	8.00	14.25	27.50	9.00

Note: "<" indicate concentrations below detection limit.  
Crustal abundances are from Fairbridge (1972).

TABLE 2.10: TRACE ELEMENT COMPOSITION  
OF VARZEA SOILS (in ug/g)

	>20 um	20-2 um	<2 um
Nb	11.00	28.00	18.00
Zr	451.00	231.00	152.00
Y	27.00	32.00	36.00
Sr	218.00	51.00	122.00
Rb	59.00	37.00	154.00
Pb	<5.00	39.00	45.00
Zn	42.00	49.00	327.00
Cu	16.00	24.00	55.00
Ni	<5.00	14.00	37.00
Co	<5.00	<5.00	28.00
Cr	18.00	24.00	48.00
Ba	378.00	227.00	428.00
V	65.00	80.00	162.00
As	6.00	30.00	32.00
Ga	5.00	<5.00	16.00
U	8.00	9.00	<5.00
Th	<5.00	17.00	14.00

Note: "<" indicate concentrations below detection limit.

(e.g. montmorillonite -  $[(Ca,Na)_x(Al,Mg,Fe)_4(Si,Al)_xO_{20}(OH)_4 \cdot nH_2O]$  and illite  $[(K,H_2O)Al_2Si_3AlO_{10}(OH)_2]$  to form (Fyfe et al., 1983). In these complex clays almost any transition metal can substitute for Al, Mg, and Fe, while halogens can be fixed in the hydroxyl sites (Fyfe et al., 1983). Therefore, as long as these clays are present with abundant unweathered minerals, many trace metals will be concentrated in the weathering process (Kronberg et al., 1979). This is shown in the  $<2 \mu m$  size fraction of the varzea soils which adsorbed significant quantities of trace metals, including Y, Rb, Pb, Zn, Cu, Ni, Co, Cr, Ba, V, and Ga (Table 2.10)

Once the primary minerals are eroded the smectite clays will be degraded to the more simple kaolin clays  $[Al_2Si_2O_5(OH)_4]$  with a corresponding decrease in major elements and trace metals (Fyfe et al., 1983). At this advanced stage of weathering, the cation-exchange capacity is minimal and enrichments in the soils will generally be limited to the elements incorporated in refractory minerals such as anatase (Ti) and zircon (Zr). This situation is also consistent with our findings in the Central Amazon where kaolinite dominates as the stable clay phase, and the trace metal contents are typically depleted relative to the soils from the varzea and crustal abundances.

#### 2.4.2 Surface Water Chemistry

The concentration of 50 elements in river water are given for several sample sites in the Rio Negro (Table 2.11), the Rio Solimões (Table 2.12), and forested streams in Carajás (Table 2.13). The 1991 values for Cu, Ni, Zn, and Pb were omitted due to contamination from the acid bottle during the sampling procedure.

These analyses indicate that there is substantial variability among individual sampling sites in all three areas. This is reflected in the large standard deviation values shown in Table (2.14). The greatest variability is shown in the waters from Carajás, where the standard deviation often exceeds the average concentration (e.g. B, P, K, Cu, Br, Mo, Nd). These high standard deviations may partially reflect the differences in location and

time of sampling, as well as the low concentrations (ppb). The least variability is exhibited by the Rio Negro samples

If the chemical composition of Amazonian waters are primarily determined by the geological source and erosional regime, then variations should be observed in water chemistry. This shown in Figure 2.3 which compares surface waters from all three regions. The largest variance exists between the whitewaters of the Rio Solimões and the blackwaters of the Rio Negro. With the exception of Zn and Se, all other elements are consistently found in greater concentrations in the former. These differences are commonly greater than an order of magnitude, and include Mg, Ca, Ti, V, As, Br, and Sr (Table 2.14). This pattern vividly reflects the differences in the metal concentrations in the surface soils.

Unlike the clear differences in chemical composition between the rivers draining the Andes Mountains and those draining the Central Amazonian lowlands, rivers from the forested areas of Carajás are much more variable. While these streams display both the highest concentrations of some elements (Mg, Li, Be, B, I, Se, Zn, Cu, Cr, Sc, Ni, Pb, Mo, and Ag) and lowest concentrations of others (Al, As, Fe, V, Sn, Th, and Zr) the overall chemistry suggests an intermediate composition (Table 2.14).

Aside from differences in concentrations, the heterogeneity of Amazonian waters is also confirmed by the relative proportions of some of the major elements (Ca, K, Mg, and Si). Calcium is the dominant element in the Rio Solimões and represents 52% of the sum of the major cations, followed by silicon at 32%, potassium 8.4%, and magnesium 7.6%. In the Rio Negro, silicon dominates at 65%, potassium 16%, calcium 14%, and magnesium 5%. Similarly, in the forested streams, silicon dominates at 56%, magnesium 20%, calcium 17%, and potassium 7% (Table 2.14). The clear dominance of calcium suggests that the solute-rich waters of the Rio Solimões could be classified as "carbonate waters" (Furch, 1984, pp 186), and are indicative of the carbonate source (mostly limestones) in the Andes Mountains (Stallard and Edmond, 1983). The solute-deficient

TABLE 2.11: CHEMICAL ANALYSIS OF WATERS FROM THE RIO NEGRO (in ug/l)

ELEMENT	M5	M6	M7	M8	M9	N1	N3	N5
Li	< 0.19	< 0.19	< 0.20	< 0.19	< 0.19	< 0.38	< 0.38	< 0.38
Be	< 0.04	< 0.04	< 0.04	< 0.04	< 0.04	< 0.07	< 0.07	< 0.07
B	0.71	0.66	0.60	0.86	0.50	0.94	0.97	1.80
Mg	150.00	140.00	150.00	160.00	170.00	74.00	74.00	110.00
Al	160.00	120.00	190.00	160.00	150.00	220.00	230.00	220.00
Si	2100.00	2100.00	2000.00	1900.00	1900.00	1500.00	1600.00	1700.00
P	8.20	6.60	16.00	8.30	7.80	8.60	< 1.20	< 1.20
K	460.00	430.00	460.00	380.00	400.00	660.00	340.00	580.00
Ca	390.00	440.00	180.00	720.00	550.00	280.00	220.00	350.00
Sc	1.50	1.20	1.60	1.30	1.00	0.30	0.21	0.32
Ti	2.10	< 0.37	< 1.40	< 0.37	< 0.37	0.20	< 0.39	< 0.20
V	< 0.27	< 0.27	< 0.27	< 0.27	< 0.27	0.36	0.32	0.31
Cr	< 0.31	< 0.31	< 0.31	< 0.31	< 0.31	1.30	0.49	2.20
Mn	7.90	11.00	9.50	10.00	10.00	8.90	8.70	11.00
Fe	430.00	420.00	420.00	390.00	370.00	350.00	320.00	380.00
Co	< 0.08	< 0.08	< 0.08	< 0.08	< 0.08	0.34	0.24	0.48
Ni	< 0.32	< 0.32	< 0.32	< 0.32	< 0.32	-----	-----	-----
Cu	< 0.21	< 0.10	< 0.27	< 0.24	< 0.76	-----	-----	-----
Zn	13.00	9.70	10.00	13.00	12.00	-----	-----	-----
As	< 0.04	< 0.04	< 0.04	< 0.04	< 0.14	0.10	0.04	0.07
Se	6.00	1.00	2.00	2.90	1.10	2.80	0.69	1.90
Br	< 0.81	< 0.81	< 0.81	< 0.81	< 0.81	< 2.20	< 0.56	< 0.56
Rb	1.60	1.30	1.20	0.98	0.74	1.40	1.20	1.50
Sr	3.60	2.90	3.20	4.00	4.00	2.50	2.50	3.70
Zr	0.04	< 0.03	< 0.03	< 0.03	< 0.03	0.16	0.13	0.13
Mo	0.09	< 0.03	< 0.09	< 0.03	< 0.03	0.84	0.45	0.46
Ag	< 0.03	< 0.03	< 0.04	< 0.03	< 0.03	0.02	< 0.02	< 0.02
Cd	0.08	0.08	0.08	0.08	0.08	0.19	0.08	0.30
Sn	0.05	0.07	< 0.05	< 0.03	< 0.03	0.75	0.24	0.48
Sb	0.11	< 0.04	< 0.07	< 0.04	< 0.04	0.28	0.07	0.13
I	0.97	1.10	1.10	0.81	0.74	1.00	0.90	1.30
Cs	0.06	< 0.06	< 0.02	< 0.04	< 0.04	< 0.05	< 0.02	< 0.02
Ba	12.00	11.00	10.00	9.00	8.70	6.50	6.80	9.30
La	0.04	0.24	0.31	0.13	0.10	0.33	0.38	0.39
Ce	0.93	0.93	0.78	0.23	0.28	0.84	1.00	1.20
Nd	0.19	0.44	0.15	0.07	0.15	0.23	0.23	0.50
Sm	0.05	0.09	0.05	0.13	0.05	0.04	0.04	0.08
Eu	< 0.04	< 0.04	< 0.04	< 0.04	< 0.04	< 0.02	< 0.02	< 0.02
Tb	< 0.02	< 0.02	< 0.02	< 0.02	< 0.02	< 0.02	< 0.02	< 0.02
Dy	< 0.03	< 0.03	< 0.03	< 0.03	< 0.03	< 0.03	< 0.03	< 0.05
Yb	0.04	< 0.04	< 0.03	< 0.04	< 0.04	< 0.02	< 0.02	< 0.03
Hf	< 0.03	< 0.03	< 0.03	< 0.03	< 0.03	< 0.02	< 0.02	< 0.05
Ta	< 0.02	< 0.02	< 0.02	< 0.02	< 0.02	< 0.02	< 0.02	< 0.02
W	< 0.03	< 0.03	< 0.03	< 0.03	< 0.03	0.17	0.04	0.12
Au	< 0.02	< 0.02	< 0.02	< 0.02	< 0.02	< 0.02	< 0.02	< 0.02
Hg	< 0.21	< 0.21	< 0.21	< 0.21	< 0.21	< 0.09	< 0.12	< 0.09
Pb	0.31	< 0.09	< 0.04	0.07	0.07	-----	-----	-----
Bi	< 0.02	< 0.02	< 0.02	< 0.02	< 0.02	< 0.02	< 0.02	< 0.02
Th	0.11	0.09	0.10	0.09	0.03	0.23	0.24	0.17
U	< 0.02	< 0.03	< 0.02	< 0.02	< 0.02	0.06	0.03	0.07

Note: "&lt;" indicate concentrations below detection limit

TABLE 2.12 CHEMICAL ANALYSIS OF WATERS FROM THE RIO SOLIMÕES (in µg l<sup>-1</sup>)

ELEMENT	M11	M12	S1	S2	S3	S4	S5	S6
Li	0.67	0.83 <	0.38	1.30 <	0.38 <	0.38 <	0.38	0.38
Be	< 0.04	0.04	0.09 <	0.07 <	0.07 <	0.07 <	0.07	0.07
B	2.90	2.50	3.00	3.80	3.60	3.80	2.40	3.80
Mg	1200.00	1200.00	1200.00	1400.00	1300.00	1300.00	1100.00	1400.00
Al	81.00	306.00	1200.00	2100.00	1000.00	1400.00	860.00	1200.00
Si	4200.00	4500.00	5700.00	6900.00	5200.00	5900.00	5000.00	5500.00
P	39.00	42.00	68.00	84.00	15.00	75.00	21.00	45.00
K	1000.00	1000.00	1200.00	1600.00	1600.00	1600.00	1600.00	1600.00
Ca	7300.00	7500.00	7700.00	8600.00	13000.00	8900.00	8100.00	9500.00
Sc	2.70	3.00	0.93	1.10	0.91	0.77	0.64	0.88
Ti	< 0.37	1.40	6.60	13.00	8.00	12.00	6.60	11.00
V	< 0.27	0.90	3.40	3.80	2.50	3.50	2.60	3.20
Cr	< 0.31	0.31	1.60	2.20	2.90	2.10	1.90	2.50
Mn	51.00	35.00	47.00	75.00	41.00	53.00	35.00	64.00
Fe	770.00	1200.00	2000.00	2800.00	1600.00	2000.00	1600.00	2400.00
Co	0.16	0.55	0.84	1.30	0.74	1.00	2.20	1.20
Ni	< 0.32	1.10	---	---	---	---	---	---
Cu	1.80	3.00	---	---	---	---	---	---
Zn	6.50	7.70	---	---	---	---	---	---
As	< 0.04	0.37	0.72	1.20	1.00	0.93	0.97	1.10
Se	3.30	0.35	0.56	0.30 <	0.26	0.56	0.56	0.46
Br	< 0.81	0.81 <	0.56	6.90	32.00	12.00	13.00	16.00
Rb	1.50	1.50	2.60	3.40	2.70	2.80	2.60	3.00
Sr	30.00	31.00	43.00	51.00	51.00	47.00	43.00	48.00
Zr	0.04	0.07	0.24	0.14	0.22	0.32	0.25	0.28
Mo	0.07	0.09	0.68	0.62	0.77	0.14	0.78	0.44
Ag	< 0.03	0.03	0.02	0.03 <	0.02 <	0.02 <	0.05 <	0.02
Cd	0.16	0.08 <	0.08	0.36 <	0.08	0.08	2.30	0.08
Sn	< 0.03	0.03	0.20	0.42	0.34	0.98	3.40	0.56
Sb	0.19	0.04	0.07	0.25 <	0.02	0.14	0.26	0.20
I	0.99	0.50	0.75	1.70	1.40	1.30	1.20	1.40
Cs	0.02	0.02	0.14	0.24	0.14	0.12	0.21	0.12
Ba	30.00	33.00	39.00	45.70	38.00	40.00	36.00	46.00
La	0.06	0.27	1.20	2.20	1.20	1.60	0.93	0.18
Ce	0.40	1.10	3.30	5.10	2.70	3.70	2.20	3.30
Nd	0.24	0.32	1.50	2.40	1.10	1.50	1.10	1.40
Sm	0.05	0.05	0.08	0.60	0.12	0.36	0.16	0.50
Eu	< 0.04	0.05	0.05	0.07	0.04	0.06	0.05	0.06
Tb	< 0.02	0.02	0.04	0.06	0.04 <	0.02	0.03 <	0.02
Dy	0.05	0.09	0.23	0.26	0.13	0.17	0.14	0.17
Yb	0.07	0.14	0.06	0.14	0.04	0.08	0.05	0.04
Hf	< 0.03 <	0.03 <	0.02 <	0.02 <	0.02 <	0.02 <	0.02 <	0.02
Ta	< 0.02 <	0.02 <	0.02 <	0.02 <	0.02	0.02 <	0.02	0.02
W	< 0.03 <	0.03	0.07	0.11	0.05	0.15	0.28	0.10
Au	< 0.02 <	0.02 <	0.02 <	0.02 <	0.02 <	0.02 <	0.02 <	0.02
Hg	< 0.21 <	0.21 <	0.09 <	0.09 <	0.09 <	0.09 <	0.09 <	0.09
Pb	0.53	0.74	---	---	---	---	---	---
Bi	0.03	0.02	0.05	0.04 <	0.02	0.06	0.20	0.06
Th	< 0.02	0.04	0.29	0.34	0.28	0.40	0.25	0.38
U	0.03	0.11	0.14	0.15	0.11	0.17	0.09	0.13

Note: "&lt;" indicate concentrations below detection limit



TABLE 2.13 CHEMICAL ANALYSIS OF WATERS FROM FOREST DAREAN CARAIAS (p. 31)

ELEMENT	C4	K2	K4	K5	K7	K9	K10	K12
Li	< 0.19	< 1.30	< 1.30	< 1.30	< 2.70	< 1.30	< 1.30	< 1.30
Be	< 0.04	0.23	0.23	0.23	0.23	0.23	0.23	0.23
B	2.00	240.00	22.00	3.40	200.00	75.00	1.80	280.00
Mg	1600.00	1900.00	2400.00	3200.00	1400.00	1000.00	2400.00	1500.00
Al	29.00	64.00	79.00	100.00	60.00	60.00	120.00	320.70
Si	4400.00	7500.00	7800.00	7400.00	3000.00	2400.00	7500.00	2800.00
P	45.00	< 3.60	< 3.60	< 3.60	< 3.60	< 3.60	< 3.60	< 3.60
K	760.00	2100.00	1200.00	1200.00	12.00	12.00	12.00	12.00
Ca	1600.00	2100.00	2400.00	3200.00	1000.00	21.00	2200.00	1000.00
Sc	3.10	17.00	16.00	14.00	4.70	2.50	13.00	4.00
Ti	1.90	< 3.00	< 3.00	< 3.00	< 3.00	< 3.00	< 3.00	< 3.00
V	< 0.27	< 0.27	< 0.27	< 0.27	< 0.27	< 0.27	< 0.27	< 0.27
Cr	0.31	12.00	16.00	12.00	16.00	16.00	15.00	26.00
Mn	13.00	32.00	45.00	24.00	15.00	20.00	49.00	52.00
Fe	360.00	350.00	300.00	320.00	78.00	210.00	720.00	310.00
Co	0.23	0.61	0.10	0.33	0.27	0.10	0.32	1.30
Ni	0.32	1.40	2.00	0.25	0.25	1.10	2.90	2.40
Cu	2.60	< 1.00	< 1.00	< 1.00	< 1.00	< 1.00	< 1.00	< 21.00
Zn	8.60	31.00	5.50	120.00	51.00	180.00	84.00	10.00
As	< 0.04	< 0.02	< 0.02	< 0.02	< 0.02	< 0.02	< 0.02	< 0.02
Se	4.20	< 2.80	< 2.80	< 2.80	< 2.80	< 2.80	< 2.80	< 2.80
Br	1.90	31.00	1.50	1.50	1.50	1.50	1.50	1.50
Rb	1.10	2.60	2.60	3.50	1.50	2.50	2.30	1.50
Sr	3.10	9.40	9.70	28.00	4.10	3.20	11.00	5.10
Zr	0.04	< 0.07	< 0.07	< 0.07	< 0.07	< 0.07	< 0.07	< 0.07
Mo	0.30	9.20	1.10	46.00	22.00	12.00	1.30	0.95
Ag	0.05	< 0.09	< 0.09	< 0.09	< 0.09	< 0.09	< 0.09	< 0.09
Cd	0.08	< 0.07	< 0.07	< 0.11	< 0.38	< 0.17	< 0.07	< 0.07
Sn	0.05	< 0.08	< 0.08	< 0.08	< 0.08	< 0.08	< 0.08	< 0.08
Sb	< 0.04	< 0.10	< 0.10	< 0.10	< 0.10	< 0.10	< 0.10	< 0.20
I	1.20	5.00	6.40	6.00	2.20	2.20	3.90	1.90
Cs	0.03	0.06	0.06	0.06	0.06	0.06	0.06	0.06
Ba	9.10	62.00	28.00	47.00	19.00	29.00	74.00	33.00
La	0.16	1.70	0.49	0.45	0.21	0.51	0.98	1.90
Ce	0.28	4.30	3.50	3.40	4.10	4.40	4.40	7.30
Nd	0.08	0.72	0.28	0.34	0.31	0.08	0.27	1.70
Sm	0.05	0.47	0.20	0.08	0.08	0.08	0.08	0.28
Eu	< 0.04	0.03	0.06	0.04	0.03	0.03	0.04	0.13
Tb	< 0.02	0.03	0.02	0.05	0.02	0.02	0.03	0.03
Dy	< 0.03	0.28	0.07	0.07	0.07	0.07	0.07	0.27
Tb	< 0.03	0.10	0.08	0.08	0.08	0.03	0.08	0.08
Hf	< 0.03	0.03	0.03	0.03	0.06	0.03	0.03	0.03
Ta	< 0.02	0.04	0.04	0.04	0.04	0.04	0.04	0.04
W	< 0.03	0.05	0.08	0.04	0.11	0.09	0.06	0.06
Au	< 0.02	0.08	0.08	0.08	0.08	0.08	0.08	0.08
Hg	< 0.21	0.25	0.25	0.25	0.25	0.25	0.25	0.25
Pb	0.05	13.00	32.00	19.00	23.00	16.00	19.00	10.00
Bi	< 0.02	0.04	0.04	0.04	0.04	0.04	0.06	0.04
Th	< 0.02	0.06	0.06	0.03	0.03	0.03	0.03	0.06
U	< 0.02	0.07	0.04	0.03	0.03	0.03	0.04	0.10

Note: "&lt;" indicate concentrations below detection limit

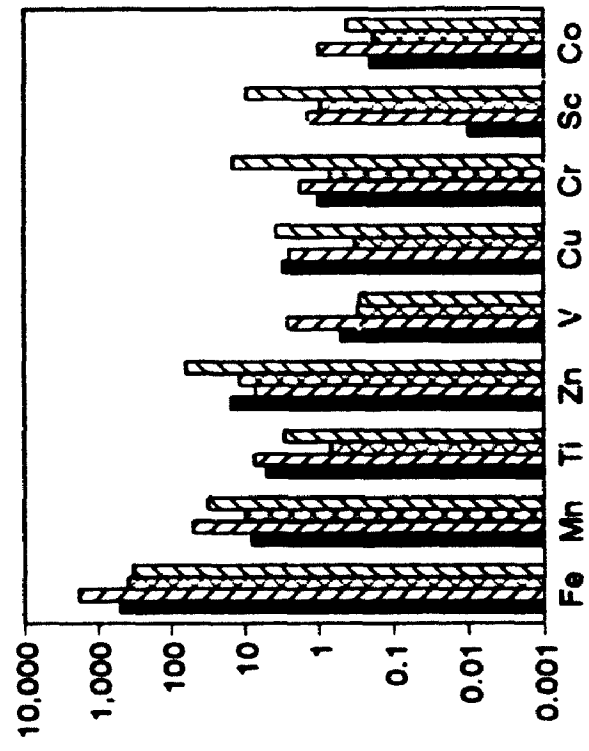
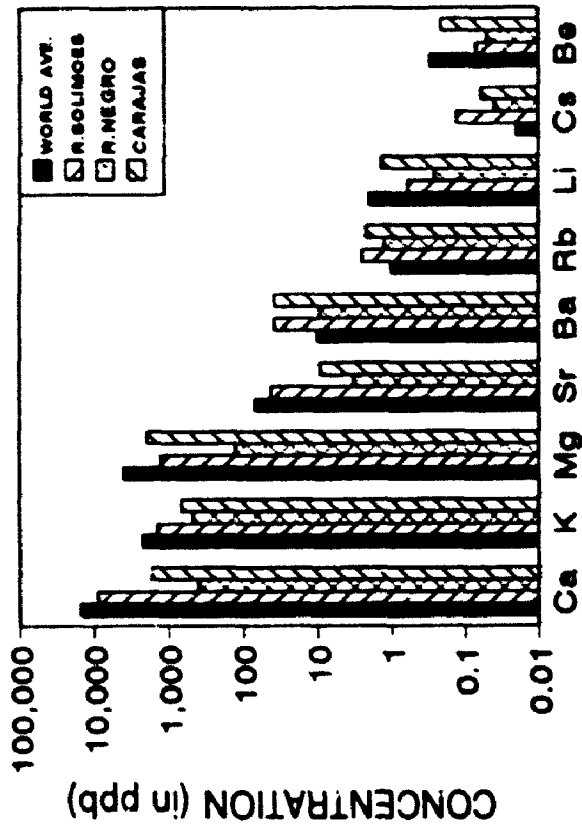
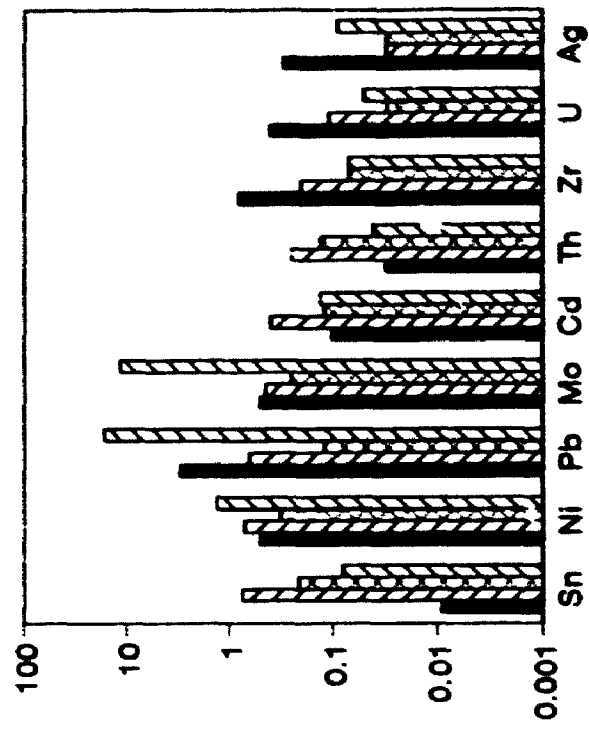
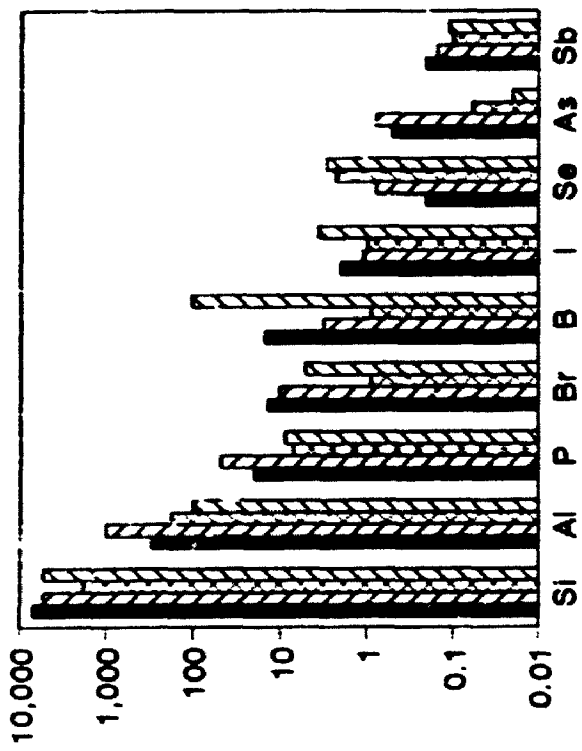
TABLE 2.14. COMPARISON OF DISSOLVED METAL CONCENTRATIONS IN AMAZONIAN RIVERS  
 TO WORLD RIVER AVERAGE: (in ug/l)

	WORLD AVERAGE:		RIO NEGRO		RIO SOLIMÕES		CARAJAS	
	AVE.	S.D.	AVE.	S.D.	AVE.	S.D.	AVE.	S.D.
Li	2.00	<	0.26	0.15	0.59	0.38	1.34	0.82
Bc	0.30	<	0.05	0.03	0.07	0.03	0.21	0.06
B	15.00		0.88	0.38	3.23	0.56	103.03	110.24
Mg	4690.00		126.50	35.45	1262.50	99.22	1925.00	660.97
Al	300.00		181.25	37.23	1017.63	591.78	99.00	88.07
Sa	7000.00		1850.00	212.13	5362.50	793.63	5350.00	2266.05
P	20.00	<	7.24	4.88	48.63	23.36	8.78	11.22
K	2300.00		463.75	99.74	1400.00	264.51	663.50	694.58
Ca	15000.00		391.25	167.22	8825.00	1725.36	1690.13	932.62
Sc	0.01		0.93	0.53	1.37	0.87	9.25	5.85
Ti	5.00	<	0.68	0.62	7.37	4.37	2.86	1.42
V	0.50	<	0.29	0.14	2.52	1.20	0.27	0.13
Cr	1.00	<	0.69	0.63	1.73	0.89	14.16	6.64
Mn	8.00		9.63	1.03	50.13	13.09	31.25	14.63
Fe	500.00		385.00	35.71	1796.25	606.30	331.00	170.55
Co	0.20	<	0.18	0.15	1.00	0.57	0.41	0.37
Ni	0.50	<	0.32	0.16	0.71	0.39	1.33	1.01
Cu	3.00	<	0.32	0.24	2.40	0.60	3.70	5.45
Zn	15.00		11.54	1.43	7.10	0.60	61.26	58.73
As	0.50	<	0.06	0.04	0.79	0.37	0.02	0.01
Se	0.20		2.30	1.59	0.79	0.93	2.98	1.51
Br	14.00	<	0.92	0.59	10.26	9.96	5.24	8.05
Rb	1.00		1.24	0.26	2.51	0.63	2.20	0.73
Sr	70.00		3.30	0.58	43.00	7.76	9.20	7.69
Zr	0.80	<	0.07	0.06	0.20	0.09	0.07	0.03
Mo	0.50	<	0.25	0.26	0.45	0.29	11.61	14.43
Ag	0.30	<	0.03	0.01	0.03	0.02	0.09	0.04
Cd	0.10	<	0.12	0.08	0.40	0.67	0.13	0.10
Sn	0.009	<	0.21	0.24	0.75	1.04	0.08	0.04
Sb	0.20		0.10	0.08	0.15	0.09	0.11	0.06
I	2.00		0.99	0.17	1.16	0.36	3.60	1.88
Cs	0.02	<	0.04	0.02	0.13	0.07	0.06	0.03
Ba	10.00		9.16	1.77	38.38	5.12	37.64	20.48
La	0.10		0.24	0.13	0.96	0.70	0.80	0.62
Ce	0.20		0.77	0.32	2.73	1.40	3.96	1.79
Nd	0.15		0.25	0.14	1.20	0.65	0.47	0.49
Sm	0.06		0.07	0.03	0.24	0.20	0.17	0.14
Eu	0.006	<	0.03	0.02	0.05	0.01	0.05	0.03
Tb	0.003	<	0.02	0.01	0.03	0.02	0.03	0.01
Dy	0.005	<	0.03	0.02	0.16	0.06	0.12	0.09
Yb	0.01	<	0.03	0.02	0.68	0.04	0.07	0.04
Hf	0.01	<	0.03	0.02	0.02	0.01	0.03	0.02
Ta	0.002	<	0.02	0.01	0.02	0.01	0.04	0.02
W	0.03	<	0.06	0.05	0.10	0.08	0.07	0.03
Au	0.002	<	0.02	0.01	0.02	0.01	0.07	0.04
Hg	0.10	<	0.17	0.09	0.12	0.07	0.25	0.12
Pb	3.00	<	0.12	0.10	0.64	0.11	16.51	8.81
Bi	0.02	<	0.02	0.01	0.06	0.06	0.04	0.02
Th	0.03		0.13	0.07	0.25	0.14	0.04	0.02
U	0.50	<	0.03	0.02	0.11	0.04	0.05	0.03
TDS	29174		3454		198%		10392	

Note: world average from Bowen (1979)

S.D. = standard deviation TDS = total dissolved inorganic solids

Figure 2.3: Comparison of dissolved metal concentrations in surface waters of the Rio Solimões, the Rio Negro, and forested streams in Carajás with world river average



CONCENTRATION (in ppb)

waters of the Rio Negro are characterized by a completely different proportion of major elements. These waters show an extremely high Si to cation ratio (Stallard and Edmond, 1983; Berner and Berner, 1987) which is indicative of the podsols in the Central Amazon, and a greater proportion of K to those of the alkaline earth metals Ca and Mg, suggesting an alkali dominance (Furch, 1984). Lastly, the forested streams in the Carajás region are once again represented by an intermediate composition.

To evaluate the magnitude of the individual elemental concentrations in all three regions, a comparison with the world rivers average (Bowen, 1979) was made. In Table (2.14), the total dissolved inorganic solids (TDS), not including Na, Cl, and S, indicate that all of the Amazonian waters studied are, as a whole, below the world average. The most solute-rich waters of the Rio Solimões contain 68% (of the TDS) of the world average, the forested streams 36%, while the most solute-deficient waters of the Rio Negro only reach 12% of the world average.

To determine the individual status of each element with respect to world river average (WRA), the data (in Table 2.14) have been divided into the following categories (Table 2.15):

sd = strongly depleted (<100%WRA)  
 d = depleted (<20-100%WRA)  
 se = strongly enriched (>100%WRA)  
 e = enriched (>20-100%WRA)  
 s = similar ( $\pm 20\%$ WRA)

The Rio Solimões is shown to have the greatest number of elements with a similar to strongly enriched status (20), followed by the forest streams (18), and lastly the Rio Negro (10). These results reinforce our other findings which indicate that the Rio Solimões is the most solute-rich river studied, while the Rio Negro is extremely solute-deficient when compared on a global basis.



## 2.5 Discussion

Similarities between the major cation and trace metal levels in the soil samples, and the dissolved metal concentrations in surface waters flowing through the varzea, the Central Amazon, and the Shield, suggest that the rivers are in chemical equilibrium with their drainage basins. Unweathered minerals in the Andes and metal-rich clays in the varzea contribute to the solute-rich waters of the Rio Solimões. This is contrasted by the solute-deficient Rio Negro which drains the highly weathered lateritic and podsolitic terrains of the Central Amazon. The composition of the soils and waters in the Shield indicates an intermediate composition.

These observations suggest that we should be able to classify the chemical composition of rivers according to the chemistry and mineralogy of the soils through which they flow. While previous work has demonstrated a relationship between geology and the chemical composition of Amazonian rivers based on a few cations (Stallard and Edmond, 1983) and trace metals (Furch, 1984), our research extends this relationship for 50 elements.

These findings have profound implications for using water chemistry as an indicator of the agricultural and mineral potential of a region. A comparison of three key macronutrients and the total dissolved inorganic solids (TDS) of several great rivers of the world speak eloquently about the state of the soils (Table 2.16). The Danube, Mississippi, Yangtze, and Nile river systems pass through younger soils that are enriched with rock-forming minerals. Since plants require a wide range of macronutrients and micronutrients, their solute-rich waters indicate a high capacity to support bioproductivity. In contrast, the extreme chemical poverty exhibited by the Rio Negro, and the inability of the lateritic soils to support agricultural activity (Leonardos et al., 1987) is probably the reason why historically this region has never been overpopulated by humans (Fyfe, 1989). Therefore, using river composition as an agricultural indicator would be a very efficient way of assuring soil potential prior to massive development projects.

**TABLE 2.16: COMPARISON OF DISSOLVED SOLUTES IN  
PRINCIPAL WORLD RIVERS (in ug/L)**

	Ca	Mg	K	TDS
Danube	49.0	9.0	1.0	307.0
Mississippi	39.0	10.7	2.8	265.0
Yangtze	45.0	6.4	1.2	232.0
Nile	25.0	7.0	4.0	225.0
Lower Negro	0.4	0.1	0.5	3.4

Note: world river values from (Berner and Berner, 1987).



Knowing the chemical composition of a river system may also be of use in determining the mineral potential of a region. The high concentration of a number of metals (such as Zn, Cu, Cr, Ni, Pb, and Mo) in the waters draining Carajás (relative to Amazonian rivers and world river average) confirms the presence of one of the greatest mining areas of the modern world. While the high aqueous concentration of some of these metals may be associated with local mining activity, many of these rivers drain completely forested areas with no anthropogenic influence. Under these conditions, river chemistry may be useful in mineral exploration.

## CHAPTER 3

### THE IMPACT OF MICROBIAL METAL SORPTION AND BIOMINERALIZATION ON AMAZONIAN RIVER CHEMISTRY

#### 3.1 Introduction

Many of the chemical processes occurring within the hydrosphere have been shown to be biologically mediated. Organisms are continuously undergoing chemical exchanges with their aqueous environment, involving the uptake and excretion of various elements. Although all forms of life possess some characteristics that make them biogeochemically important, much of the focus today is being directed towards the role of microorganisms in the cycling of elements.

The significance of microorganisms, such as bacteria and algae, arises from their ability to live in a variety of habitats, many of which are devoid of higher organisms. Microorganisms have been isolated from hostile environments such as hypersaline waters (Steinhorn and Gat, 1983), low pH-hydrothermal waters (Mann et al., 1987), and acid mine effluents (Mann et al., 1989)

Within most freshwater systems, the typical concentration of dissolved metals is extremely low. Microorganisms, however, possess the ability to adsorb and concentrate metallic ions from solution. Experimental work by Beveridge (1978), Beveridge and Murray (1976), Hoyle and Beveridge (1983), and Mullen et al., (1989) have demonstrated that substantial quantities of several metals can be bound and accumulated by bacterial cells at their surfaces. Many transition metals showed extremely high affinities for the cell-wall fabric (e.g.  $U^{+4}$ ,  $Zr^{+4}$ ,  $Hf^{+4}$ ,  $Fe^{+3}$ ,  $Pd^{+2}$ ,  $Ru^{+3}$ , and  $In^{+3}$ ), and have proven suitable as contrasting agents for electron microscopy (Beveridge, 1978).

The sorption and immobilization of dissolved metals have also been documented in both filamentous and unicellular algae. In a study of mine tailing ponds in Elliot Lake, Timmins, and Sudbury, filamentous algae were shown to concentrate a wide variety of

metals by over  $10^2$  times their natural aqueous concentration with Fe, Co, and Zr up to  $10^6$  (Mann and Fyfe, 1988). Even elements with exceedingly low dissolved concentrations in rivers, such as uranium (global river average for U,  $0.6 \mu\text{g/L}$ ) were shown to be concentrated over  $10^3$  times (Mann and Fyfe, 1988).

The importance of algae in sequestering dissolved metals is manifested by unicellular algae, such as diatoms. Diatoms are commonly the most abundant freshwater eucaryotic microorganisms, and the development of large populations is invariably accompanied by a marked decline in the amount of dissolved silicon from the waters in rivers (Lack, 1971) and lakes (Schelske and Stoermer, 1971).

Biologically mediated processes can also have profound effects on the precipitation of mineral phases. Through the process of biomineralization, microorganisms are able to form mineralized deposits from several of the elements taken out of solution. There appears to exist two different processes of mineral formation (Lowenstam, 1981). The first process is characterized by the absence of any regulated control over mineral precipitation (Simkiss, 1986). Lowenstam (1981, pp. 1126) refers to this process as "biologically induced mineralization"; a process involving bulk intercellular and/or extracellular mineral formation, without the formation of organic matrices. Biominerals are commonly generated as secondary events from interactions between the activity of the organism and its surrounding environment (S. Mann, 1986), whereby minor perturbations such as the introduction of biologically produced metabolic end products (such as  $\text{OH}^-$ ,  $\text{CO}_2$ ,  $\text{H}^+$ , and  $\text{NH}_3$ ), the release of cations by the cell, or the development of a charged surface, such as a cell wall, can all induce the nucleation of minerals (Lowenstam and Weiner, 1989).

In bacteria, the fixation of metallic ions arises through interaction with the anionic surfaces of the cell wall (Beveridge, 1981, Beveridge and Fyfe, 1985). Constituent carboxyl and phosphoryl groups interact passively with available cations and have been shown to be major sites for metal deposition (Beveridge and Murray, 1980, Ferris and

Beveridge, 1984) In addition, some cells may have an extracellular sheath or capsule comprised of acidic polysaccharides whose molecular components are similarly reactive and consequently accumulate metals around the cell (Ferris and Beveridge, 1985). Once bound to the bacteria, the metals seem to serve as nucleation sites for the formation and growth of authigenic mineral phases. In the laboratory, bacterial cells promote phosphate mineralization in simulations of sediment diagenesis (Beveridge et al., 1983) and the precipitation of both metal sulphides and complex (Fe, Al) - silicate polymorphs in natural environments (Ferris et al., 1987).

The second process of biomineralization is characterized by the development of an organic framework or mold into which various ions are actively introduced. This process has been described by S. Mann (1983, pp. 126) as "biologically controlled mineralization". During biologically controlled mineralization an area is sealed off from the environment allowing specific ions of choice to diffuse into the space delineated for mineral precipitation. The cell therefore, creates an internal environment completely independent of the external conditions. It is under these "ideal" conditions that mineralization may occur (Simkiss, 1986).

Diatoms are examples of biologically-controlled mineralizers that remove silicon to fulfill physiological functions such as DNA synthesis and to form their siliceous skeletons (Sullivan and Volcani, 1981). The skeleton (also referred to as the frustule) is comprised of the mineral opal, an amorphous variety of silica, which at surface temperatures (25°C) has a solubility of approximately 120 ppm (Kastner et al., 1977). Since freshwater environments are usually undersaturated with respect to opaline silica, the diatoms must actively take-up dissolved silicon, the undissociated monomeric form of silicic acid,  $\text{Si(OH)}_4$ .

Upon extraction, diatoms deposit the silicic acid intracellularly within a deposition vesicle where supersaturated solutions of dissolved silicon are attained. In these supersaturated solutions, dissolved silicon polymerizes forming first oligomers and later

higher molecular weight polymers through a combination of silanol (-Si-OH) groups (Williams et al., 1985). The actual mechanisms for silica polymerization within the deposition vesicle is still largely speculative, however, it has been suggested that the structural components of the vesicle, such as the silicalemma, play a critical role in the mineralization process (Volcani, 1983). This specialized membrane is composed of several proteins which are believed to serve as templates for silica mineralization by presenting a layer of hydroxyl groups whose surfaces could hydrogen bond to the hydroxyl groups of the silicic acid molecules (Volcani, 1983).

During the mineralization process, the vesicles arrange themselves into a specific pattern that in essence acts as the molding for the future skeleton. Upon completion, the mature cell wall of a diatom is comprised of the mineral phase, the silicalemma, and an exterior organic casing (Lowenstam and Weiner, 1989). The organic casing is believed to be actively involved in protecting the mineralized fraction from dissolution (Lowenstam and Weiner, 1989) since diatom frustules dissolve more rapidly from killed cells than from live cells (Lewin, 1961).

The freshwater habitat of bacteria and algae include both planktonic and benthic species. Planktonic microbes are found freely floating in the open water column, whereas benthic communities in the littoral zone of lakes or rivers must exhibit a strong adhesion to substrates to avoid detachment due to wave energy (Hoagland and Peterson, 1990) or high flow rates. The benthic communities can be classified according to their substrata, thus episammic, epiphytic, epizoic, and epilithic communities may be distinguished by growing on various sediment, plant, animal, or mineral surfaces, respectively.

The ability of microorganisms to undergo chemical exchanges with their aqueous environment, involving both the sorption and excretion of various elements, has been overlooked as an important factor in determining the chemistry of Amazonian rivers. In view of the general paucity of information on microbial activity in these rivers, this chapter

was designed to investigate the role of microorganisms in various Amazonian river systems

### 3.2 Sampling and Analytical Methodology

In the Manaus area, water, filamentous microorganisms (later identified as filamentous algae), and sediment samples were collected upstream of Manaus on the Rio Negro (and some of its tributaries) and on the Rio Solimões during early July/90 and mid-June/91 sampling periods. Submerged wood samples coated by gelatinous biofilms were collected from sites M8 and M14, and several submerged leaves and rocks, also covered by biofilms, were taken randomly from both rivers. In the Carajás area, water, microbial, and sediment samples were collected randomly from a variety of streams. Some of the streams drained forested areas, while others drained areas having undergone almost complete deforestation.

Large populations of filamentous algae were gathered from below the water surface by hand using surgical gloves to avoid contamination. The microorganisms were washed in the natural river water to remove loose detritus, placed in polyethylene bags, and drained of excess water. Sediment was collected from the river bottom at depths of approximately 5 m below the water surface, and then placed in polyethylene bags and allowed to air dry. Samples of wood, leaves, and rocks were similarly gathered from below the water surface by hand, again, using surgical gloves, dried in the sun, and stored as above. Immediately after removal from the water, small portions of microorganisms and sediment were also placed into 5 mL metal-free plastic tubes, containing aqueous 2.0% (v/v) glutaraldehyde, a fixative for electron microscopy (Hayat, 1981).

In the laboratory, sections of wood were cut away from the outer surface for observation by scanning electron microscopy (SEM). Random samples of leaves and rocks, selected from the sealed polyethylene specimen bags, were also selected for SEM observation. To determine the presence of planktonic diatoms, water samples (taken

midstream from all sample sites) were pressure filtered through 0.2  $\mu\text{m}$  Nuclepore membranes (Costar Corp). The membranes which contained suspended materials were subsequently allowed to air dry. In preparation for analysis, all samples were mounted on specimen stubs with conductive carbon paint and sputtered with gold for 3 minutes. Samples were examined with an SEM model ISI DS 130, coupled with a Tracor Northern EDX Analyzer, model TN 5500.

Prior to analysis, the filamentous algae were placed in 500 mL Nalgene bottles, half filled with deionized water and then submerged in a Crest ultrasonic bath for 30 minutes (on "heavy cleaning" setting) to remove excess sediment particles. Samples were then weighed wet and digested in pure nitric acid at elevated pressures in a Teflon pressure vessel. Concurrently, a percent moisture was determined so that all data could be reported relative to dry weight. After digestion, the samples were diluted to appropriate volumes. Multi-element analyses of the filamentous algae were performed on the aqueous digestates by ICP-MS.

Filamentous algae and sediment samples were prepared for thin-sectioning by washing in a solution of 0.05 M N-2-hydroxyethylpiperazine-N'-2-ethane-sulfonic acid (HEPES) buffer (Sigma Chem. Co.) adjusted to pH 7.2 to remove the glutaraldehyde, dehydrating through an acetone series, and embedding in epoxy resin (EPON 812, CanEM). Thin sections, ranging in thickness from approximately 50 nm to 130 nm, were obtained with a Reichert-Jung Ultracut E ultramicrotome, and mounted on Formvar carbon-coated copper grids. To increase the electron contrast of cytoplasmic material inside intact cells, some thin sections were stained with uranyl acetate and lead citrate before imaging in the electron microscope. Whole mounts of sediment were prepared by washing random samples (several  $\mu\text{g}$ ) in HEPES, and pipetting approximately 10  $\mu\text{L}$  of solution onto carbon-coated copper grids, which were then allowed to air dry.

Electron microscopy was done at 100 KeV in a Philips EM400T TEM/STEM (transmission electron microscope/scanning transmission electron microscope) which was

equipped with a Link Analytical energy dispersive X-ray spectrometer EDS analysis was conducted using electron beam spot sizes of 200 nm or less with a beam current of 50 nA, and spectra were obtained by collecting counts for 100 s (live-time) Crystalline mineral phases were determined using SAED (selected area electron diffraction) with a camera length of 800 mm Amorphous phases were identified by EDS spot analyses run with the Link quantification program to determine stoichiometric ratios

### **3.3 Results**

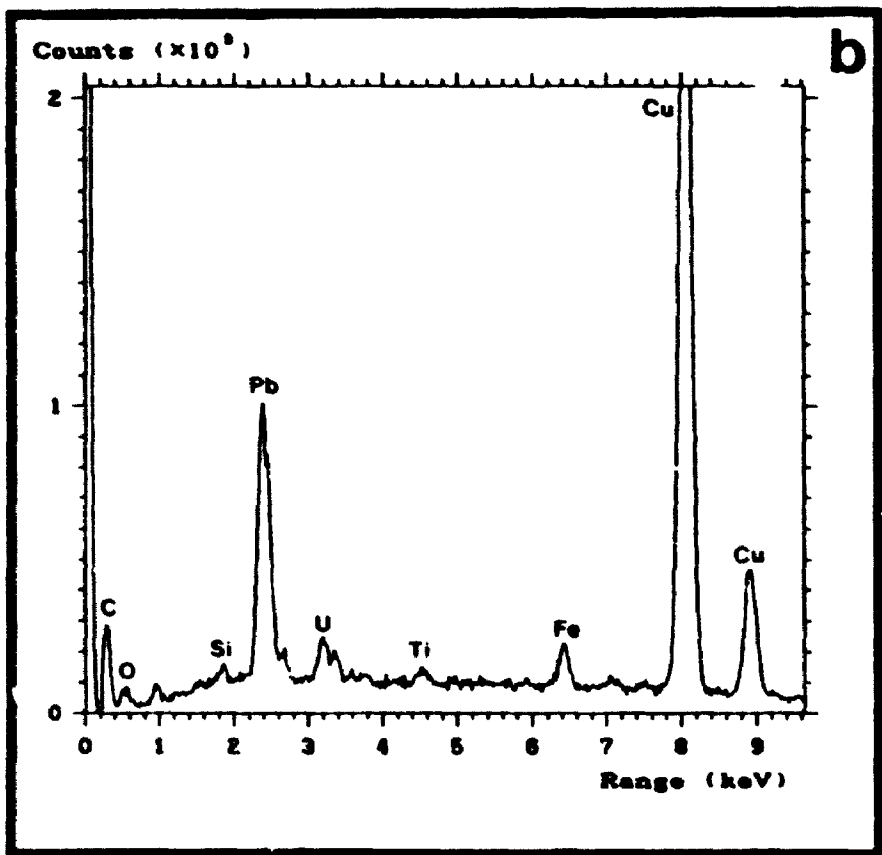
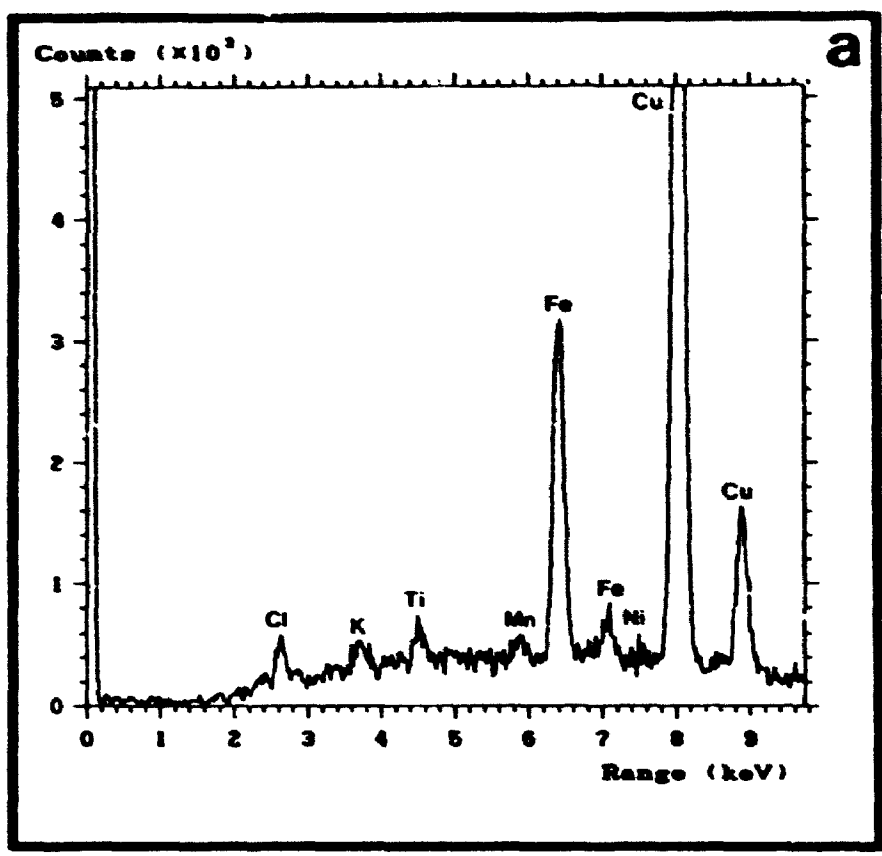
#### **3.3.1 Metal Sorption and Biomineralization by Bacteria**

TEM analyses indicated that the filamentous algae and sediment samples (from both river systems) served as substrata for epiphytic and epibenthic bacterial communities. The abundance of these benthic microorganisms suggested that any available surface would serve as a solid interface for their growth. These surfaces provide desirable locations for the growth of microorganisms due to the high concentration of organics and inorganics that accumulate at interfaces (Costerton et al., 1981).

Epiphytic bacterial cells taken from the waters of the Rio Solimões showed abundant mineralization, ranging from Fe-rich capsules to fine-grained (<500 nm) authigenic mineral precipitates. Many of the cells exhibited capsules which varied greatly in their proportions, some encapsulated only an individual cell (Plate 3.1a), while other microorganisms produced so much extracellular material that a number of cells became encapsulated to produce a so-called "microcolony" (Costerton et al., 1981, Ferris and Beveridge, 1985). EDS analyses indicated that these capsules had sequestered significant amounts of iron from solution, with lesser amounts of K, Ti, Mn, and Ni (Figure 3.1a). The accumulation of trace metals such as Mn and Ni, which are found in low aqueous concentrations in the Rio Solimões (Table 2.14), suggests a selective accumulation by the cell wall. Conversely, calcium, which is the most abundant dissolved species, is not complexed in detectable amounts.



**Figure 3 1** EDS spectra of (a) mineralized capsule (unstained) of an epiphytic bacterial cell from the Rio Solimões and (b) unmineralized capsule (stained) of an epiphytic bacterial cell from the Rio Negro. Cu peaks are from the supporting grid, the Cl peak is due to contamination from the EPON, and the U and Pb peaks are due to staining



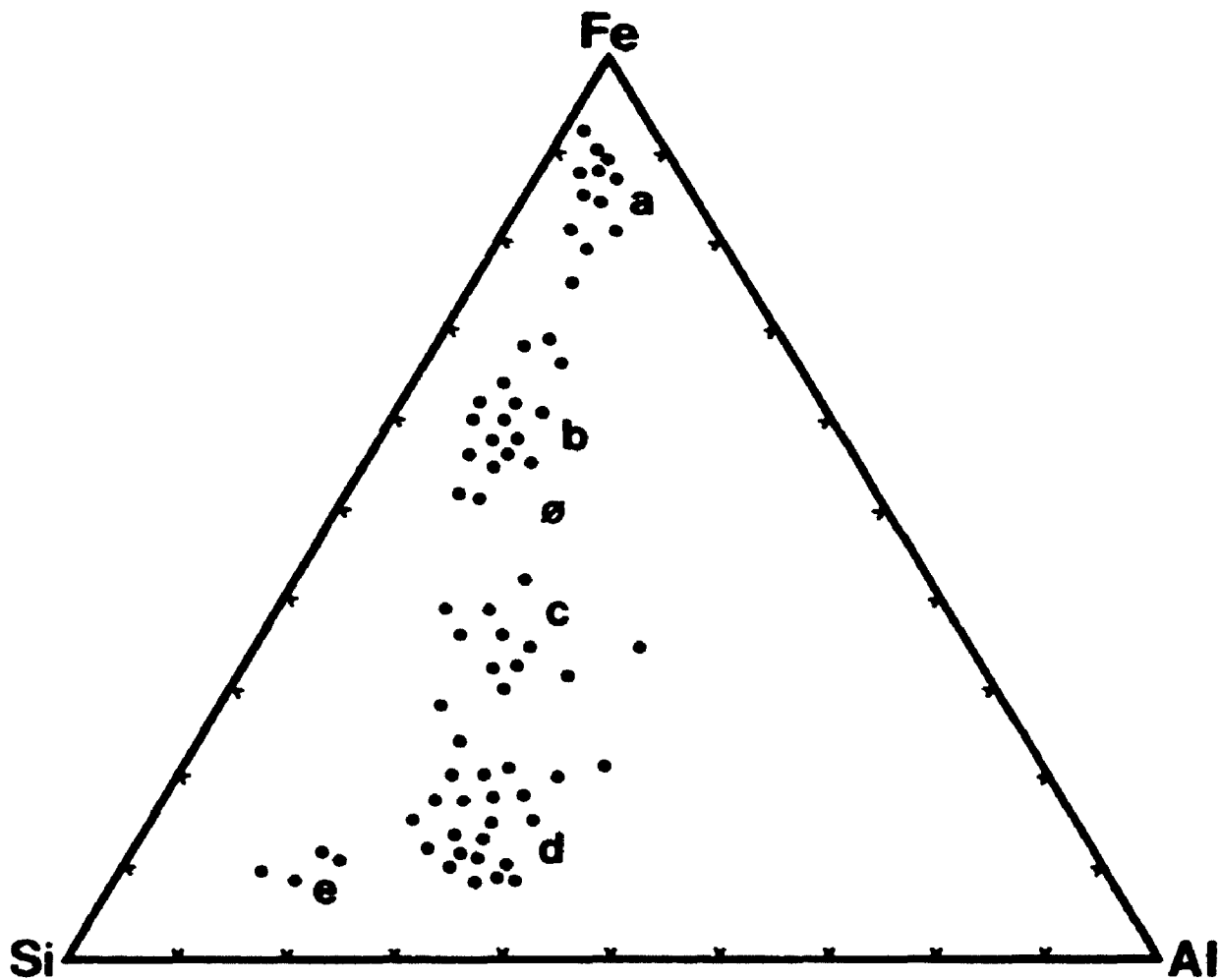
In the same samples, other cells showed the nucleation of small (approximately 100 nm in diameter), dense aggregates on the outer surfaces of the capsule (Plates 3.1b and 3.2a). Predominantly Fe-rich (Figure 3.2), these aggregates suggested an early stage of mineralization within the metal-loaded capsule, as represented in Plate 3.1a

Progressive mineralization, leading to the partial (Plates 3.2b and 3.3a) and complete encrustation (Plate 3.3b) of some bacterial cells was also observed. The authigenic grains exhibited a wide range of morphologies, ranging from amorphous "gel-like" to crystalline structures. The most abundant mineral phase associated with the epiphytic bacteria was a complex (Fe,Al) - silicate with a composition characteristic of a chamositic clay  $[(Fe_xAl)(Si_3Al)O_{10}(OH)_x]$ . EDS analyses indicated that the gel-like areas were typically Fe-rich precursors of the clay mineral, while the crystalline phases were increasingly siliceous in composition. Intermediate compositions, corresponding to the transition from a low-order state to a high-order state, were also identified (Figure 3.2). SAED patterns generated on the samples with good crystallinity indicated principal diffraction at  $d = 2.56$  and  $4.58 \text{ \AA}$ . This pattern is typical of an intercalated clay such as chamosite.

Variable (Fe,Al) - silicates were also evident in the sediment samples. Commonly, large ( $1.5 \mu\text{m}$ ) mineral grains were identified in association with bacterial cells (Plate 3.4b), or their remains (Plate 3.4a). EDS analyses indicated that many of these grains are extremely siliceous in composition (Figure 3.2). Although many of the cells seem to have detrital material (e.g. kaolinite) adsorbed to their outer surfaces (Plate 3.4a), the siliceous grains shown in Plate 3.4b appear to be authigenic since their compositions are unlike the suspended sediment of the Rio Solimões.

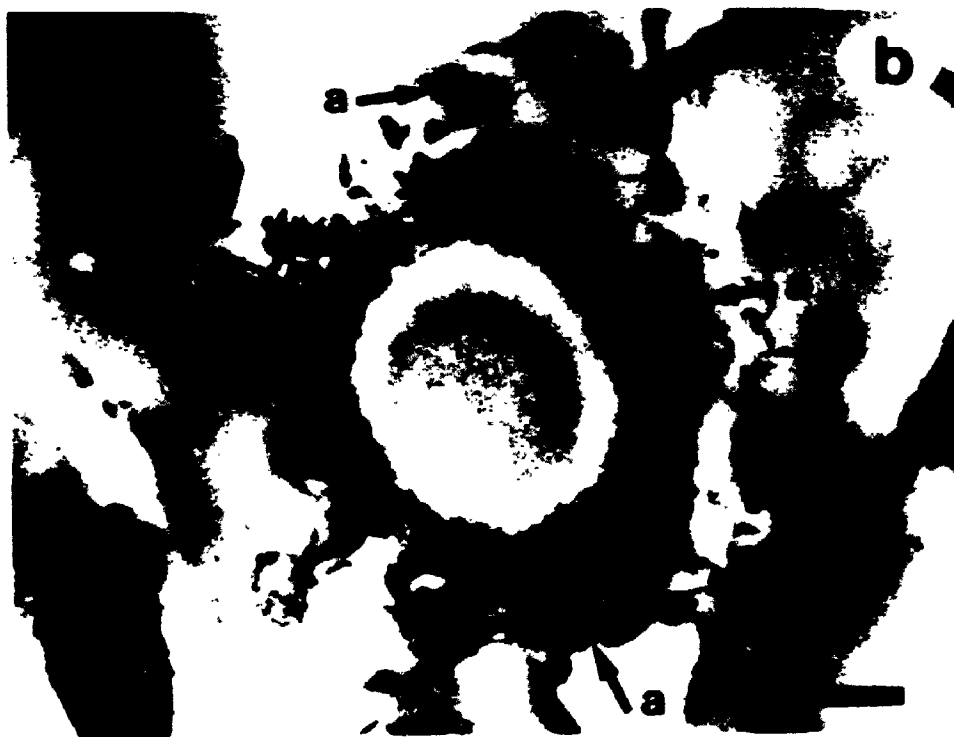
The precipitation of (Fe,Al) - silicates was not restricted to cells with encapsulating material. Colonies of epiphytic cyanobacteria (identified by their intracytoplasmic membranes), which were found attached to a larger eucaryotic algal cell (Plate 3.5a) showed minerals directly on the outer surface of the cell wall (Plate 3.5b). Similar to that

Figure 3 2 Distribution of Fe, Al, and Si in dense aggregates (a), "gel-like" phases (b), transition phases (c), crystalline phases in epiphytic bacteria (d), and siliceous grains in episammic bacteria (e) The Fe, Al, and Si content for chamosite ( $\emptyset$ ) is marked



**PLATE 3.1**

- a) Transmission electron micrograph (TEM) of an iron mineralized capsule (arrow) from an epiphytic bacterial cell in the Rio Solimões. Sample has been stained to increase the electron contrast inside the intact cell. Scale bar, 180 nm.
  
- b) TEM image of an epiphytic bacterial cell (unstained) from the Rio Solimões with the formation of Fe-rich, dense aggregates (a). Scale bar, 180 nm.



**PLATE 3.2**

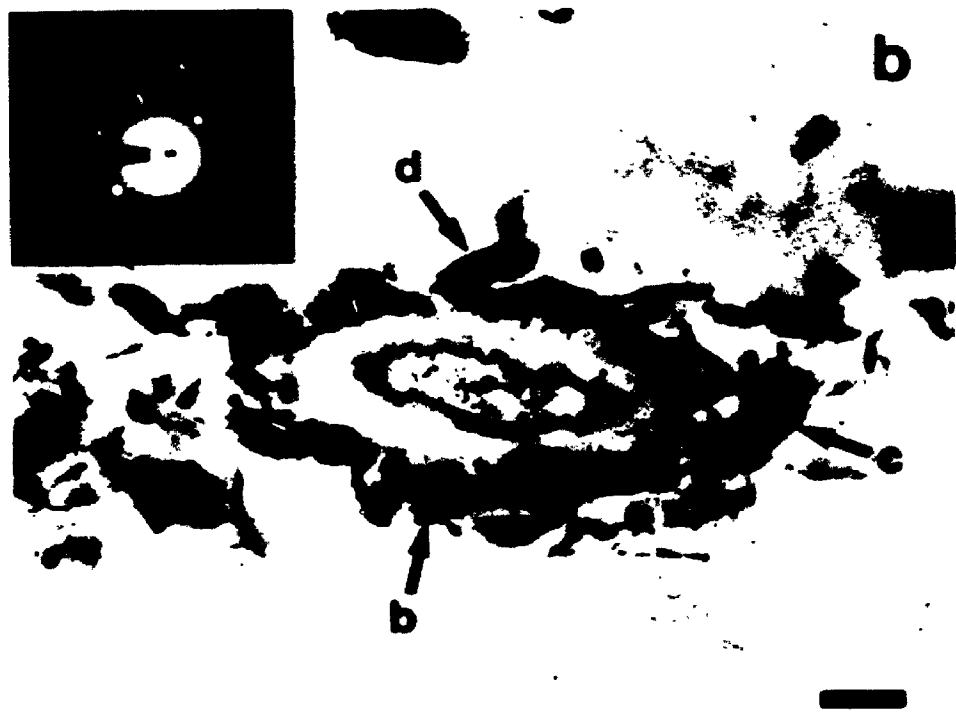
- a) TEM image of an epiphytic bacterial cell (stained) from the Rio Solimões with abundant Fe-rich aggregates (a) on the outer surface of the mineralized capsule. Scale bar, 290 nm.
  
- b) TEM image of the "gel-like" structures (b) associated with the epiphytic bacterial cell (stained) from the Rio Solimões. Scale bar, 380 nm





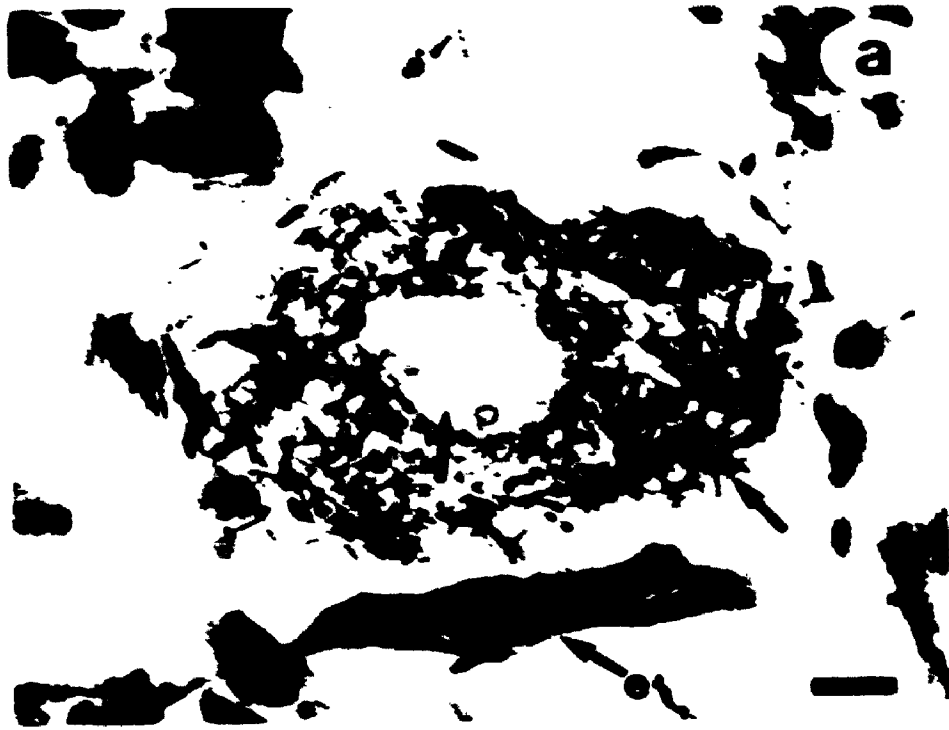
**PLATE 3.3**

- a) TEM image of a partially encrusted bacterial cell (stained) from the Rio Solimões showing the "gel-like" phases (b) and the transition phase (c). Scale bar, 230 nm.
  
- b) TEM image of a completely encrusted bacterial cell (stained) from the Rio Solimões with a complete range of mineral morphologies including the "gel-like" phase (b), the "transition" phase (c), and the crystalline phase (d) with SAED pattern indicative of an intercalated clay such as chamosite. Scale bar, 380 nm.



**PLATE 3.4**

- a) TEM image of episammic bacteria (stained) from the Rio Solimões. Arrows indicate lysed cell, mineralized capsule, and large Fe-aluminosilicate grain (e) associated with many of the bacterial cells in the sediment. Scale bar, 230 nm
- b) TEM image of episammic bacteria (stained) from the Rio Solimões with mineralized capsule, "gel-like" phase (b), "transition" phase (c), crystalline phase (d), and Fe-aluminosilicate grains (e). Scale bar, 290 nm



**PLATE 3.5**

- a) TEM image of a colony of epiphytic cyanobacteria (as determined by their intracytoplasmic membranes) from the Rio Solimões. Bacteria are attached to a large algal cell (arrow). Scale bar, 2.0  $\mu\text{m}$
  
- b) Magnified view of a cyanobacteria (stained) with "gel-like" structures (arrows) formed on the outside of the cell wall. Scale bar, 600 nm



—

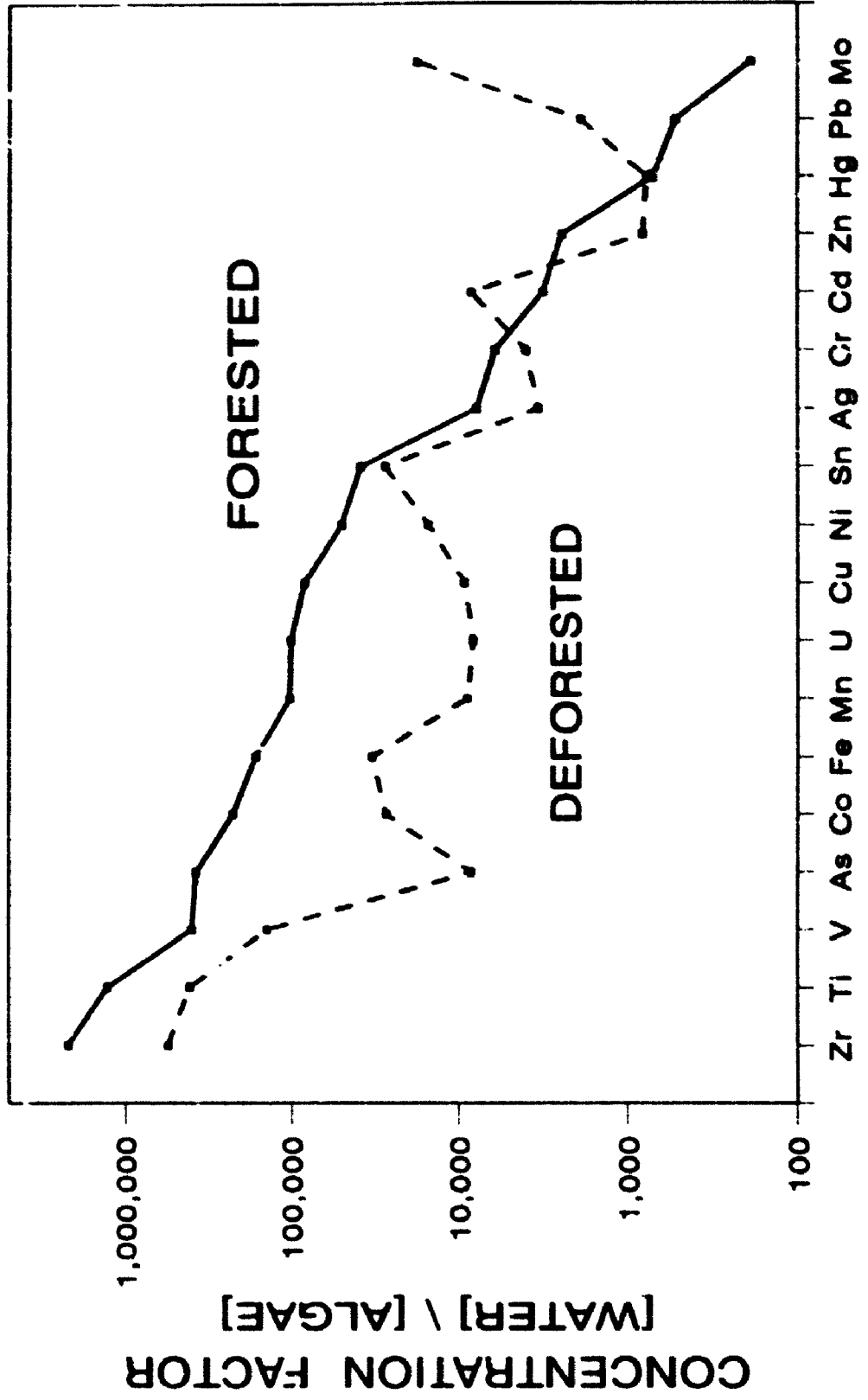


**PLATE 3.6**

- a) TEM image of an epiphytic bacterial cell (stained) from the Rio Negro. Arrows indicate unmineralized capsule and detrital kaolinite grain entrapped by the cell. Scale bar, 600 nm
  
- b) Small colony of epiphytic bacteria (stained) from the Rio Negro, loosely encapsulated by organic material. Arrow indicates the low levels of mineralization on the outer cell wall. Scale 480 nm



# CONCENTRATION FACTORS IN ALGAE FORESTED vs. DEFORESTED



found with the epiphytic bacteria, a complete range of Si, Fe, Al compositions and morphologies were identified, with grain sizes typically larger in dimension ( $1 \mu\text{m}$ ). This may reflect a greater efficiency of mineral precipitation, since cations do not have to diffuse through a capsule, and furthermore, the available reactive sites on the cell wall are filled with metallic ions more rapidly.

In contrast to the prolific mineralization by bacteria in the Rio Solimões, cells with capsules (Plate 3.6a) or without capsules (Plate 3.6b) collected from the Rio Negro remained unmineralized (Figure 3.1b). The Pb and U peaks in the EDS spectrum attest to the highly reactive nature of the capsule, and their predominance further indicates the absence of any substantial metal sorption. Also, compared to the Rio Solimões, the presence of bacteria on biological and/or abiological substrata was greatly limited in the number of cells observed.

### 3.3.2 Metal Sorption by Filamentous Algae

Filamentous algae (as identified by H. Mann, personal commun., 1991) growing in waters from the Rio Negro (Table 3.1) and the Rio Solimões (Table 3.2) were characterized by high concentrations of a wide array of heavy metals. A comparison of the two rivers indicated that the metal concentrations in the algae of the Rio Solimões were consistently higher than in the algae from the waters of the Rio Negro.

Using a plot of concentration factors (concentration in algae/concentration in water), the algae are characterized by enrichments of between  $10^2$  to  $10^6$  for the metals studied (Figure 3.3). Exceptionally high concentration factors ( $>10^5$ ) are indicated for Ti, Zr, and Ag, while low concentration factors ( $<10^3$ ) are indicated for Cd and Hg. Figure 3.3 also displays a difference in concentration factors between the two main rivers. Concentration factors for the metals analyzed are typically higher in the algae from the Rio Solimões than in the algae from the Rio Negro.

TABLE 3.1: CONCENTRATION OF METALS IN WATER AND ALGAE FROM THE RIO NEGRO

ELEMENT	WATER (ug/L)	M5-90 (ug/g)	M6-90 (ug/g)	M8-90 (ug/g)	M8-91 (ug/g)	AVERAGE (ug/g)	CONC. FACTOR
TITANIUM	0.68	580.00	75.00	400.00	290.00	336.25	494,485
VANADIUM	0.29	17.00	3.20	21.00	10.00	12.80	44,138
CHROMIUM	0.69	11.00	0.83	5.70	21.00	9.63	13,960
MANGANESE	9.63	110.00	95.00	130.00	14.00	87.25	9,060
IRON	385.00	15000.00	4000.00	16000.00	2900.00	9475.00	24,610
COBALT	0.18	2.80	1.00	2.20	1.90	1.98	10,972
NICKEL	0.32	6.00	1.40	4.90	4.50	4.20	13,125
COPPER	0.32	11.00	4.00	5.80	8.50	7.33	22,891
ZINC	11.54	74.00	21.00	73.00	27.00	48.75	4,224
ARSENIC	0.06	0.90	0.35	2.10	0.64	1.00	16,625
ZIRCONIUM	0.07	17.00	1.80	7.20	7.30	8.33	118,929
MOLYBDENUM	0.25	0.49	0.11	1.40	0.89	0.72	2,890
SILVER	0.03	0.12	0.02	0.08	2.40	0.66	21,892
CADMIUM	0.12	0.16	0.05	0.09	0.11	0.10	863
TIN	0.21	0.83	0.21	0.60	0.55	0.55	2,607
MERCURY	0.17	0.08	0.04	0.17	0.06	0.09	506
LEAD	0.12	16.00	2.10	9.90	3.00	7.75	64,583
URANIUM	0.03	0.84	0.17	0.65	0.26	0.48	16,000

Note: conc. factor = concentration of metal in algae / concentration of metal in water.

TABLE 3.2: CONCENTRATION OF METALS IN WATER AND ALGAE FROM THE RIO SOLIMÕES

ELEMENT	WATER (µg/L)	M11-90 (µg/g)	S4-91 (µg/g)	S5-91 (µg/g)	S6-91 (µg/g)	AVERAGE (µg/g)	CONC. FACTOR
TITANIUM	7.37	2400.00	7500.00	3500.00	10000.00	5850.00	793,758
VANADIUM	2.52	170.00	230.00	150.00	290.00	210.00	83,333
CHROMIUM	1.73	71.00	250.00	86.00	160.00	141.75	81,936
MANGANESE	50.13	9300.00	17000.00	4500.00	2800.00	8400.00	167,564
IRON	1796.25	110000.0	59000.00	44000.00	49000.00	65500.00	36,465
COBALT	1.00	61.00	110.00	21.00	36.00	57.00	57,000
NICKEL	0.71	49.00	120.00	40.00	59.00	67.00	94,366
COPPER	2.40	74.00	190.00	49.00	66.00	94.75	39,479
ZINC	7.10	200.00	160.00	200.00	270.00	207.50	29,225
ARSENIC	0.79	47.00	4.00	30.00	24.00	26.25	33,228
ZIRCONIUM	0.20	64.00	160.00	58.00	150.00	108.00	540,000
MOLYBDENUM	0.45	4.20	2.00	1.60	2.30	2.53	5,611
SILVER	0.03	0.76	3.80	16.00	3.50	6.02	200,500
CADMIUM	0.40	3.60	0.55	2.20	2.10	2.11	5,281
TIN	0.75	4.30	2.10	3.00	6.00	3.85	5,133
MERCURY	0.12	0.40	0.46	0.36	0.61	0.46	3,813
LEAD	0.64	72.00	18.00	26.00	41.00	39.25	61,328
URANIUM	0.11	6.10	4.10	2.90	5.50	4.65	42,273

Note: conc. factor = concentration of metal in algae / concentration of metal in water

**Figure 3.3: Concentration factor plot for algae in the Rio Negro and the Rio Solimões**

# CONCENTRATION FACTORS IN ALGAE RIO NEGRO vs. RIO SOLIMOES

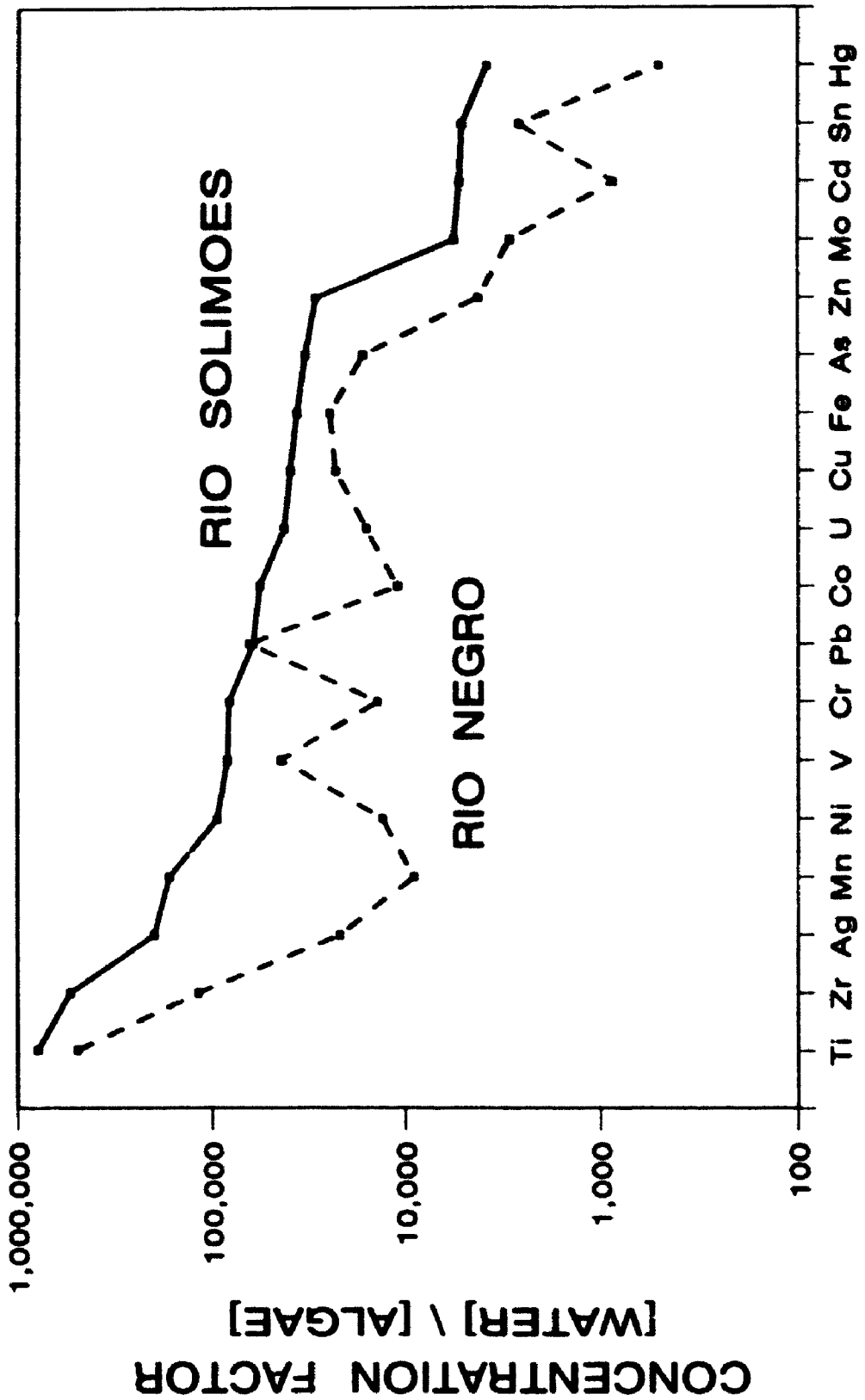


TABLE 3.3: CONCENTRATION OF METALS IN WATER AND ALGAE FROM FORESTED AREAS

ELEMENT	WATER (ug/L)	K3-91 (ug/g)	K8-90 (ug/g)	K9-90 (ug/g)	K11-90 (ug/g)	AVERAGE (ug/g)	CONC. FACTOR
TITANIUM	2.86	12000.00	1200.00	600.00	910.00	3677.50	1,285,839
VANADIUM	0.27	310.00	59.00	22.00	42.00	108.25	400,926
CHROMIUM	14.16	240.00	55.00	7.60	44.00	86.65	6,119
MANGANESE	31.25	2400.00	2400.00	1800.00	6200.00	3200.00	102,400
IRON	331.00	100000.0	51000.00	22000.00	45000.00	54500.00	164,653
COBALT	0.41	140.00	28.00	22.00	180.00	92.50	225,610
NICKEL	1.33	110.00	30.00	17.00	110.00	66.75	50,188
COPPER	3.70	370.00	74.00	65.00	730.00	309.75	83,716
ZINC	61.26	330.00	120.00	53.00	100.00	150.75	2,461
ARSENIC	0.02	12.00	7.80	0.82	9.60	7.56	377,750
ZIRCONIUM	0.07	530.00	44.00	19.00	26.00	154.75	2,210,714
MOLYBDENUM	11.61	5.30	0.93	0.55	2.00	2.20	189
SILVER	0.09	2.50	0.06	0.04	0.23	0.71	7,867
CADMIUM	0.13	0.77	0.28	0.12	0.48	0.41	3,173
TIN	0.08	4.50	1.40	5.60	0.85	3.09	38,594
MERCURY	0.25	0.25	0.02	0.02	0.42	0.18	711
LEAD	16.51	22.00	6.20	2.20	4.00	8.60	521
URANIUM	0.05	14.00	2.10	1.20	2.80	5.03	100,500

Note: conc. factor = concentration of metal in algae / concentration of metal in water.

TABLE 3.4: CONCENTRATION OF METALS IN WATER AND ALGAE FROM DEFORESTED AREAS

ELEMENT	WATER (ug/L)	C1-90 (ug/g)	K1-90 (ug/g)	K15-91 (ug/g)	AVERAGE (ug/g)	CONC. FACTOR	AZ4-91 (ug/g)
TITANIUM	3.00	1500.00	1000.00	1200.00	123.33	411,111	8800.00
VANADIUM	0.50	55.00	59.00	97.00	70.33	141,801	340.00
CHROMIUM	12.20	42.00	47.00	57.00	48.67	3,989	190.00
MANGANESE	403.67	3400.00	4300.00	3100.00	3600.00	8,918	89000.00
IRON	1596.67	47000.00	85000.00	26000.00	52666.67	32,985	230000.0
COBALT	2.09	43.00	110.00	18.00	57.00	27,273	110.00
NICKEL	2.11	28.00	22.00	46.00	32.00	15,166	80.00
COPPER	8.73	18.00	180.00	44.00	80.67	9,240	140.00
ZINC	170.00	140.00	64.00	210.00	138.00	812	150.00
ARSENIC	0.81	11.00	1.80	7.90	6.90	8,487	46.00
ZIRCONIUM	0.06	46.00	32.00	17.00	31.67	558,495	370.00
MOLYBDENUM	0.17	0.82	6.80	1.20	2.94	17,711	16.00
SILVER	0.07	0.10	0.36	0.25	0.24	3,381	1.50
CADMIUM	0.15	0.42	0.27	3.20	1.30	8,475	1.40
TIN	0.08	2.20	2.40	1.70	2.10	27,632	5.40
MERCURY	0.24	0.058	0.38	0.11	0.18	774	0.66
LEAD	6.27	14.00	3.70	18.00	11.90	1,898	130.00
URANIUM	0.37	3.30	4.00	1.70	3.00	8,174	4.30

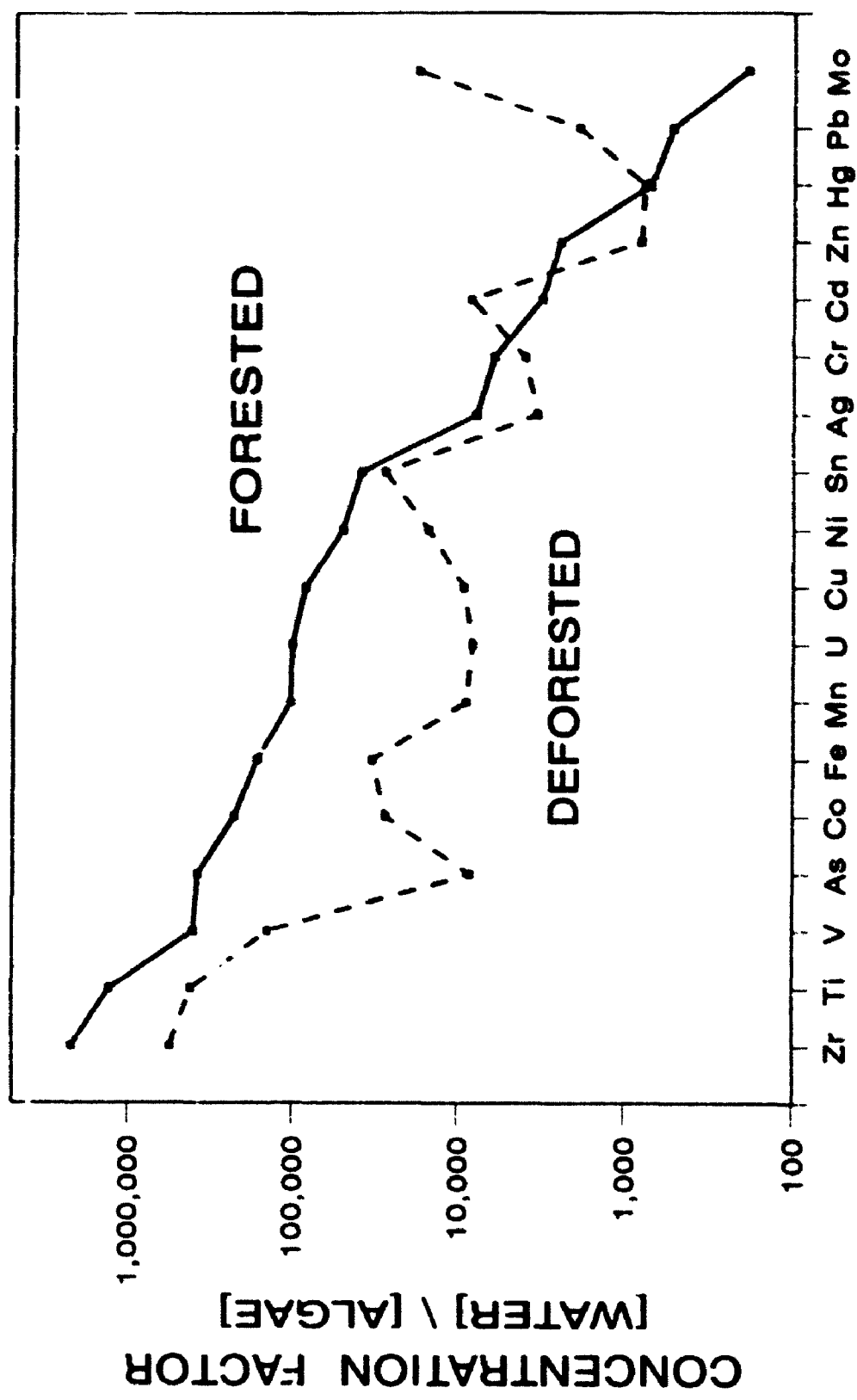
Note: conc. factor = concentration of metal in algae / concentration of metal in water.





**Figure 3.4: Concentration factor plot for algae in streams draining forested and deforested terrains.**

# CONCENTRATION FACTORS IN ALGAE FORESTED vs. DEFORESTED



Algal communities living in the waters of Carajás also contained high metal concentrations relative to their water source. A comparison of algal samples collected from pristine forested regions (Table 3.3) to regions deforested several years earlier (Table 3.4) indicated that metal concentrations were generally higher in the forested environment. An exception to this pattern is sample site AZ4 (deforested area). The algal samples were collected from a stream draining an active manganese mining operation, which supplied metal-rich sediment to the stream.

The concentration factors for the Carajás area ranged from  $10^2$  to  $10^7$  (Figure 3.4). Zr and Ti are characterized by high concentration factors ( $>10^6$ ) while Zn, Hg, Pb, and Mo all have low factors ( $<10^3$ ). In addition, Figure 3.4 illustrates that, for a majority of metals analyzed, the concentration factors for algae were higher in streams draining forested sites.

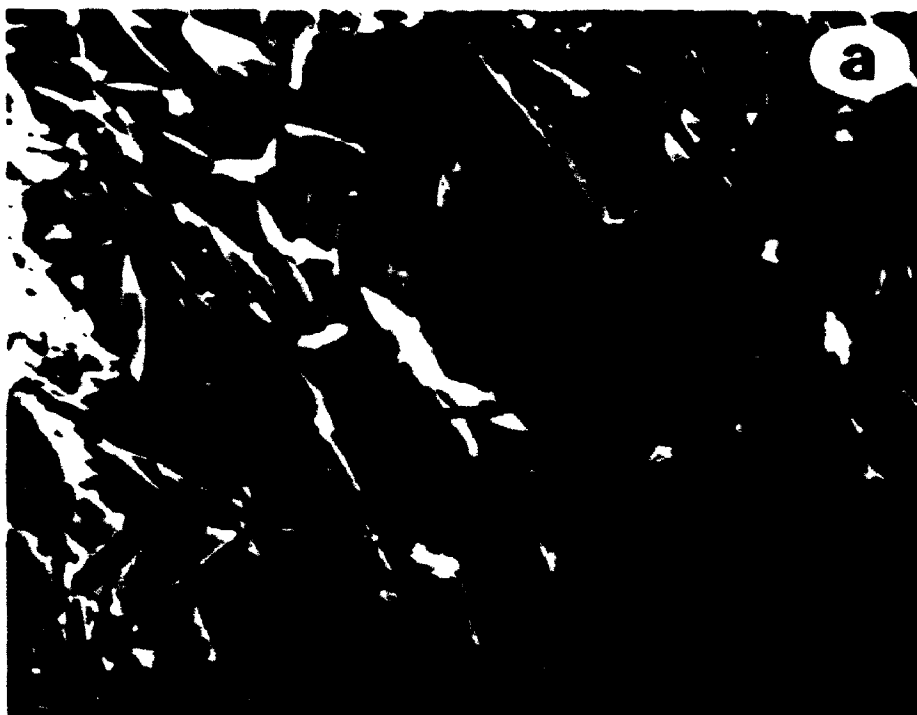
### 3.3.3 Silica Precipitation by Diatoms

The SEM indicates that wood, leaf, and rock samples served as substrata for siliceous epiphytic algae. The abundance of these benthic communities suggested that where light intensity is sufficient to support photosynthesis, any available surface would serve as their solid interface for growth. This explains the absence of living diatoms in the sediments collected (by the dredging device) from the deeper waters, below the euphotic zone.

Samples obtained from the submerged wood revealed morphologically different diatom species on the surface and 3 mm within the wood. The surface community of diatoms (*Navicula* sp.) ranges in size from 50 to 120  $\mu\text{m}$  and are shown oriented in a rosette pattern (Plates 3.7a and 3.7b). The density of diatoms on the surface suggest that the wood serves as both a favorable solid substrate and as a nutrient source. Remnant frustules are also shown (Plates 3.8a and 3.8b) covered by blankets of siliceous "gel" (Figure 3.5a).

**PLATE 3.7**

- a) Scanning electron micrograph (SEM) of diatoms (*Navicula* sp ) on outer wood surface collected from sample site M8. Arrows indicate radiating orientation of cells.
  
- b) SEM image of diatoms (*Navicula* sp ) on outer wood surface collected from sample site M14. Arrow indicates similar radiating orientation as above.



**PLATE 3.8**

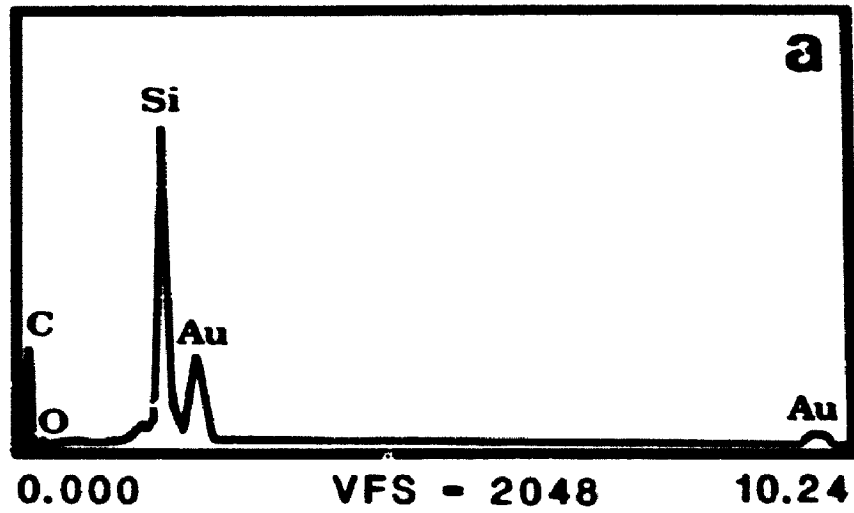
- a) SEM image of outer wood surface covered by siliceous gel. Arrows indicate remnant frustule and siliceous gel
  
- b) SEM image of a group of diatoms on the outer wood surface covered by a thin veneer of siliceous gel (arrows)



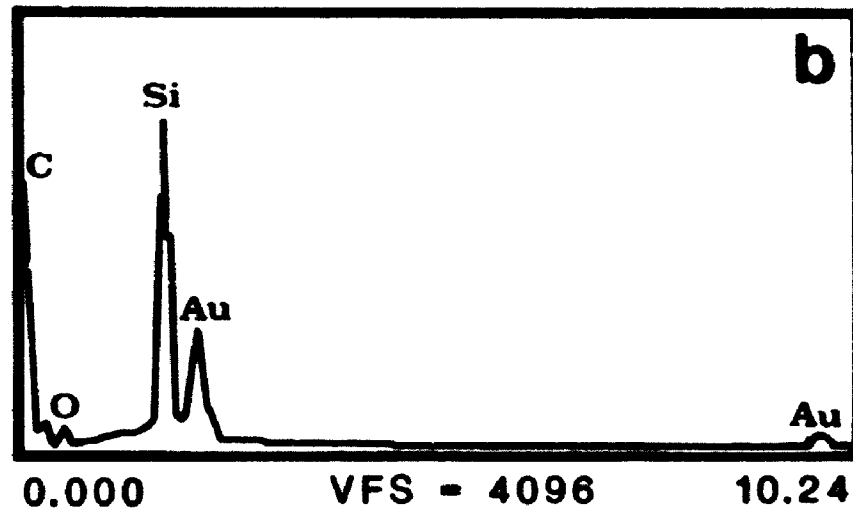
Figure 3.5 EDS spectra of (a) siliceous "gel" on outer wood surface and (b) siliceous "gel" 3 mm deep in wood. Au peaks are due to scanning electron microscope preparation.



Cursor:0.0 KeV - 1315

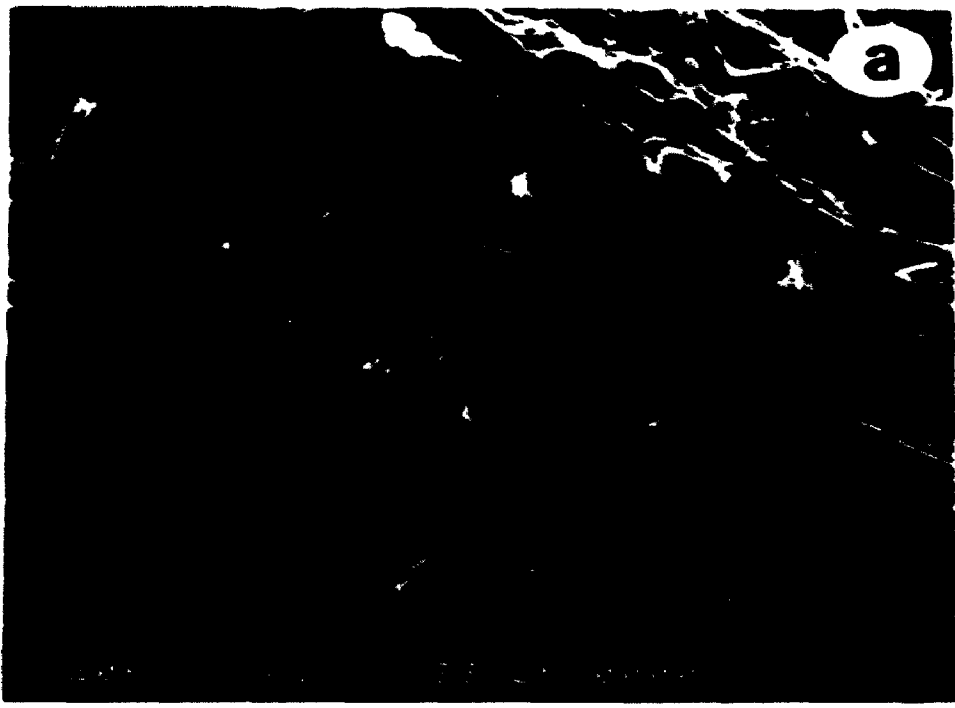


Cursor:0.0 KeV - 1297



**PLATE 3.9**

- a) SEM image of diatoms (*Eunotia* sp. and *Synedra* sp.) from 3 mm below the surface of wood. Arrows indicate wood fibres (long structure), diatoms, and a patch of siliceous gel (amorphous area at top right).
  
- b) Magnified view of diatoms in above sample.



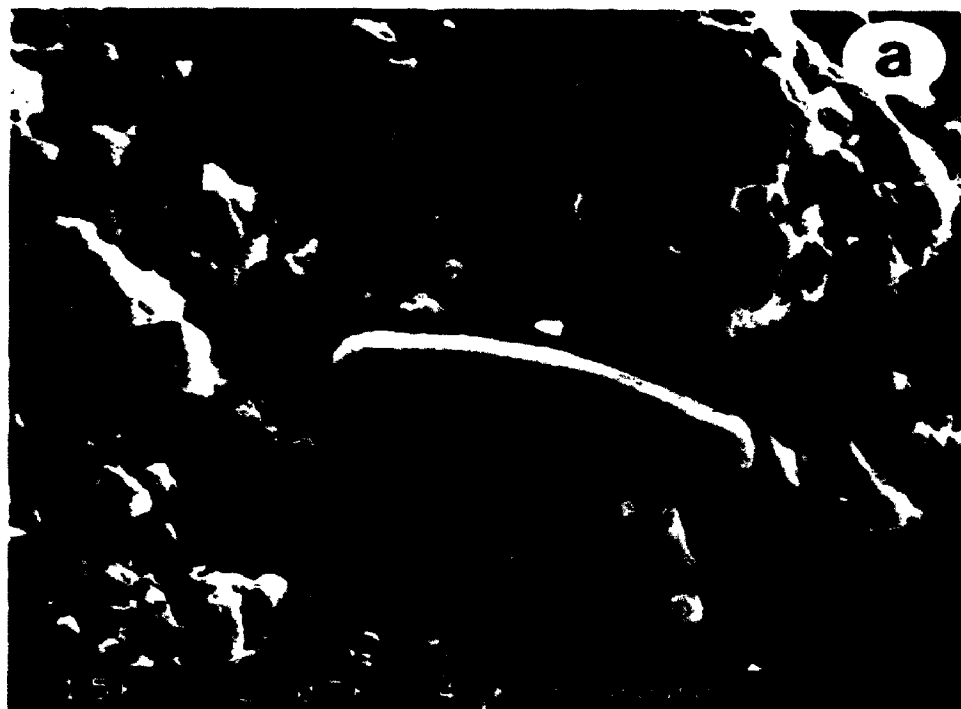
**PLATE 3.10**

- a) SEM image of partial leaf structure (arrow) with *Navicula* sp. different from that of the wood. Sample collected from site M6.
  
- b) SEM image of another submerged leaf (sample site M8) with benthic diatoms. Arrows indicate leaf structure (stomata?), unidentified diatoms, and a patch of siliceous gel (amorphous area at top centre).



**PLATE 3.11**

- a) SEM image of diatoms (*Navicula* sp.) collected off the surface of a submerged laterite sample (site M7).
  
- b) SEM image of *Navicula* sp. collected from the cavity of a laterite sample at site N4.



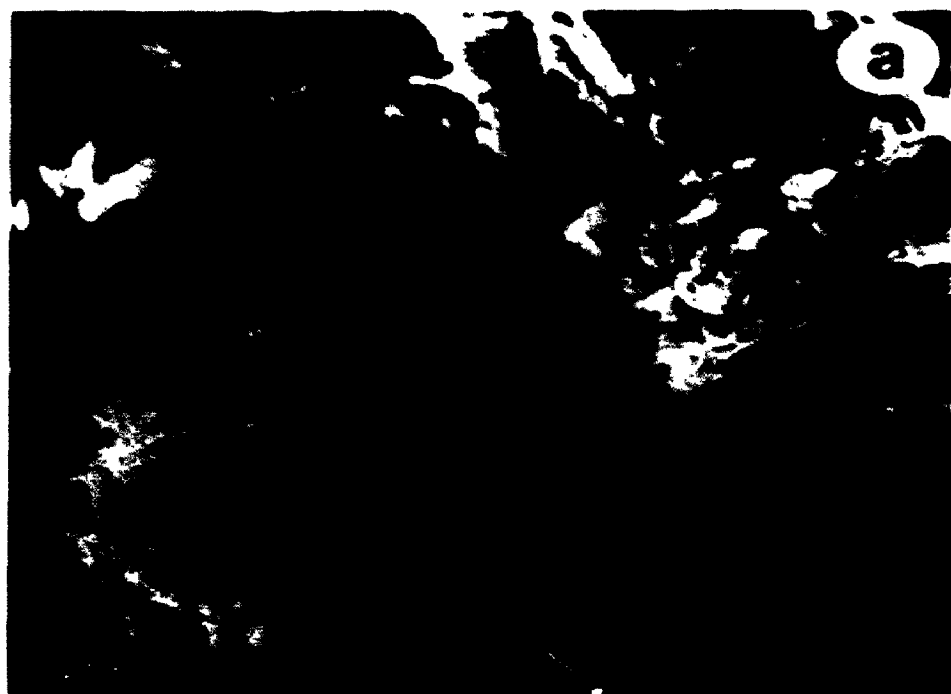
**PLATE 3.12**

- a) SEM image of diatom fragment in the sediments (sample site M14) of the Rio Negro.
  
- b) TEM image of similar diatom fragments isolated in whole mounts Scale bar, 480 nm



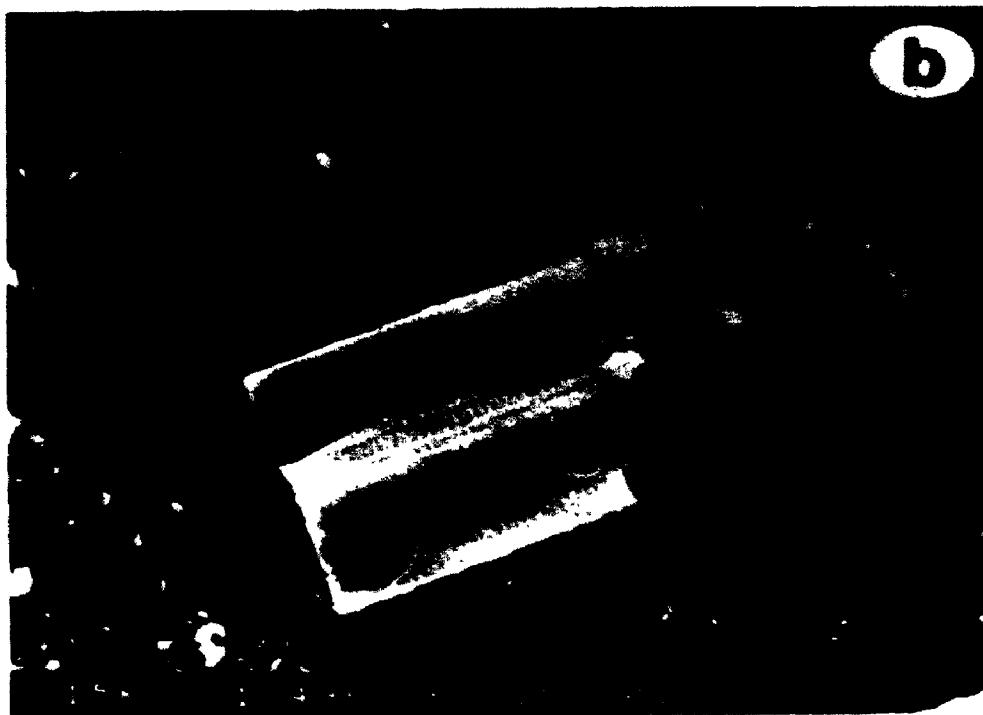
**PLATE 3.13**

- a) SEM image of diatom fragment (arrow) in sediment sample M7 from the Rio Negro
  
- b) TEM whole mount of fragments from similar environment as above. Arrows indicate partial frustule and sediment. Scale bar, 1 10  $\mu\text{m}$



**PLATE 3.14**

- a) SEM image of unidentified planktonic diatoms collected from the surface waters of the Rio Negro.
  
- b) SEM image of different planktonic species in the Rio Negro



The section of wood obtained from 3 mm depth within the wood revealed completely different species of diatoms (*Synedra* sp and *Eumittia* sp ) (Plates 3.9a and 3.9b) These diatoms are characteristically smaller (15 to 45  $\mu\text{m}$ ), which suggested lower available nutrient levels within the porous wood (C Trick, 1990, personal commun ) Overlying some of the wood fibres are patches of a siliceous gel (Figure 3.5b) less extensive than the gel in Plates (3.8a and 3.8b)

Samples obtained from the submerged leaves (Plates 3.10a and 3.10b) and submerged laterites (Plates 3.11a and 3.11b) show different diatom species from that seen on the wood Various diatom species (quantitatively fewer than on the wood surface) were randomly oriented and overlie a siliceous and kaolinitic sediment Diatoms (*Navicula* sp ) were also found on the outer surface of a submerged rock chemically composed of Fe, Al-silicates

SEM and TEM analyses of sediment samples from sites M14 (Plates 3.12a and 3.12b) and M7 (Plates 3.13a and 3.13b) indicate the presence of highly fragmented diatom skeletons This suggests that the sediments, over large distances (several km) along the Rio Negro, are in part composed of highly reactive, amorphous silica Through filtration of the surface waters of the Rio Negro, several varieties of unidentified, planktonic diatoms were recovered (Plates 3.14a and 3.14b) Some filters analyzed on the SEM indicated prolific numbers of these siliceous microorganisms in the water column

### **3.4 Discussion**

#### **3.4.1 The Role of Bacteria**

The role of bacteria in forming authigenic minerals involves a complex interaction between metals in solution with the reactive components of the cell The anionically-charged cell wall and the encompassing layers provide special microenvironments for the deposition of iron and other soluble cationic species Ferric iron, which exhibits unstable aqueous chemistries, was bound in significant amounts, and previous studies indicate that

this may be sufficient to induce transformations to the insoluble hydroxide form (e.g.  $[\text{Fe}(\text{OH})_2]$ ) (Ferris et al., 1986). This corresponds closely to the dense Fe-rich aggregates formed on the outer surfaces of our sample cells.

Through progressive mineralization, these Fe-rich aggregates served as nucleation sites for the precipitation and growth of the complex (Fe,Al) - silicates. It is likely that the initial (Fe,Al) - silicate phases precipitated directly through the reaction of dissolved silicon and aluminum to the bound metallic cations, a process which inhibits the conversion of the Fe-hydroxides (e.g. ferrihydrite) to more stable Fe-oxide forms (e.g. goethite) (Carlson and Schwertmann, 1981). Continued aggregation of these hydrous precursors results in the formation of low-order, "gel-like" phases (Ferris et al., 1987) which are characterized by large surface areas with a high adsorptive affinity for additional metal cations (Wada, 1981).

Due to their lack of a regular crystal structure, these hydrous compounds are unstable and will, over time dehydrate, converting to more stable crystalline forms. In a study by Ferris et al. (1987), the authors found that an increasing incorporation of Fe (in a metal contaminated lake sediment) accompanied the transformation of low-order (Fe,Al) - silicates into a crystalline form of chamosite. In our study area, the hydrous Fe-rich chamosite appeared especially reactive to silicic acid, and continued adsorption of silicon accompanied the conversion of the low-order phase to the crystalline phase. Eventually this process led to the complete encrustation of the bacterial cell within a Fe+Si-rich mineral matrix. The preferential accumulation of silicon is most likely a reflection of the high ratio of dissolved silicon to dissolved iron in the river system (Table 2.14).

It is an interesting observation that all bacterial populations examined in the Rio Solimões consistently formed identical mineral phases. This suggests that the bacteria from our sampling area, regardless of their physiology, were capable of serving as passive nucleation sites for (Fe,Al) - silicate precipitation. Conversely, all bacteria from the Rio Negro showed a conspicuous absence of mineralization.

It is clear then, that the differences in mineral accumulation exhibited by bacterial cells in the Rio Solimões and the Rio Negro must reflect differences in the physical and chemical conditions of their riverine environments. The Rio Solimões is a fertile river, rich in suspended sediments and dissolved inorganic solutes. As a result, the bacteria will have an abundant supply of metals in solution with which to complex and to accumulate. In contrast, the Rio Negro is an extremely infertile river characterized by low levels of major cations and trace metals (Table 2.14). With very dilute waters, the bacteria presumably are unable to bind sufficient quantities of metals to form authigenic mineral phases, suggesting that both metal sorption and biomineralization largely reflect the availability of dissolved solutes in the water column.

The absence of mineralization in the Rio Negro may also be partially attributed to the high concentration of dissolved organic carbon (e.g. humic acid) (Chapter 4). Under these conditions, interactions of organic material with metallic ions may effectively deplete the river water of dissolved metals (Beck et al., 1974), with a majority of reactive sites occupied by strongly bound metals such as  $Fe^{3+}$  and  $Al^{3+}$  (Reuter and Perdue, 1977). In addition, dissolved organic compounds substantially perturb the interactions of aluminum ions with silicic acid and thus inhibit the formation of aluminosilicate phases (Huang, 1991).

In a solute-rich river system, the fate of the metal-loaded bacteria has profound implications for the transfer of metals from the hydrosphere to the sediment (Beveridge et al., 1983). Given that planktonic bacterial populations in the Rio Solimões are typically on the order of  $1 \times 10^6$  to  $4 \times 10^6$  cells/mL (Wissmar et al., 1981), in addition to the unknown benthic populations, it is not difficult to imagine that these microorganisms could effectively cleanse the water of dissolved metals and partition them into the sediments (Beveridge and Fyfe, 1985). As the epiphytic cells lyse and settle to the sediment/water interface, or as the episammic cells lyse in situ, the organo-metallic complexes may undergo a series of microbial or chemical transformations (Degens and Ittekkot, 1982).

Through diagenesis, the bound metals may either be recycled to the overlying water column or become immobilized as stable mineral phases. If the latter occurs, then during diagenesis in an oxic environment, micro-deposits of Fe-aluminosilicates could develop in the sediments.

### 3.4.2 The Role of Algae

Algal samples collected from different riverine environments in both the Manaus and Carajás areas indicated that metals were consistently removed from the waters by these microorganisms. The pattern which seems to arise is that algae effectively sequester and concentrate the metals available to them within their aqueous environment. Some metals are extracted from their surrounding environment to fulfill essential physiological functions (Table 3.5). These functions range from cell synthesis (O'Kelley, 1974) to the formation of skeletal and supporting tissues (Borowitzka, 1986; Sullivan and Volcani, 1981). The extraction of other metals without known cellular functions largely reflects the strong complexing ability of the reactive organic components of the living cell. For example, Kuyucak and Volesky (1989) have shown that the cellulosic materials of the cell wall played an important role in the experimental biosorption of gold. The availability of these metals in solution may, therefore, lead to high metal accumulations by algae.

If we conclude that metal concentrations within the algal biomass are a direct reflection of availability, then it is not surprising that the concentration of metals in the filamentous algae of the Rio Solimões greatly exceeds those of the Rio Negro. A similar relationship of metal concentration also arises between algal samples obtained from forested and completely deforested regions. Tropical plant species have adapted over millions of years to the highly leached and weathered soils of the tropics by developing a closed system that effectively conserves and recycles needed nutrients (Jordan, 1985). Under these forested conditions the river system is continuously supplied with nutrients through the slow leaching from leaves, soils, and decaying organic matter. Removal of the



**TABLE 3.5: INORGANIC ELEMENTS REQUIRED  
BY ONE OR MORE ALGAL SPECIES**

---

**Macro nutrient elements**

**S, K, Ca, Mg, N, and P**

**Micronutrient elements essential to all algae**

**Fe, Mn, Cu, Zn, Mo, and Cl**

**Elements required by some algae**

**Co, B, Si, Na, V, and I**

---

**Note: taken from O'Kelley (1974)**

vegetation through logging and slash-and-burn agricultural practices, however, disrupts the nutrient-conserving mechanisms. Initial losses will consist of those in the standing biomass (Salati and Vose, 1984), and those liberated as aerosols by the burning of the felled forest (Ewel et al., 1981). Over time, increased soil erosion causes the level of soil nutrients to fall below the level of an undisturbed forest (Jordan, 1985). Eventually, the nutrient input into the river system will be minimal. This situation appears consistent with the data from these algal samples which show a higher metal concentration in the microorganisms from the forested streams.

The role of algae in biogeochemical cycling extends beyond trace metal extraction. Siliceous microorganisms, such as the diatoms, sequester silicon from the surface waters of the Rio Negro, where the dissolved silicon levels were a maximum of 2100  $\mu\text{g/L}$ . While many might suggest that the high silica to cation ratios in the river (Table 2.11) argues against a significant biological removal of silica, a comparison of these ratios to both the ratios in average shield rocks and adjacent lateritic soils (Table 3.6) indicates that processes for silica removal are at work. Dissolved silicon levels have typically been attributed to an abiological buffering mechanism, whereby sorption reactions involving dissolved silicon and solid phases (i.e. sediments) control the concentration in freshwater environments (Edwards and Liss, 1973). Although the geochemical cycle of Si in freshwater ecosystems is dominated by physico-chemical processes, the widespread occurrence of both benthic and planktonic diatoms in the waters of the Rio Negro suggests that these levels are in part influenced by biological activity.

Despite low silicon levels, which are characteristic of Central Amazon rivers, the waters from the Rio Negro were capable of supporting prolific diatom growth with wood, rocks, and submerged leaves serving as solid substrates. Even at these low levels, as compared to the worldwide average concentration of 13,100  $\mu\text{g/L}$  (Livingstone, 1963), silicon will not become a limiting factor, except during intensive diatom blooms where concentrations may drop below 100  $\mu\text{g/L}$  (Lewin and Guillard, 1963).

**TABLE 3.6: COMPARISON OF DISSOLVED SOLUTES (NORMALIZED AGAINST SILICON) IN THE RIO NEGRO WITH AVERAGE SHIELD AND LATERITIC SOILS**

<b>ELEMENT</b>	<b>Rio Negro</b>	<b>Average Shield</b>	<b>Lateritic Soil</b>
Potassium	0.2130	0.0620	0.0006
Magnesium	0.0770	0.0420	0.0007
Calcium	0.2280	0.0690	0.0001
Phosphorous	0.0047	N.A.	0.0009
Silicon	1.0000	1.0000	1.0000

Note: Average Shield values are from Stallard and Edmond (1983).

In accordance with low weathering rates exhibited in the Central Amazon, the source of silicon for diatom growth will be largely sustained through the recycling of biogenic silica (Reynolds, 1986). Studies in large, non-flowing lakes (Kingston et al., 1983) and in the marine environment (Hein et al., 1978) have shown that recycled silicon provides >90% of that consumed annually by diatom blooms. Similar processes of silicon recycling should be expected within the almost non-flowing waters of the flooded forests. Calculation of silica recycling in the flowing (2 km/hr, N. Falcao, personal commun.) mainstream of the Rio Negro is much more difficult to determine.

The recycling of silicon in diatoms involves the dissolution of opaline skeletons and subsequent biological uptake. Sediment samples collected along the Rio Negro indicate the ubiquitous presence of diatom fragments which must serve as a major source of dissolving silica. Furthermore, within the small tributaries and flooded forests of the Rio Negro where benthic communities (e.g. *Navicula* sp.) are abundant, dissolution may begin in situ on the substratum. Upon death of the microorganism, the remnant siliceous frustules become fragmented, partially dissolve, and within micrometres to millimetres of the surface, reprecipitate as silica overgrowths (Hein et al., 1978; Williams et al., 1985). These amorphous overgrowths are formed when the dissolved silicon levels become locally supersaturated before opal-A dissolution has gone to completion (Hesse, 1990). Dissolution, therefore, becomes interrupted by the re-precipitation of a less soluble, nonbiogenic, siliceous ooze referred to as opal-A (Hein et al., 1978).

Results from our studies suggest that we are witnessing the first stages of a dissolution-reprecipitation process in which the opal-A skeletons of diatoms are transformed in situ into a textureless, siliceous gel, with an amorphous composition. Under ideal pressure and temperature conditions, this process may continue to follow the diagenetic sequence: opal-A -- opal-CT -- chert (Carr and Fyfe, 1958; Kastner et al., 1977; Williams et al., 1985; Hesse, 1990).

This dissolution-precipitation process may alter the structure of the wood sample. The ubiquitous nature of the diatoms and the precipitation of the silica gel suggest that the wood sample is undergoing a void-filling process of silicification (Sigleo, 1978). In our samples this process begins with the dissolution of diatoms on the surface and within. The silicic acid produced from the dissolving frustules may permeate throughout the wood. Hydrogen bonding between the hydroxyl groups in the silicic acid and the hydroxyl groups in the cellulose then leads to the deposition of opaline silica on the surfaces of individual wood cells (Sigleo, 1978). It is, therefore, no surprise to see a siliceous gel, both on the wood surface and within the wood.

The extent of this silicification process may be significant when the vast number of partially submerged trees in the study area is considered. The slow flowing movement of water within the flooded forests and the preferential attachment of diatoms to the outer wood surfaces may allow for silicon levels to build up sufficiently in microenvironments. Therefore, many of the trees within these flooded forests potentially can become reservoirs of highly reactive silica, disrupting the amount of silicon locally recycled through the freshwater system.

The key question now is whether the net uptake of silicon by diatoms significantly affects the silicon budget of the Rio Negro on a regional scale. To determine the mass balance of silicon in the river system, we would require knowing the population of diatoms and their silicon recycling efficiency in the flowing mainstream. While these calculations are presently impossible to make, continued research in the area will shed more light on this question.

## **CHAPTER 4**

### **METAL COMPLEXATION BY ORGANIC MATERIAL**

#### **4.1 Introduction**

Most studies of biogenic materials in Amazonian rivers have been confined to bulk measurements of the concentration of particulate organic carbon (POC) and dissolved organic carbon (DOC), traditionally defined by separation with a 0.5  $\mu\text{m}$  filter (Schlesinger and Melack, 1981). The POC is largely unreactive, and consists of a coarse fraction ( $>63 \mu\text{m}$ ) comprised of tree leaf debris and some wood, with the fine fraction ( $<63 \mu\text{m}$ ) derived primarily from soils and grasses (Hedges et al., 1986). The DOC consists predominantly of humic substances, such as humic acids (HA) and fulvic acids (FA) (Lamar, 1986). These humic substances are generally thought to be refractory, terrestrially derived organic matter leached from the surrounding soils (Reuter and Perdue, 1977). The remaining DOC includes potentially labile biochemical components such as proteins and carbohydrates (Degens, 1982).

In recent years, it has become increasingly apparent that consequential interactions exist between dissolved organic matter and the inorganic materials of freshwater systems. Studies have shown that significant quantities of trace metals are bound on the anionic surfaces of particulate humic substances (Rashid, 1974). Constituent carboxyl and phenolic hydroxyl groups interact passively with available cations in solution (Beck et al., 1974), forming organo-metallic complexes through ion exchange, surface adsorption, and chelation, with stabilities much higher than those of corresponding inorganic metal complexes (Reuter and Perdue, 1977).

Generally the concentration of dissolved solutes in a river system (approximately 30 mg/L, Bowen, 1979) are more abundant than dissolved organic carbon (0.1 to 10 mg/L, with the upper value restricted to polluted systems (Stumm and Morgan, 1970). Under conditions of low DOC, interactions with metallic ions may cause only slight changes in

the overall chemical composition of river water (Beck et al., 1974). Further, a majority of the reactive sites would be occupied by strongly bound metals such as  $\text{Fe}^{3+}$  or  $\text{Al}^{3+}$ , such that complexation of trace metals would be insignificant (Reuter and Perdue, 1977). It would, therefore, be advantageous to study a river system in which the relative abundance of dissolved organics to dissolved solutes would be much greater.

In the Amazon Basin, many of the rivers (blackwater varieties) are characterized by their high organic content and their solute-deficiency; the most notable being the Rio Negro with a TDS (total dissolved inorganic solids) of only 3.5 mg/L (Table 2.14). The Rio Negro is the largest contributor of DOC to the Amazon River, whose average concentrations of 10.8 mg C/L greatly exceed those of the Rio Solimões with only 3.8 mg C/L (Ertel et al., 1986). The Rio Negro is the major humic acid flux to the Amazon River system at 2.5 times the input of the Rio Solimões and also the largest fulvic acid flux amounting to 70% of the mainstream concentration. With a DOC:TDS of 3:1, the Rio Negro was chosen as an ideal study site for the role of dissolved organic matter in the complexation of dissolved metals. As the major tributary of the Amazon, which represents anywhere from 5 to 25% of the Amazon's discharge (Ertel et al., 1986), any significant processes of metal cycling will have a marked influence on regional fluvial processes.

#### **4.2 Sampling and Analytical Methodology**

Samples of water (approximately 250 mL) were collected upstream of Manaus on the Rio Negro and some of its tributaries in early June/91. Samples were left unacidified to retain the organo-metallic complexes.

Whole mounts of unfixed organic material (DOC and POC) were prepared for electron microscopy by pipetting approximately 10  $\mu\text{L}$  of water sample onto carbon-coated copper grids. After allowing the water to evaporate off, the grids were analyzed by TEM. Energy-dispersive X-ray spectroscopy (EDS) was used to determine the trace metal composition of the organic matter.

### 4.3 Results

Results from the EDS analyses indicated that organic material in both the "dissolved" and "particulate" size ranges (Plates 4a-4b) were capable of binding detectable quantities of metals (Figures 4.1a-4.1b). An entire spectrum of metals were shown to be adsorbed, including Fe, Ca, K, P, Si, Al, Mg, Ni, Cr and Ti. Major cations in the waters of the Rio Negro, such as Fe and Si were shown to form the greater part of the organo-metallic complexes, while trace metals such as Ni, Cr, and Ti were (based on X-ray counts) adsorbed in lesser amounts.

To determine the concentration of dissolved metals, waters are typically passed through a 0.45  $\mu\text{m}$  filter to remove suspended materials. Our results, however, indicated that many of the metals which presumably occurred in "solution" may exist as colloidal metal-organic complexes (Beck et al., 1974)

### 4.4 Discussion

Results from this rather simple exercise reveal the reactive nature of the dissolved organic matter. Major cations in the Rio Negro, such as Fe, Al, and Si were bound into organo-metallic complexes, contributing largely to the mobilization and transport of these metals in the river (Beck et al., 1974). The high organic-inorganic matter ratio of the river also seems to provide sufficient reactive sites for adsorption of trace metals. As a whole, this process has profound implications for metal cycling in rivers which drain highly leached and low relief, podsolitic terrains.

The interaction between dissolved organics and dissolved solutes may, however, be limited in other Amazonian river systems. In the Rio Negro, where suspended solids are found in extremely low concentrations, the humic substances behave rather conservatively with a HA:FA of 0.64. However, in the Amazon mainstream, the hydrophobic humic acids become selectively adsorbed onto fine suspended particles from the Rio Solimões (Leenheer, 1980), such that the HA:FA drops to only 0.31 (Ertel et al., 1986). Although



### **PLATE 4.1**

- a) TEM image of "dissolved" organic material (DOC) from the Rio Negro. Arrows indicate areas of high metal adsorption. Scale bar, 100 nm.**
  
- b) TEM image of "particulate" organic material (POC) from the Rio Negro. Dark patches represent areas of high metal adsorption, whereas the arrow indicates remaining unmineralized organic material. Scale bar, 500 nm.**

a

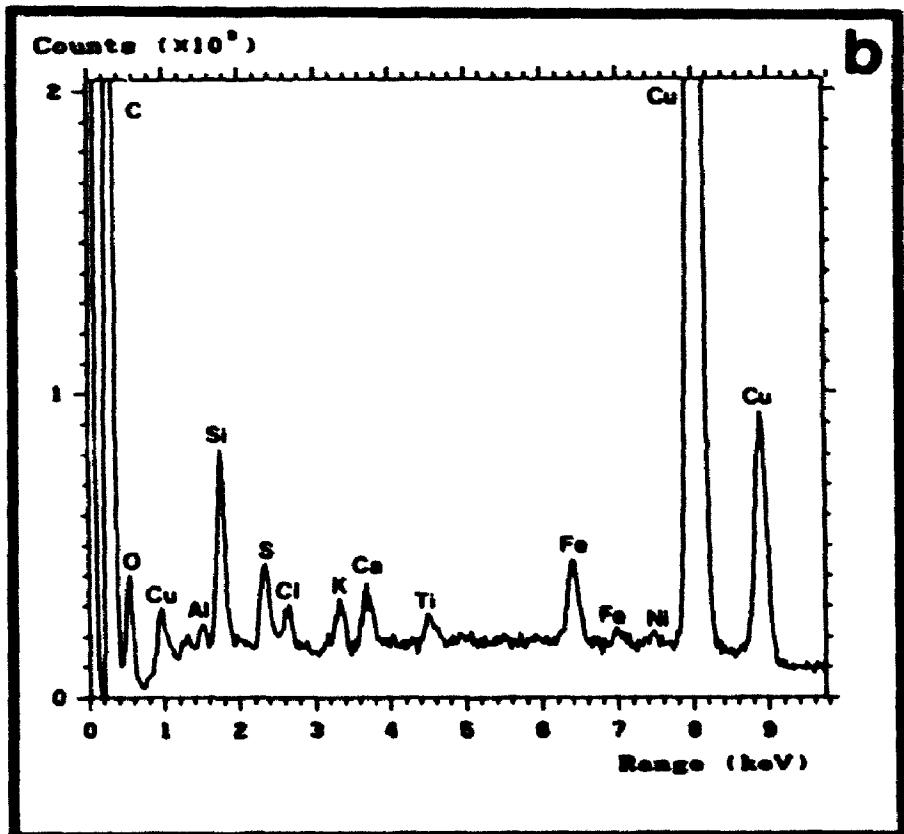
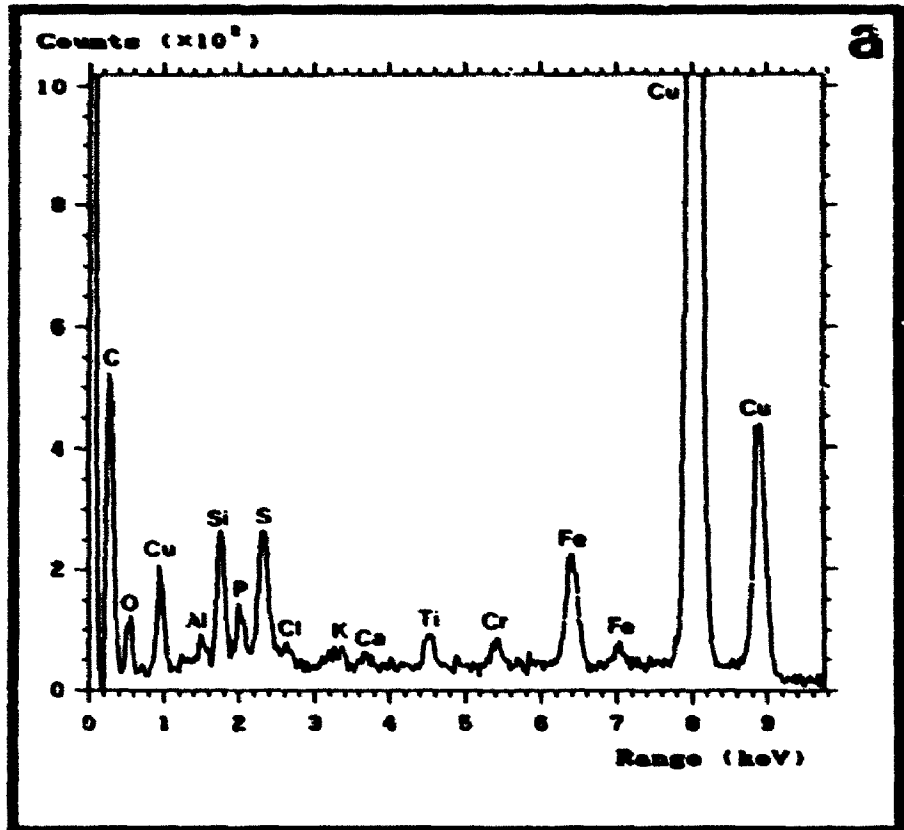


b



4

Figure 4.1: EDS spectra of metals complexed to (a) "dissolved" organic material and (b) "particulate" organic material from the Rio Negro. Cu peaks are from the supporting grid



- c) The  $^{206}\text{Pb}/^{204}\text{Pb}$  isotopic ratios in the rain water are generally lower than all other components analyzed, with an extremely pronounced depletion in the  $^{207}\text{Pb}/^{204}\text{Pb}$  ratio

#### Manaus

- a) Isotopic ratios for the rainfall in Manaus indicates that the  $^{206}\text{Pb}/^{204}\text{Pb}$  ratio for the rainfall is slightly enriched relative to the Rio Solimões, yet depleted relative to the Rio Negro. These results reconfirm the radiogenic nature of the soils and waters of the Central Amazon
- b) The  $^{206}\text{Pb}/^{204}\text{Pb}$  value for the vegetation in the Rio Solimões Basin are anomalously higher than both the soils and river water. Evidently the plants are deriving some of their lead from a more radiogenic source. Surprisingly, the rainfall does not appear to be that source, however, this may merely represent the low  $^{206}\text{Pb}/^{204}\text{Pb}$  values of the rainfall on that particular day.

#### 5.4 Discussion

Results from this study clearly indicate that precipitation is a major source of dissolved metals to solute-deficient river systems such as the Rio Negro. This corresponds to earlier work by Gibbs (1970) who observed that in many of the low-salinity rivers of the Amazon, the chemical composition was determined primarily by the dissolved salts supplied by precipitation. The marine component of the precipitation was shown to consist of Na, K, Mg, and Ca in approximately sea-salt proportions (Gibbs, 1970, Stallard and Edmond, 1981), and this flux may account for the high concentrations of K, Ca, and Mg found in the rainfalls over both locations.

While the marine origin can clearly account for the high concentration of a limited number of dissolved metals in the rainfall, the question which needs to be addressed is, what is the source for the numerous other metals in the rainfall? To trace the source of these metals, Sr and Pb isotopic ratios were employed. In the past, this method has proven successful in distinguishing far-traveled aerosols from local bedrock inputs into vegetation

## **CHAPTER 5**

### **THE IMPACT OF BIOMASS BURNING ON AMAZONIAN RIVER CHEMISTRY**

#### **5.1 Introduction**

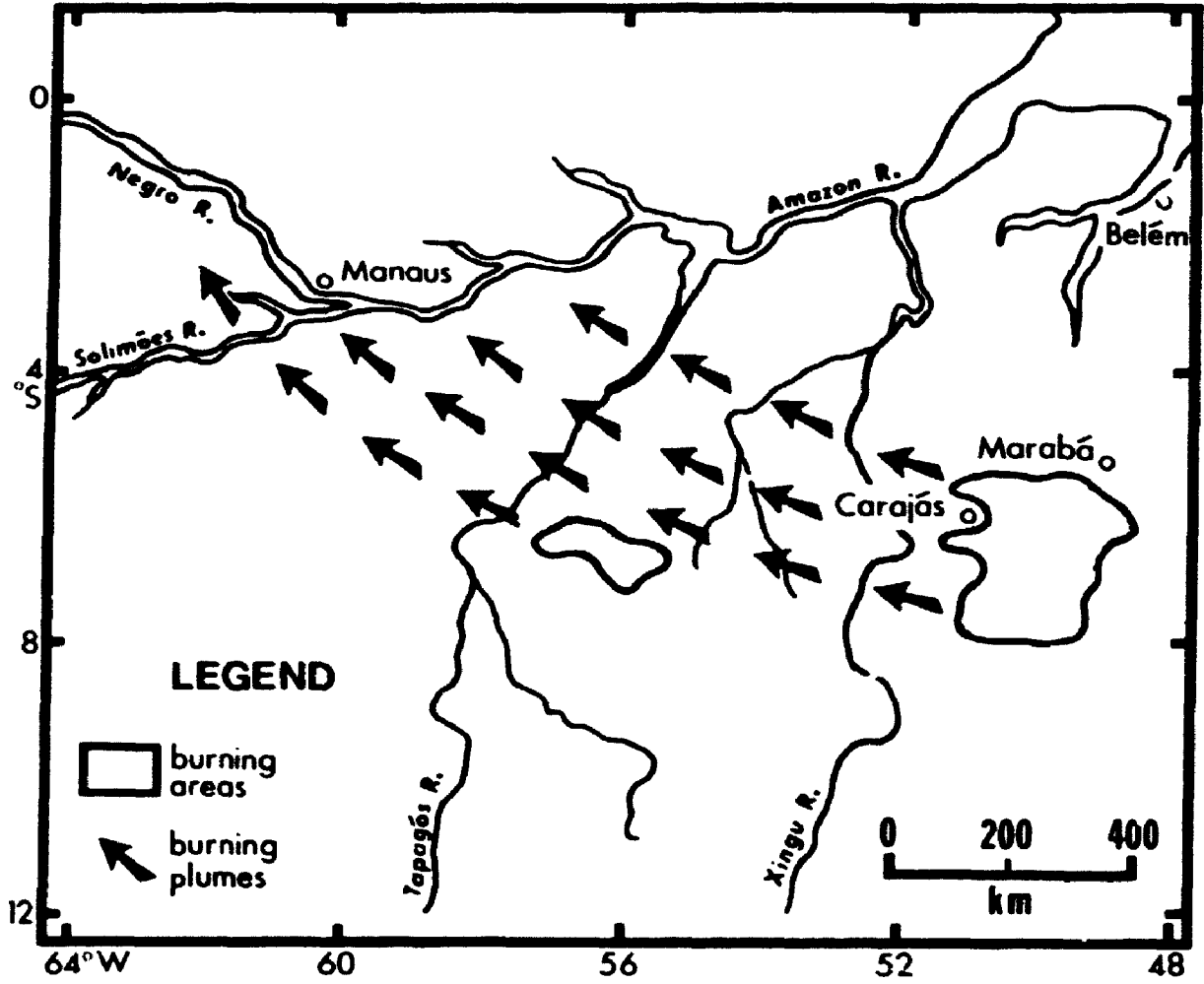
Within the last 30 years, as human settlement into the Amazon Basin has expanded, it has become apparent that anthropogenic forces now influence the nutrient dynamics of the forest ecosystem. As population pressures increase, large tracts of undisturbed forest are converted to agriculture and pastoral lands. Both practices typically remove the vegetation through slash-and-burn methods of forest clearing.

Although biomass burning has been a common practice for several decades, the magnitude of these burnings are only now becoming understood. Through the use of satellite imagery, Setzer and Pereira (1991) have estimated that biomass burning in Brazil during the dry season of 1987 involved 350,000 independent fires, corresponding to about 20 million hectares of vegetation burned, of which 8 million were associated with recent deforestation.

The emissions from biomass burnings are transported over the continent with the prevailing winds in a northwesterly direction. Data from the Amazon Boundary Layer Experiment (ABLE 2A) conducted during the dry season of July/August 1985 indicated the long-range transport of the burn plumes. The trajectories suggested that some plumes traveled about 1000 km between their point of origin and the sampling area in a time period of just 24 hours (Figure 5.1) (Andreae et al., 1988). Giant haze layers, derived from the biomass-burning plumes, extended over millions of km<sup>2</sup> (Setzer and Pereira, 1991).

Through the traditional slash-and-burn methods of forest removal, many of the elements originally tied up in the biomass are released. Initially, an entire suite of metals will be concentrated in a nutrient-rich ash (Jordan, 1985). The fate of this ash is two-fold: some will be leached and washed into the local river system after a few rainfalls, while

**Figure 5.1: Location of major burning areas in the state of Pará, with the movement of the burn plumes in a 24 hr period shown After Andreae et al . (1988)**





some will be dispersed into the atmosphere (Leslie, 1981) It is also well documented that biomass burning is a substantial source of carbon dioxide (Wong, 1978; Seiler and Crutzen, 1980), carbon monoxide (Greenberg et al., 1984), and many other trace gases (Crutzen et al., 1979; Crutzen and Andreae, 1990) to the atmosphere Large quantities of aerosols are produced as well. These are composed of organic matter, black (soot) carbon, and inorganic materials (Crutzen and Andreae, 1990).

The release of inorganic aerosols during biomass burning (in the Amazon) has previously been documented. Leslie (1981) has observed that forest and grassland burnings were responsible for the release of P, S, Cl, Mg, Al, Si, K, Ca, Ti, and Fe into the atmosphere. In comparison to natural Amazon aerosol concentrations, Artaxo et al., (1988) found that several elements (Al, Si, P, S, Cl, K, Ca, Ti, V, Cr, Mn, Fe, Ni, Cu, Zn, Br, and Pb) were greatly enriched in the aerosols from forest burning sites This coincides with the findings of Cachier et al., (1985) who found that during the dry season, the aerosol concentrations over various tropical regions were dominated by biomass burning emissions

While atmospheric enrichment of nutrients (through biomass burning) has been reported, their transport and fate has not yet been addressed Therefore, in this chapter we attempt to determine the significance of biomass burning as a nutrient source into Amazonian river systems To facilitate this study a method was needed which could trace the spatial movement of the released aerosols A technique that has proven effective in quantifying atmospheric inputs into forested watersheds has been the use of Radiogenic isotopes. Straughan et al., (1981), Gosz et al., (1983), and Graustein and Armstrong (1983) have found that the strontium isotopic composition ( $^{87}\text{Sr}/^{86}\text{Sr}$ ) was an effective tracer in distinguishing far-traveled aerosols from bedrock inputs to the nutrient reservoir of a forest.

Similar to the previous chapters, both the Carajás and Manaus areas were chosen for sampling Presently the area around Carajás serves as the focus of burning in the eastern

part of the Amazon. This provided us with the opportunity to collect vegetation which potentially serves as a source of nutrients for the western part of the Basin. The Manaus area was selected as a second sampling site for two reasons:

- a) the influence of man on this area has been negligible, and
- b) with the prevailing winds moving in a northwesterly direction, it should be possible to detect the burning emissions from the Carajás area.

## 5.2 Sampling and Analytical Methodology

In Manaus, rainfall was collected on both May 30/91 and May 31/91. River water, soils and vegetation (leaves and wood) were randomly collected from both river basins. In Carajás, rainfall was collected only on July 22/90. River water, soil, and vegetation samples were collected from streams draining both completely forested and clear-cut regions.

Approximately 1 L samples of river water were collected and placed in two 500 mL Nalgene bottles and then acidified on site with 5 mL analytical grade  $\text{HNO}_3$ . Rainfall was collected with 25 cm diameter plastic funnels into 500 mL Nalgene bottles and treated as above. Prior to multi-element analysis, materials in suspension were removed in the laboratory by pressure filtration through 0.2  $\mu\text{m}$  Nuclepore membranes. The dissolved metal content of the water samples were analyzed by ICP-MS.

To determine the composition of the inorganic aerosols released from forest burning, samples of vegetation were mixed, placed in a ceramic bowl, and then ignited. This methodology was an attempt to mirror the slash-and-burn techniques employed in the Amazon. To collect the fine particulate matter liberated from the combustion of the vegetation, a *Sphagnum* moss bag (serving as a highly adsorptive filter) was suspended between 10-20 cm above the bowl. The moss bags (those exposed to the burning biomass and a separate, unused one which served as a standard) and the accompanying residual ash (which was collected from the bowl) were subsequently analyzed by ICP-MS. The percent

ash was determined by drying samples at 100°C for 24 hrs and then ashing a known quantity at 550°C for 24 hrs in a furnace

Strontium and lead isotopic ratios were determined for river waters, rainfall, vegetation (in the form of an ash), and soils from both Carajás and Manaus. Initially, the samples were dissolved with  $\text{HNO}_3$ , and then converted to chlorides ( $\text{HCl}$ ) for Sr analysis and bromides ( $\text{HBr}$ ) for Pb analysis. Sr and Pb were separated through ion exchange chromatography which involves the reversible exchange of ions between a solid phase (the ion exchange resin itself) and a mobile phase (ion solution). The resins were packed into glass (for Sr) and plastic (for Pb) vertical columns while the sample solution was loaded onto the top. Samples were then eluted by washing its ionic components through the column using suitable solvents (e.g.  $\text{HCl}$  for Sr and  $\text{HBr}$  for Pb) at predetermined controlling rates. Ions were subsequently separated from one another due to their different affinities towards the ion exchange resins. For Sr and Pb, the columns were pre-calibrated so that the elements of interest would be eluted with a known fraction. After drying the eluent, samples were analyzed on a Finnigan MAT 262 thermal ionization mass spectrometer

### **5.3 Results**

#### **5.3.1 Composition of Aerosols and Residual Ash**

Analyses of the moss filters indicated that an entire spectrum of metals were released as aerosols through biomass burning (Table 5.1). Values for Si and K are not given due to interferences encountered with acid digestion and the Ar plasma during sample preparation and ICP-MS analysis, respectively. The most significant metals released in quantity included, Al, P, Ca, Ti, Fe, B, and Br, while many other metals were released in lesser amounts. Previous studies on the emissions from coal-fired and peat-fired burning plants have also documented that the submicron particles were predominantly composed of Si, Al, K, Fe, and Ti (Kauffer and Lichtman), 1984, Hasanen

et al., 1986, Tazaki et al., 1989), with lower concentrations of several other trace metals (Klein et al., 1975, Kaakinen et al., 1975). Taking into account that the residual ash comprises only 1% of the original vegetation, it becomes apparent that a number of metals are selectively volatilized, including B, Mg, Al, P, Ti, Cr, Fe, Co, Ni, Cu, Zn, Zr, I, Ba, La, Ce, Th, and U. Also, of the 99% of the biomass which is volatilized, less than 1% consists of inorganic material.

The high concentration of Br is unexpected since under high temperature ashing, the halogen would tend to form a gaseous state. This could explain the low concentration of other halogens such as I, or the absence of highly volatile elements such as Hg and Se (values of 0.00 for aerosols released in Table 5.1), which are commonly discharged to the atmosphere as gases (Billings and Matson, 1972, Andren et al., 1975).

Analysis of the residual ash (Table 5.1) indicates elevated concentrations of several metals, with over 50% of the total composition comprised of Si, Ca, Fe, and Al. The remainder consists of a myriad of trace metals.

### 5.3.2 Chemical Composition of Rainfall

Chemical analyses of the rainfall collected over Manaus indicated that all metals (with the exception of Sc, Se, and Hg) were found in higher concentrations in precipitation than in the waters of the Rio Negro (Table 5.2) some metals were precipitated at over 100 times their concentration in the surface waters, including K, Ca, V, Sr, and Sn. A comparison of the rainfall collected between the two consecutive days in Manaus also indicates an extreme difference in chemical composition. Rainfall from May 31/91 is consistently more depleted in dissolved solutes, suggesting that a) many of the metals may have been washed out in the previous storm, or b) the second day storm was greater in intensity, and therefore, a dilution effect may have taken place.

In the rainfall collected over Carajás, only a limited number of elements (e.g. B, K, Cu, Zn, Se, Rb, I and Hg) were found in concentrations exceeding those in the waters of

TABLE 51. INORGANIC COMPOSITION OF AEROSOLS AND RESIDUAL ASH (in  $\mu\text{g/g}$ )

ELEMENT	STANDARD FILTER	FILTER 1	FILTER 2	FILTER 3	AVERAGE FILTER	AEROSOLS RELEASED	RESIDUAL ASH
LITHIUM	1.20	1.80	1.80	1.60	1.73	0.53	10.00
BERYLLIUM	0.05	0.05	0.18	0.05	0.09	0.04	0.19
BORON	25.00	60.00	140.00	190.00	130.00	105.00	5.60
MAGNESIUM	1300.00	1300.00	1400.00	1400.00	1366.67	66.67	2200.00
ALUMINIUM	1200.00	3800.00	4200.00	2700.00	3566.67	2366.67	34000.00
SILICON	-----	-----	-----	-----	-----	-----	280000.00
PHOSPHOROUS	38.00	65.00	62.00	360.00	162.33	124.33	320.00
POTASSIUM	-----	-----	-----	-----	-----	-----	5100.00
CALCIUM	4800.00	5100.00	5300.00	5400.00	5266.67	466.67	98000.00
SCANDIUM	30.00	29.00	26.00	24.00	25.33	0.00	16.00
TITANIUM	49.00	120.00	150.00	1100.00	456.67	407.67	3400.00
VANADIUM	0.22	0.63	0.66	0.58	0.62	0.40	-----
CHROMIUM	1.40	2.60	3.00	2.70	2.77	1.37	2.80
MANGANESE	360.00	350.00	370.00	380.00	366.67	6.67	830.00
IRON	740.00	1900.00	2200.00	1600.00	1900.00	1160.00	86000.00
COBALT	0.56	0.92	1.20	0.97	1.03	0.47	4.10
NICKEL	2.80	2.90	3.80	3.80	3.50	0.70	15.00
COPPER	3.80	3.90	3.60	6.60	4.70	0.90	4.10
ZINC	39.00	38.00	37.00	43.00	39.33	0.33	1600.00
ARSENIC	0.01	1.20	0.76	0.01	0.66	0.65	-----
SELENIUM	0.34	0.33	0.33	0.32	0.33	0.00	6.80
BROMINE	150.00	280.00	250.00	360.00	296.67	146.67	-----
RUBIDIUM	16.00	15.00	14.00	15.00	14.67	0.00	10.00
STRONTIUM	17.00	21.00	25.00	23.00	23.00	6.00	830.00
ZIRCONIUM	0.63	2.80	3.20	2.20	2.73	2.10	84.00
MOLYBDENUM	0.13	0.13	0.13	0.13	0.13	0.00	2.10
SILVER	0.15	0.06	0.06	0.06	0.06	0.00	0.20
CADMIUM	0.12	0.12	0.12	0.29	0.18	0.06	0.20
TIN	0.13	0.14	0.07	0.14	0.12	0.00	13.00
ANTIMONY	0.12	0.14	0.14	0.17	0.15	0.03	3.30
IODINE	2.50	2.80	2.70	2.80	2.77	0.27	0.18
CAESIUM	0.28	0.44	0.37	0.41	0.41	0.13	0.10
BARIUM	32.00	38.00	44.00	41.00	41.00	9.00	130.00
LANTHANUM	0.06	0.10	1.20	0.15	0.48	0.42	12.00
CERIUM	1.10	2.00	2.20	2.10	2.10	1.00	16.00
NEODYMIUM	0.34	0.85	0.85	0.77	0.82	0.48	3.10
SAMARIUM	0.07	0.07	0.06	0.10	0.08	0.01	1.30
EUROPIUM	0.04	0.03	0.03	0.03	0.03	0.00	0.32
TERBIUM	0.01	0.02	0.02	0.02	0.02	0.01	0.08
DYSPROSIUM	0.06	0.05	0.04	0.04	0.05	0.00	0.22
YTTERBIUM	0.03	0.03	0.03	0.03	0.03	0.00	0.21
HAFNIUM	0.04	0.08	0.08	0.04	0.07	0.03	1.60
TANTALUM	0.03	0.03	0.03	0.03	0.03	0.00	0.35
TUNGSTEN	0.05	0.05	0.05	0.05	0.05	0.00	2.80
GOLD	0.04	0.02	0.03	0.03	0.03	0.00	0.14
MERCURY	0.35	0.33	0.33	0.33	0.33	0.00	0.44
LEAD	11.00	9.60	10.00	10.00	9.87	0.00	250.00
BISMUTH	0.02	0.02	0.03	0.02	0.03	0.01	0.30
THORIUM	0.10	0.44	0.47	0.26	0.39	0.29	6.40
URANIUM	0.07	0.10	0.11	0.08	0.09	0.02	0.82

Note: aerosols released = average filter - standard filter

TABLE 5.2: COMPARISON OF SURFACE WATERS TO PRECIPITATION IN STUDY AREAS (in ug/l.)

ELEMENT	AVERAGE NEGRO	MANAUS RAINFALL MAY 30/91	MANAUS RAINFALL MAY 31/91	FOREST STREAMS	CARAJAS RAINFALL JUL. 22/90
LITHIUM	0.26 <	0.38	0.75	0.59	0.22
BERYLLIUM	0.05 <	0.07 <	0.07	0.07 <	0.04
BORON	0.88	3.10	4.70	3.23	15.00
MAGNESIUM	128.50	910.00	480.00	1262.50	1300.00
ALUMINUM	181.25	2300.00	160.00	1017.63	170.00
SILICON	1850.00	3000.00	1600.00	5362.50	540.00
PHOSPHOROUS	7.24	2000.00	23.00	48.63	40.00
POTASSIUM	463.75	12000.00	6200.00	1400.00	3500.00
CALCIUM	391.25	5200.00	8000.00	8825.00	2300.00
SCANDIUM	0.93	0.51	0.34	1.37	0.44
TITANIUM	0.68	5.80	3.30	7.37	1.50
VANADIUM	0.29	120.00	7.90	2.52 <	0.27
CHROMIUM	0.69	5.60	3.60	1.73	0.33
MANGANESE	9.63	92.00	6.60	50.13	65.00
IRON	585.00	1700.00	130.00	1796.25	190.00
COBALT	0.18	1.20	0.67	1.00	0.18
ARSENIC	0.06 <	0.02	0.13	0.79 <	0.04
SELENIUM	2.30 <	0.26	0.70	0.79	2.20
BROMINE	0.92 <	0.56	9.60	10.26	7.30
RUBIDIUM	1.24	35.00	11.00	2.51	7.30
STRONTIUM	3.30	30.00	51.00	43.00	6.00
ZIRCONIUM	0.07	0.36	0.39	0.20 <	0.03
MOLYBDENUM	0.25 <	0.09	2.60	0.45	0.03
SILVER	0.03	0.05	0.02	0.03 <	0.03
CADMIUM	0.12	1.70	0.24	0.40	0.08
TIN	0.21	13.00	8.00	0.75	0.05
ANTIMONY	0.10	0.39	0.33	0.15	0.04
IODINE	0.99	0.56	2.00	1.16	2.70
CAESIUM	0.04	0.44	0.14	0.13	0.15
BARIUM	9.16	50.00	16.00	38.38	6.20
LANTHANUM	0.24	11.00	0.32	0.96	0.08
CERIUM	0.77	9.30	0.26	2.73	0.27
NEODYMIUM	0.25	5.80	0.23	1.20	0.12
SAMARIUM	0.07	0.55	0.10	0.24	0.05
EUROPIUM	0.03	0.04 <	0.02	0.05 <	0.04
TERBIUM	0.02	0.10 <	0.02	0.03 <	0.02
DYSPROSIUM	0.03	0.33 <	0.03	0.16 <	0.03
YTTREBIUM	0.03	0.16 <	0.02	0.08 <	0.03
HAENIUM	0.03 <	0.02	0.03	0.02 <	0.03
TANTALUM	0.02 <	0.02 <	0.02	0.02 <	0.02
TUNGSTEN	0.06	0.05	0.2	0.10 <	0.03
GOLD	0.02 <	0.02 <	0.02	0.02 <	0.02
MERCURY	0.17 <	0.09 <	0.12	0.12 <	0.21
BISMUTH	0.02	0.11	0.05	0.06 <	0.02
THORIUM	0.13	0.20	0.15	0.25	0.05
URANIUM	0.03	0.13	0.08	0.11 <	0.02

Note. "<" indicate concentrations below detection limit.

the forested streams. Since the forested streams are inherently more solute-rich than the Rio Negro, the addition of dissolved metals through precipitation will be less pronounced.

### 5.3.3 Determination of Isotopic Ratios

#### 5.3.3.1 Sr Ratios

Sr isotopic data for water, soils, and vegetation are presented in Table (5.3). Our results indicate several interesting features from both study areas.

#### Carajás

- a) The water, soils, and vegetation all have high  $^{87}\text{Sr}/^{86}\text{Sr}$  ratios reflecting the highly radiogenic nature of the granitic and gneissic Precambrian Shield (Tassinari et al., 1982).
- b) Extremely variable  $^{87}\text{Sr}/^{86}\text{Sr}$  compositions for both water (0.734893-0.757355) and soils (0.723426-0.791215) are evident. This suggests that the soils are of diverse origin, and therefore, the rivers draining these different soil types (Table 2.2) will show dissimilar isotopic ratios.
- c) Unlike the soils and water, the vegetation appears much more uniform in composition, with  $^{87}\text{Sr}/^{86}\text{Sr}$  values ranging from 0.731424 to 0.732788. This uniformity may indicate that the different vegetation types receive significant amounts of their Sr from a similar source, much of which, however, originates from a source other than the soils.
- d) The rainfall collected on July 22/90 has significantly lower ratio (0.722968) than the river water and vegetation, indicating that the water precipitated over Carajás is not solely derived from local evapotranspiration. This coincides with previous studies which have estimated that 52% of the rainfall in the region between Belém and Manaus comes from water vapor from the Atlantic Ocean, while the remaining 48% is water vapor evapotranspired from the forest ecosystem (Marques et al., 1977).

### Manaus

- a) Ratios for water (Rio Solimões and Rio Negro), soil (varzea and Central Amazon), and vegetation are considerably less radiogenic than their counterparts from Carajás. The Rio Solimões has an extremely low ratio "reflective of" the carbonate (Faure, 1986) and andesitic (Dickinson, 1970) source rocks in the Andes (Klammer, 1984). In contrast, the Rio Negro is characterized by higher  $^{87}\text{Sr}/^{86}\text{Sr}$  ratios indicative of soils primarily derived from a Precambrian Shield source (Klammer, 1984)
- b) The vegetation in both the Rio Negro Basin and the Rio Solimões Basin have lower isotopic ratios than the soils and river water, suggesting once again that the source of their nutrients may be derived from multiple sources

### 5.3.3.2 Pb Ratios

Many of the observations made with the strontium isotopes are enhanced by the use of lead isotopic ratios (Table 5.4) of which the  $^{206}\text{Pb}/^{204}\text{Pb}$  ratios seem the most useful. Unlike the strontium data, however, the lead values are all quite varied, and due to the low levels of lead in some samples, isotopic ratios could not be determined.

### Carajás

- a)  $^{206}\text{Pb}/^{204}\text{Pb}$  isotopic ratios for the river water, soils, and vegetation indicate that the soils are typically the most radiogenic components. Similar to the strontium ratios, the lead ratios for the soils are extremely varied, leading to variable ratios in the river water
- b) The isotopic values for the vegetation are not as uniform as the Sr values. This heterogeneity may be attributable to the leachable lead that the vegetation acquires from the soils. The fact that the Pb ratios in the vegetation are not as variable as the soils confirms that the soils are not the only source of lead. If they were, then the Pb ratios in the vegetation would correspond more closely to the soil values



TABLE 5.3: Sr ISOTOPIC RATIOS

WATER	DESCRIPTION	87/86	2SIGMA
K2	Carajas stream	0.757355	0.000022
C1	Carajas stream	0.734893	0.000013
RC	Rain - Carajas	0.722968	0.000017
S5	Rio Solimoes	0.709007	0.000039
N3	Rio Negro	0.722426	0.000021
RM1	Rain - Manaus	0.708551	0.000016
RM2	Rain - Manaus	0.710183	0.000029
	Oceans	0.70906	0.00003

SOIL	DESCRIPTION	87/86	2SIGMA
C1	Carajas	0.786563	0.000120
K4	Carajas	0.791215	0.000042
K9	Carajas	0.757485	0.000063
PO	Carajas	0.741668	0.000049
C5	Carajas	0.723426	0.000035
S5	Varzea	0.708683	0.000026
M8	Central Amazon	0.721219	0.000267

VEG.	DESCRIPTION	87/86	2SIGMA
C5A	Carajas	0.732365	0.000038
C5B	Carajas	0.732788	0.000024
C1A	Carajas	0.731424	0.000112
C1B	Carajas	0.738754	0.000061
S5	Varzea	0.707746	0.000044
M8	Central Amazon	0.715473	0.000174

NBS-987	Standard	0.710244	0.000025
---------	----------	----------	----------

Note: Sr ratio for ocean water from Faure et al. (1965).

Veg. = vegetation

TABLE 5.4 Pb ISOTOPIIC RATIOS

WATER DESCRIPTION	206/204	2SIGMA	208/204	2SIGMA	207/204	2SIGMA	208/206	2SIGMA
K2 Carajas Stream	18.670174	0.004144	37.853386	0.008726	15.670512	0.003525	2.027478	0.000071
C1 Carajas Stream	21.337430	0.002188	55.709192	0.912074	---	---	2.624860	0.000110
RC Rain - Carajas	19.010310	0.531730	38.278039	0.002933	8.861624	0.165703	3.974119	0.106205
S5 Rio Solimoes	17.978463	0.009474	38.041360	0.020484	15.646353	0.008299	2.116034	0.000391
N3 Rio Negro	17.859870	0.068110	37.608200	0.143300	15.506950	0.060900	2.106090	0.000990
RM2 Rain - Manaus	19.601386	0.000250	45.592030	4.911000	0.847976	0.042069	2.326152	0.128299

SOIL DESCRIPTION	206/204	2SIGMA	208/204	2SIGMA	207/204	2SIGMA	208/206	2SIGMA
C1 Carajas	16.775462	0.488000	33.583810	2.704800	12.746418	0.022300	1.878756	0.203300
K4 Carajas	53.604085	1.111000	63.848421	1.261900	17.201595	0.516000	1.193386	0.032900
PO Carajas	43.613726	0.186800	58.436070	1.397800	16.726990	0.007300	1.348902	0.018300
C5 Carajas	69.185250	0.223280	44.829030	0.145080	24.936450	0.816520	0.647954	0.000091
S5 Varzea	18.652400	0.011300	38.584100	0.024100	15.633500	0.009500	2.068500	0.000100

VEG. DESCRIPTION	206/204	2SIGMA	208/204	2SIGMA	207/204	2SIGMA	208/206	2SIGMA
C5A Carajas	19.876368	0.258771	39.663815	0.501515	16.210688	0.210738	1.997287	0.013992
C5B Carajas	18.153450	0.212940	37.768820	0.455370	15.639710	0.228280	2.080200	0.002000
C1B Carajas	19.471921	0.297633	40.302984	0.111871	16.409260	0.246138	2.071260	0.024246
S5 Varzea	21.901487	1.357892	43.675613	4.549801	19.276352	1.195133	2.096657	0.024736
M8 Central Amazon	18.450865	0.129156	38.594955	0.298431	15.919684	0.111437	2.105191	0.010145

0.11% Standard amu-982	36.739043	0.000027					1.000016	0.000360
---------------------------	-----------	----------	--	--	--	--	----------	----------

Note: veg. = vegetation

- c) The  $^{206}\text{Pb}/^{204}\text{Pb}$  isotopic ratios in the rain water are generally lower than all other components analyzed, with an extremely pronounced depletion in the  $^{207}\text{Pb}/^{204}\text{Pb}$  ratio

#### Manaus

- a) Isotopic ratios for the rainfall in Manaus indicates that the  $^{206}\text{Pb}/^{204}\text{Pb}$  ratio for the rainfall is slightly enriched relative to the Rio Solimões, yet depleted relative to the Rio Negro. These results reconfirm the radiogenic nature of the soils and waters of the Central Amazon.
- b) The  $^{206}\text{Pb}/^{204}\text{Pb}$  value for the vegetation in the Rio Solimões Basin are anomalously higher than both the soils and river water. Evidently the plants are deriving some of their lead from a more radiogenic source. Surprisingly, the rainfall does not appear to be that source, however, this may merely represent the low  $^{206}\text{Pb}/^{204}\text{Pb}$  values of the rainfall on that particular day.

#### 5.4 Discussion

Results from this study clearly indicate that precipitation is a major source of dissolved metals to solute-deficient river systems such as the Rio Negro. This corresponds to earlier work by Gibbs (1970) who observed that in many of the low-salinity rivers of the Amazon, the chemical composition was determined primarily by the dissolved salts supplied by precipitation. The marine component of the precipitation was shown to consist of Na, K, Mg, and Ca in approximately sea-salt proportions (Gibbs, 1970, Stallard and Edmond, 1981), and this flux may account for the high concentrations of K, Ca, and Mg found in the rainfalls over both locations.

While the marine origin can clearly account for the high concentration of a limited number of dissolved metals in the rainfall, the question which needs to be addressed is, what is the source for the numerous other metals in the rainfall? To trace the source of these metals, Sr and Pb isotopic ratios were employed. In the past, this method has proven successful in distinguishing far-traveled aerosols from local bedrock inputs into vegetation

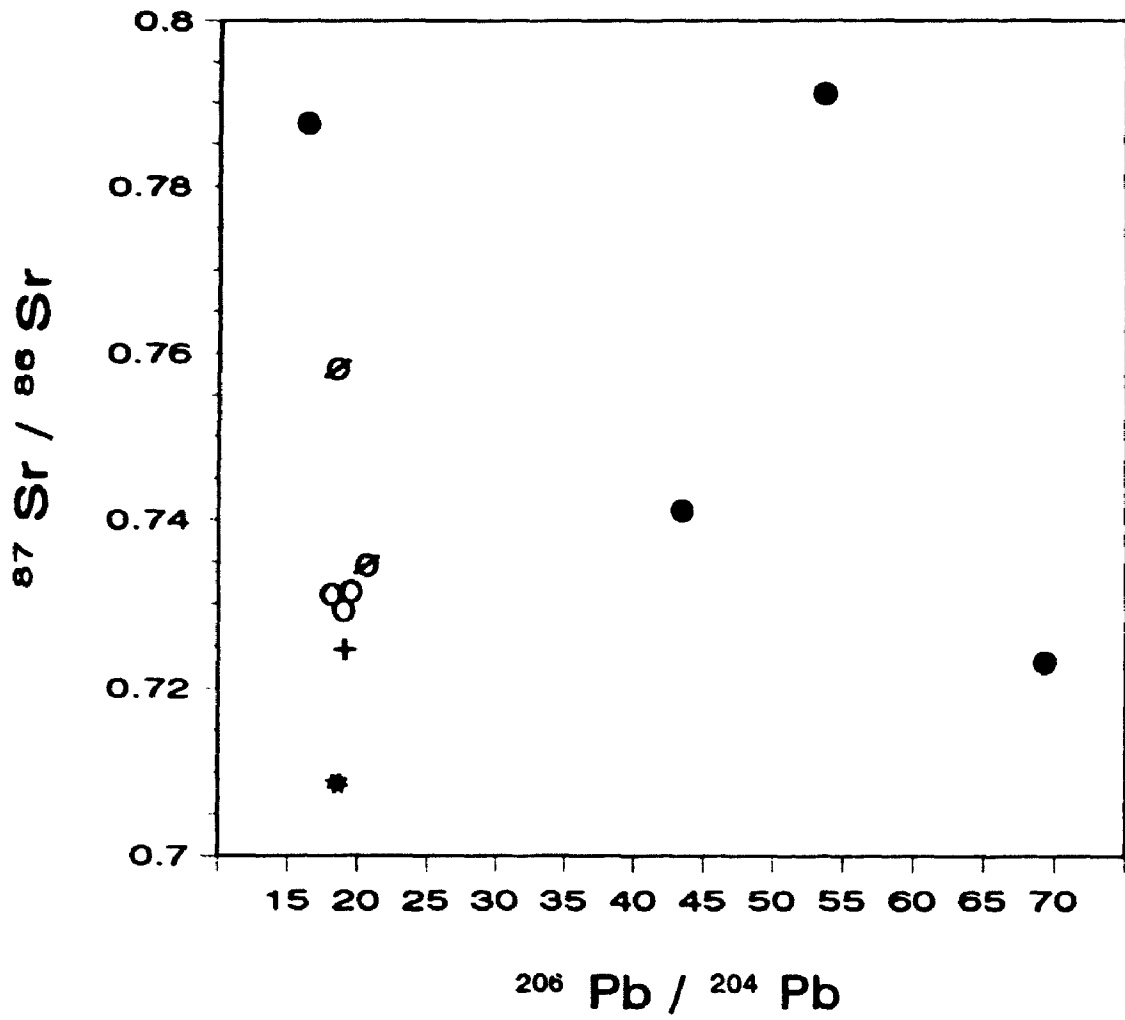
(Gosz et al., 1983), as well as determining the provenance of river systems (Fisher and Stueber, 1976)

Using a plot of  $^{87}\text{Sr}/^{86}\text{Sr}$  and  $^{206}\text{Pb}/^{204}\text{Pb}$  isotopic ratios (Figure 5.2), it becomes apparent that the composition of the rainfall indicates a multi-component mixing of marine water with local components in the Carajás area. The isotopic ratio of the rainwater lies intermediate between the extremely low values for marine water and the extremely radiogenic values for river water, vegetation, and soils. Although evapotranspiration off the surface of the river or vegetation would supply some radiogenic strontium to the atmosphere, this process would be limited in its efficiency in supplying particulate matter to the atmosphere (Faure, 1986). A more likely factor determining the isotopic nature of the rainfall is that as water vapor moves across the continent, it picks up aerosols (needed to serve as nuclei for cloud formation) from other sources, including both biomass burning and wind-blown soils.

Results from the burning experiment have shown that a significant amount of both major elements and trace metals are released into the atmosphere as aerosols and vapors. In Carajás, the vast areas of forests undergoing burning may provide sufficient amounts of these aerosols. For example, from the standpoint of strontium, it seems that the  $6 \mu\text{g/g}$  released as aerosols, and possibly the other  $8.3 \mu\text{g/g}$  that are now concentrated in the ash, may provide sufficient particles to account for much of the  $6 \mu\text{g/L}$  in the rainfall. Since the winds in the Amazon Basin move in a northwesterly direction, these newly released aerosols will be transported, along with water vapor into the Manaus area in the course of 1-2 days (Andreae et al., 1988). Through this process, particulate matter from Carajás can influence the nutrient dynamics over Manaus.

While many metals seem to be found in extremely high concentrations in the rainfall over Manaus compared to the Rio Negro, isotopic analyses indicate that the Sr and Pb ratios are progressively decreasing as the rainfall moves westward. This suggests that much of the radiogenic Sr and Pb may have been washed out during transport, with the

Figure 5.2:  $^{87}\text{Sr}/^{86}\text{Sr}$  and  $^{206}\text{Pb}/^{204}\text{Pb}$  isotopic ratios for ocean water (●), river water (○), soils (●), vegetation (○), and rainfall (+) collected in Carajás. Pb values for ocean water were determined based on marine sediment values (Faure, 1986)



remaining ions being continuously mixed with evapotranspired water from waters and vegetation in the Manaus area, both of which are characterized by lower isotopic ratios

The emission of gases through biomass burning may also play an important role locally for metals such as Hg and Se. Since most of the burning takes place in the eastern part of the Amazon Basin, these elements could be found in significant concentrations in the rainfall. Rainfall collected over Carajás indicates just this. However, since these elements are short-lived in the atmosphere (Andren et al., 1975), their high concentrations may dissipate over regional distances, explaining their low concentrations in the rainfall over Manaus.

The high concentration of mercury found in the precipitation has proven to be one of the interesting observations made in this study. Recently concern over this metal in the Amazon has arisen due to its indiscriminate use in gold mining, particularly in the state of Pará (Mallas and Benedicto, 1986). Mercury is used extensively in the gold recovery process to separate the fine gold particles from other minerals present in the river sediment. Initially, heavy metallic particles are concentrated gravimetrically in riffles and amalgamated with mercury to form a Au-Hg complex. After amalgamation, the complex is burned and the Hg vapor is released to the atmosphere (Malm et al., 1990). During the entire process, it has been estimated that for production of 1 kg of gold, 0.72 kg of Hg are lost as vapor (Pfeiffer and Lacerda, 1988). Once in the atmosphere, the residence time for Hg is on the order of several days under high humidity (Lindquist and Rodhe, 1985), thus in the Amazon, Hg vapor emitted during gold recovery could be expected to return rapidly to adjacent forests (Lacerda et al., 1989)

The other source of aerosols to the atmosphere, wind-blown soil, can also be indirectly attributed to deforestation, since prior to settlement, the Amazon was forested. The causes of deforestation are numerous, however, in the Carajás area, the most common cause is the mining industry. The Carajás mining operation, which has considerable deposits of Fe, Mn, Ni, Sn, Cu, Al, and Au, represents one of the largest mining

operations today. Aside from the mines, vast tracts of land have been cleared to make way for a railroad, which links the mine to a port on the Atlantic, as well as the construction of smelters fueled by charcoal (Fearnside, 1989). The net result of these activities is that previously forested lands are now exposed to erosive agents such as water and wind. Invariably, erosion due to runoff carries the soil into regional fluvial systems, whereas increased wind erosion effectively transports particles finer than 50  $\mu\text{m}$  to 100  $\mu\text{m}$  long distances away from their source (Lyles and Tatarko, 1986).

In addition to these regional sources of aerosols, large volcanic eruptions, such as Mt. Pinatubo in the Philippines, release enormous quantities of volcanic ash into the atmosphere. These particles have lengthy atmospheric residence times which allows them to be dispersed globally. The influence of volcanic ash on the Amazon, however, is unclear.

Although isotopic ratios suggest that land-derived aerosols are a major source of metals in rainfall, the results proved inconclusive in determining whether the source was actually from biomass burning. This study suffered from an extremely limited number of samples (in particular rainfall) which made identifying the source of its dissolved metals highly speculative. Also, any attempt at quantifying the flux of metals released through biomass burning, based on only a few vegetation samples, was clearly impossible. Therefore, as a future study, a more extensive sampling program will be required, with an emphasis on collecting a number of rainfall samples (preferably during both dry and wet seasons) for radiogenic analyses and a multitude of various vegetation types (with known proportions in the Amazon ecosystem) to provide a data base large enough to make reasonable nutrient budget calculations.



## CHAPTER 6

### SUMMARY AND CONCLUSIONS

Rivers transport most of the materials which enter the oceans, yet our knowledge of the processes influencing their chemical composition remains inadequate. Much of what is known has been based on a compilation of data from extremely diverse sources. However, the inconsistencies suffered by fragmented data can be overcome through the study of large river systems which encompass a range of geological, climatic, and ecological variability to permit study of the concomitant effects determining river chemistry on a continental scale.

Unfortunately, the difficulty encountered with most river basins is that much of their catchment has been influenced by man through agricultural and pastoral activities, industry, logging, hydroelectric projects, and settlement. The Amazon Basin, however, provided (by today's standards) an unusually ideal study area primarily because much of it remains largely undisturbed.

During the course of the last four years, I have attempted to consider some of the influences which effect not only the source of solutes to Amazonian river systems, but also some of the factors which control the distribution of metals within their water columns and sediments. Without question, the largest source of metals to the river systems has proven to be weathering of the substrate lithology in source regions and within the erosional regime. Weathering not only governs the distribution of major elements and trace metals, but it also determines the concentration of organic matter in the river and the activity of microbial populations. These factors have proven to be of profound implication since organic material, both cellular and non-cellular, were shown to partially control the concentration of dissolved metals in both solute-rich rivers and solute-deficient rivers, respectively.

Although the influence of man on the Amazon Basin has remained largely negligible, anthropogenic activities are now also being felt. While obvious disturbances such as the discharge of sewage effluent into the river or large-scale projects such as the building of hydroelectric plants commonly are discussed with reference to river composition, more discreet human activities, such as biomass burning, and to a lesser extent, mining, may also become important factors in transferring metals to regional fluvial systems via the atmosphere

From this study I think one of the most important observations which can be made is that Amazonian rivers are extremely complicated systems which receive their individual characteristics from multiple sources. Although my research has focused solely on this river system, I believe that this conclusion can be extended to almost any river system.

**APPENDIX 1**

**GEOCHEMICAL DATA FOR STANDARDS:**

**SOIL SAMPLES**

TABLE A1.1: XRF DATA FOR MAJOR OXIDE COMPOSITION IN SOIL STANDARDS  
 SY-2 AND MRG-1 AND COMPARISON WITH ACCEPTED VALUES (in wt.%)

	SY-2		MRG-1	
	ACCEPTED	THIS STUDY	ACCEPTED	THIS STUDY
SiO <sub>2</sub>	60.05	60.07	39.09	39.21
TiO <sub>2</sub>	0.14	0.12	3.77	3.78
Al <sub>2</sub> O <sub>3</sub>	12.04	12.09	8.46	8.31
Fe <sub>2</sub> O <sub>3</sub>	6.31	6.22	17.93	17.83
MnO	0.32	0.29	0.17	0.17
MgO	2.69	2.58	13.55	13.39
CaO	7.96	8.01	14.71	14.74
K <sub>2</sub> O	4.44	4.52	0.18	0.15
P <sub>2</sub> O <sub>5</sub>	0.43	0.41	0.08	0.04
Na <sub>2</sub> O	4.31	4.20	0.74	0.42

TABLE A1.2: XRF DATA FOR TRACE ELEMENT COMPOSITION IN SOIL STANDARDS  
G-2 AND BHVO-1 AND COMPARISON WITH ACCEPTED VALUES (in ug/g)

	G-2		BHVO-1	
	ACCEPTED	THIS STUDY	ACCEPTED	THIS STUDY
Nb	12.00	12.00	19.00	20.00
Zr	309.00	300.00	129.00	175.00
Y	11.00	10.00	27.60	24.00
Sr	478.00	485.00	403.00	389.00
Rb	120.00	169.00	11.00	11.00
Pb	30.00	29.00	2.60	6.50
Zn	86.00	90.00	105.00	102.00
Cu	11.00	12.00	136.00	134.00
Ni	5.00	6.00	121.00	120.00
Co	4.60	5.00	45.00	49.00
Cr	8.70	5.00	289.00	286.00
Ba	1882.00	1845.00	139.00	130.00
V	36.00	42.00	139.00	312.00
Ga	23.00	24.00	21.00	20.00

TABLE A1.3: PRECISION CALCULATIONS (in wt.%)

	M13A	DUPLICATE	S4A	DUPLICATE
SiO <sub>2</sub>	53.32	53.57	61.55	62.46
TiO <sub>2</sub>	0.74	0.76	0.89	0.91
Al <sub>2</sub> O <sub>3</sub>	32.70	32.30	16.30	16.34
Fe <sub>2</sub> O <sub>3</sub>	1.18	1.19	6.28	6.29
MnO	0.01	0.01	0.11	0.10
MgO	0.03	0.02	1.56	1.78
CaO	0.00	0.00	1.29	1.27
K <sub>2</sub> O	0.08	0.09	2.25	2.26
P <sub>2</sub> O <sub>5</sub>	0.02	0.02	0.15	0.17
Na <sub>2</sub> O	0.00	0.00	1.29	1.12
LOI	12.60	12.80	7.81	7.80
TOTAL	100.67	100.76	99.48	100.50

TABLE A1.4: PRECISION CALCULATIONS (in ug/g)

	M130A	DUPLICATE	S4A	DUPLICATE
Nb	28.00	27.00	18.00	17.00
Zr	403.00	406.00	279.00	275.00
Y	7.50	7.30	32.00	35.00
Sr	22.00	22.00	215.00	220.00
Rb	7.40	8.70	109.00	110.00
Pb	30.00	28.00	20.00	18.00
Zn	19.00	19.00	109.00	107.00
Cu	10.00	12.00	32.00	32.00
Ni	5.80	6.30	36.00	38.00
Co	<5.00	<5.00	18.00	17.00
Cr	142.00	142.00	56.00	56.00
Ba	43.00	39.00	107.00	99.00
V	42.00	35.00	474.00	479.00
As	.00	5.00	10.00	10.02
Ga	27.00	29.00	21.00	25.00

Note: "<" indicate concentrations below detection limit.

**APPENDIX 2**

**GEOCHEMICAL DATA FOR STANDARDS:**

**WATER SAMPLES**



TABLE A2.1: ICP-MS DATA FOR WATER STANDARDS ERI CN1 AND ERI CN2 AND COMPARISON WITH ACCEPTED VALUES (in ug/L)

	ERI CN1			ERI CN2	
	ACCEPTED	THIS STUDY		ACCEPTED	THIS STUDY
As	50.0	41.0	Al	100.0	94.0
Ba	100.0	100.0	Sb	100.0	110.0
Cd	5.0	5.5	Be	10.0	8.9
Cr	50.0	57.0	Co	50.0	44.0
Cu	50.0	42.1	Fe	50.0	47.0
Pb	50.0	69.0	Mn	10.0	9.4
Hg	2.0	2.6	Mo	30.0	36.0
Sc	50.0	53.0	Ni	30.0	26.0
Ag	10.0	10.0			

TABLE A2.2. PRECISION CALCULATIONS(in ug/L)

	AZ1-91	DUPLICATE	A1-91	DUPLICATE	RAIN-91	DUPLICATE
Li	0.38	0.49	0.90	0.38	1.00	0.75
Be	0.07	0.07	0.07	0.07	0.07	0.07
B	1.00	0.80	2.90	3.40	4.00	4.70
Mg	1400.00	1300.00	1100.00	1100.00	480.00	480.00
Al	24.00	21.00	820.00	800.00	150.00	160.00
Si	4000.00	3400.00	5000.00	5000.00	1600.00	1600.00
P	1.20	1.20	31.00	43.00	29.00	23.00
K	1100.00	990.00	1200.00	1200.00	5900.00	6200.00
Ca	2000.00	1900.00	7800.00	7400.00	17000.00	17000.00
Sc	0.51	0.30	0.72	0.73	0.31	0.34
Ti	0.20	0.20	4.90	4.50	3.00	3.30
V	0.28	0.26	2.60	2.60	7.80	7.90
Cr	0.32	0.27	1.20	0.98	3.50	3.60
Mn	4.00	3.70	33.00	32.00	6.50	6.60
Fe	29.00	22.00	1500.00	1500.00	120.00	130.00
Co	0.14	0.13	0.50	0.52	0.81	0.67
As	0.13	0.10	0.82	1.10	0.52	0.33
Se	0.69	0.37	0.43	1.20	3.90	1.70
Br	17.00	28.00	1.50	3.40	2.80	9.60
Rb	2.50	2.40	2.30	2.30	11.00	11.00
Sr	4.10	3.90	41.00	41.00	50.00	51.00
Zr	0.04	0.06	0.18	0.22	0.37	0.39
Mo	0.85	0.73	0.73	0.76	0.26	0.26
Ag	0.02	0.07	0.03	0.04	0.03	0.02
Cd	0.08	0.22	0.08	0.08	0.14	0.24
Sn	3.30	3.90	0.26	0.28	0.41	0.60
Sb	0.68	0.09	0.38	0.11	0.14	0.33
I	1.90	2.00	1.10	1.20	2.00	2.00
Cs	0.07	0.02	0.1	0.11	0.13	0.14
Ba	53.00	57.00	33.00	35.00	17.00	16.00
La	0.21	0.19	0.83	0.93	0.30	0.32
Ce	0.21	0.17	2.20	2.30	0.36	0.26
Nd	0.08	0.14	1.10	0.99	0.13	0.23
Sm	0.03	0.06	0.19	0.28	0.04	0.10
Eu	0.02	0.02	0.04	0.05	0.02	0.02
Th	0.02	0.02	0.02	0.03	0.02	0.02
Dy	0.03	0.03	0.05	0.09	0.03	0.03
Yb	0.02	0.02	0.03	0.07	0.02	0.02
Hf	0.02	0.02	0.02	0.02	0.02	0.03
Ta	0.02	0.02	0.02	0.02	0.02	0.02
W	0.13	0.06	0.03	0.05	0.28	0.20
Au	0.02	0.02	0.02	0.02	0.02	0.02
Hg	0.09	0.09	0.09	0.09	0.12	0.12
Bi	0.02	0.02	0.02	0.03	0.03	0.05
Th	0.07	0.04	0.41	0.31	0.23	0.15
U	0.03	0.03	0.10	0.11	0.08	0.08

**APPENDIX 3**

**GEOCHEMICAL DATA FOR STANDARDS:  
ORGANIC SAMPLES**

TABLE A3.1: ICP-MS DATA FOR THE BIOLOGICAL STANDARDS TORT-1, NOAA BT2, AND PACS-1 AND COMPARISON WITH ACCEPTED VALUES (in ug/g)

TORT-1		NOAA BT2		PACS-1	
ACCEPTED	THIS STUDY	ACCEPTED	THIS STUDY	ACCEPTED	THIS STUDY
As	25.70	Cr	1.06	Sb	178.00
Cd	27.40	Mn	8.84	Cd	2.48
Cr	2.70	Fe	133.00	Cr	117.00
Co	0.45	Ni	1.07	Co	18.10
Cu	450.00	Cu	7.45	Cu	460.00
Fe	191.00	Zn	128.00	Pb	414.00
Pb	11.40	As	9.70	Mn	476.00
Mn	23.90	Se	2.90	Mo	12.80
Mo	0.37	Ag	0.15	Ni	45.10
Mo	1.65	Cd	0.64	Sr	283.00
Ni	2.45	Sn	0.04	Sn	42.70
Se	7.20	Sb	0.10	Zn	835.00
Sr	115.50	Hg	0.09		
Sn	0.15	Pb	4.37		
V	1.55				
Zn	187.00				

TABLE A3.2. PRECISION CALCULATIONS (in  $\mu\text{g/g}$ )

	ALGAE		FILTER	
	M2-90B	DUPLICATE	F1-90	DUPLICATE
Li	45.00	56.00	1.90	1.10
Be	2.50	2.70	0.043	0.064
B	79.00	150.00	32.00	4.40
Mg	6200.00	6600.00	840.00	990.00
Al	3400.00	2800.00	1400.00	1400.00
Ca	18000.00	12000.00	6900.00	6300.00
Sc	120.00	100.00	3.90	3.10
Ti	1500.00	1400.00	35.00	35.00
V	96.00	95.00	1.20	1.10
Cr	42.00	42.00	23.00	11.00
Mn	3900.00	3100.00	380.00	380.00
Fe	49000.00	49000.00	920.00	980.00
Co	26.00	17.00	0.44	0.42
Ni	65.00	19.00	30.00	2.90
Cu	130.00	30.00	8.90	5.90
Zn	210.00	110.00	47.00	39.00
As	22.00	15.00	0.34	0.22
Se	3.50	1.70	0.15	0.70
Br	47.00	54.00	57.00	62.00
Rb	25.00	52.00	16.00	23.00
Sr	94.00	74.00	11.00	12.00
Zr	30.00	32.00	1.40	1.10
Mo	5.60	1.40	0.29	0.26
Ag	0.39	0.17	0.11	0.05
Cd	16.00	1.30	0.50	0.26
Sn	1.90	1.70	0.38	0.26
Sb	1.40	0.89	0.21	0.14
I	13.00	3.30	1.10	1.50
Cs	2.20	3.10	0.35	0.47
Ba	500.00	430.00	33.00	37.00
La	5.30	11.00	0.72	0.68
Ce	17.00	25.00	1.56	1.40
Nd	6.50	11.00	0.50	0.53
Sm	1.50	2.30	0.074	0.098
Eu	0.42	0.59	0.019	0.017
Tb	0.25	0.34	0.008	0.012
Dy	1.40	1.90	0.065	0.096
Yb	0.77	1.10	0.047	0.039
Hf	1.80	2.00	0.044	0.067
Ta	0.74	0.70	0.26	0.21
W	1.60	1.40	0.10	0.11
Au	0.017	0.03	0.009	0.009
Hg	0.055	0.08	0.043	0.035
Pb	32.00	29.00	8.90	8.50
Bi	0.43	0.41	0.12	0.085
Th	4.20	6.60	0.20	0.16
U	3.30	2.60	0.074	0.092

**APPENDIX 4**

**GEOCHEMICAL ANALYSES**

**OF**

**WATER, SOILS, AND ALGAE**

UNABLE TO FILM THE MATERIAL ON THE FOLLOWING PAGE 138 (DISKETTE).  
PLEASE CONTACT THE UNIVERSITY LIBRARY.

INCAPABLE DE MICROFILMER LE MATERIEL SUR LES PAGES ...  
VEUILLEZ CONTACTER LA BIBLIOTHEQUE DE L'UNIVERSITE.

NATIONAL LIBRARY OF CANADA    BIBLIOTHEQUE NATIONALE DU CANADA  
CANADIAN THESIS SERVICE        LE SERVICE DES THESES CANADIENNES

## REFERENCES

- Andreae, M O , Browell, E V , Garstang, M , Gregory, G L , Harriss, R C , Hill, G F , Jacob, D L , Pereira, M C , Sachse, G W , Setzer, A W , Silva Dias, P L , Talbot, R W , Torres, A L , and Wofsy, S C , 1988. Biomass-burning emissions and associated haze layers over Amazonia. *J. Geophys. Res.*, 93:1509-1527.
- Andren, A W , Klein, D H , and Talmi, Y , 1975. Selenium in coal-fired steam plant emissions *Environ Sci. Technol.*, 9:856-858
- Artaxo, P., Storms, H , Bruynseels, F , Van Grieken, R., and Maenhaut, W., 1988. Composition and sources of aerosols from the Amazon Basin. *J. Geophys. Res.*, 93 1605-1615
- Beck, K C., Reuter, J H , and Perdue, E.M . 1974. Organic and inorganic geochemistry of some coastal plain rivers of the southeastern United States. *Geochim. Cosmochim. Acta*, 38:347-364.
- Berner, E.K and Berner, R A , 1987. *The Global Water Cycle* Prentice-Hall, New Jersey, 397 pp.
- Beveridge, T J and Murray, R.G.E., 1976 Uptake and retention of metals by cell walls of *Bacillus subtilis*, *J. Bacteriol.*, 127:1502-1518.
- Beveridge, T J , 1978 The response of cell walls of *Bacillus subtilis* to metals and to electron-microscopic stains *Can J. Microbiol.* , 24:89-104
- Beveridge, T J and Murray, R G E , 1980 Sites of metal deposition in the cell wall of *Bacillus subtilis*, *J. Bacteriol.*, 141 876-887
- Beveridge, T J , 1981 Ultrastructure, chemistry, and function of the bacterial wall *Int Rev Cytol.* , 72 229-317
- Beveridge, T J , Meloche, J.D , Fyfe, W S , and Murray, R G.E . 1983. Diagenesis of metals chemically complexed to bacteria Laboratory formation of metal phosphates, sulphides, and organic condensates in artificial sediments *Appl Environ Microbiol.* , 45 1094-1108
- Beveridge, T J and Fyfe, W S , 1985 Metal fixation by bacterial cell walls *Can J Earth Sci.* , 22 1893-1898
- Billings, C E and Matson, W R , 1972 Mercury emissions from coal combustion *Science*, 176 1232-1233



- Borowitzka, M A , 1986 Physiology and biochemistry of calcification in the Chlorophyceae In B S C Leadbeater and R Riding (Editors), Biomineralization in Lower Plants and Animals Systematics Association Special Volume 30 Clarendon Press, Oxford, pp 107-124
- Bowen, H.J.M., 1979 Environmental Chemistry of the Elements Academic Press, London, pp. 237-272
- Boyle, E A , 1978 Trace element geochemistry of the Amazon and its tributaries Eos, 59 276.
- Cachier, H , Buat-Ménard, P , Fontugne, M , and Rancher, J , 1985 Source terms and source strengths of the carbonaceous aerosol in the tropics. J. Atmos. Chem., 3:469-489.
- Carlson, L. and Schwertmann, U , 1981 Natural ferrihydrites in surface deposits from Finland and their association with silica Geochim Cosmochim Acta, 45 421-429
- Carr, R M and Fyfe, W S , 1958 Some observations on the crystallization of amorphous silica Am. Mineral., 43 908-916.
- Costerton, J W., Irvin, R. T , and Cheng, K.J., 1981 The role of bacterial surface structures in pathogenesis. CRC Crit. Rev. Microbiol , 8 303-338.
- Crutzen, P J , Heidt, L E , Krasnec, J P , Pollock, W H , and Seiler, W , 1979 Biomass burning as a source of atmospheric gases CO, H<sub>2</sub>O, N<sub>2</sub>O, NO, CH<sub>3</sub>Cl, and COS Nature, 282 253-256
- Crutzen, P.J. and Andreae, M.O., 1990. Biomass burning in the tropics: Impact on atmospheric chemistry and biogeochemical cycles Science, 250 1669-1678
- Degens, E. T and Ittekkot, V. I , 1982 *In situ* metal-staining of biological membranes in sediments. Nature, 298:262-264.
- Degens, E T . 1982 Transport of carbon and minerals in major world rivers, part I Mitt Geol Palaont. Inst Univ. Hamburg SCOPE/UNEP Sonderb, 52 1-12
- Dickinson, W R , 1970. Relation of andesites, granites, and derivative sandstones to arc-trench tectonics. Rev. Geophys Space Phys., 8 813-860
- Edwards, A M C. and Liss, P S., 1973 Evidence for buffering of dissolved silicon in fresh waters Science, 173 341-342

- Ertel, J R , Hedges, J I , Devol, A H , Richey, J E , and Ribeiro, M N G , 1986  
Dissolved humic substances of the Amazon River system *Limnol Oceanogr* , 31:739-754
- Ewel, J , Berish, C , Brown, B , Ponce, N , and Raich, J , 1981 Slash and burn impacts on a Costa Rican wet forest site *Ecology*, 62:816-829
- Fairbridge, R W , 1972 *The Encyclopedia of Geochemistry and Environmental Sciences - Encyclopedia of Earth Sciences Series, Vol. IVA* Van Nostrand and Reinhold, New York, 1321 pp
- Faure, G , Hurley, P M , and Powell, J L , 1965 The isotopic composition of strontium in surface water from the North Atlantic Ocean. *Geochim. Cosmochim. Acta*, 29:209-220.
- Faure, G . 1986 *Principles of Isotope Geology* John Wiley & Sons, New York, 589 pp
- Fearnside, P.M., 1989 Deforestation in Brazilian Amazonia: The rates and causes of forest destruction *The Ecologist*, 19:214-218
- Ferris, F G and Beveridge, T.J., 1984. Binding of a paramagnetic metal cation to *Escherichia coli* K-12 outer membrane vesicles. *FEMS Microbiol. Lett.*, 24:43-46.
- Ferris, F G and Beveridge, T.J., 1985. Functions of bacterial cell surface structures. *Bioscience*, 35:172-177.
- Ferris, F G , Beveridge, T J , and Fyfe, W S , 1986. Iron-silica crystallite nucleation by bacteria in a geothermal sediment. *Nature*, 320:609-611
- Ferris, F G , Fyfe, W S , and Beveridge, T J , 1987 Bacteria as nucleation sites for authigenic minerals in a metal-contaminated lake sediment. *Chem Geol.*, 63:225-232
- Fisher, S.R and Stueber, M., 1976 Strontium isotopes in selected streams within the Susquehanna River Basin. *Water Resources Res.*, 12:1061-1068.
- Fittkau, E J , Irmiler, U , Junk, W J , Reiss, F , and Schmidt, G.W., 1975. Productivity, biomass, and population dynamics in Amazonian water bodies. In: F.B Golley and E. Medina (Editors), *Tropical Ecological Systems. Trends in Terrestrial and Aquatic Research* Springer Verlag, New York, pp 289-311
- Furch, K , Junk, W J , and Klinge, H , 1982 Unusual chemistry of natural waters from the Amazon Region *Acta Cient. Venez.*, 33:269-273.

- Furch, K., 1984. Water chemistry of the Amazon Basin. The distribution of chemical elements among freshwaters. In: H. Sioli (Editor), *The Amazon*. W. Junk Publishers, Dordrecht, pp. 167-200.
- Fyfe, W.S., Kronberg, B.I., Leonardos, O.H., and Olorunfemi, N., 1983. Global tectonics and agriculture. A geochemical perspective. *Agriculture, Ecosystems and Environment*, 9:383-399.
- Fyfe, W.S., 1989. Soil and global change. *Episodes*, 12:249-254.
- Gibbs, R.J., 1967. The geochemistry of the Amazon River System. Part I. The factors that control the salinity and the composition and concentration of the suspended solids. *Geol. Soc. Amer. Bull.*, 78:1203-1232.
- Gibbs, R.J., 1970. Mechanisms controlling world water chemistry. *Science*, 170:1088-1090.
- Gibbs, R.J., 1972. Water chemistry of the Amazon River. *Geochim. Cosmochim. Acta*, 36:1061-1066.
- Gibbs, R.J., 1973. Mechanisms of trace metal transport in rivers. *Science*, 180:71-73.
- Gibbs, R.J., 1977. Transport phases of transition metals in the Amazon and Yukon Rivers. *Geol. Soc. Amer. Bull.*, 88:829-843.
- Gosz, J.R., Brookins, D.G., and Moore, D.I., 1983. Using strontium isotope ratios to estimate inputs to ecosystems. *BioScience*, 33:23-30.
- Graustein, W.C. and Armstrong, R.L., 1983. The use of strontium-87/strontium-86 ratios to measure atmospheric transport into forested watersheds. *Science*, 219:289-292.
- Greenberg, J.P., Zimmerman, P.R., Heidt, L., and Pollock, W., 1984. Hydrocarbon and carbon monoxide emissions from biomass burning in Brazil. *J. Geophys. Res.*, 89:1350-1354.
- Guerra, A.T., 1959. *Geografia do Brasil. Grande Região norte*. Instituto Brasileiro de Geografia e Estatística, Rio de Janeiro, 422 pp.
- Hasanen, E., Pohjola, V., Hakkala, M., Zilliacus, R., and Wickström, K., 1986. Emissions from power plants fueled by peat, coal, natural gas and oil. *Sci. Total Environ.*, 54:29-51.
- Hayat, M.A., 1981. *Principles and Techniques of Electron Microscopy. Biological Applications*. University Park Press, Baltimore, 522 pp.

- Hedges, J I , Clark, W A , Quay, P D , Richey, J E , Devol, A H , and Santos, U M , 1986 Compositions and fluxes of particulate organic material in the Amazon River *Limnol Oceanogr* , 3 717-738
- Hein, J R , Scholl, D W , Barron, J A , Jones, M.G , and Miller, J., 1978 Diagenesis of late Cenozoic diatomaceous deposits and formation of bottom simulating reflector in the southern Bering Sea. *Sedimentology*, 25:155-181.
- Hesse, R. 1990 Origin of chert: Diagenesis of biogenic siliceous sediments, In: I.A. McIlreath and D.W. Morrow (Editors), *Diagenesis*. Geological Association of Canada, Geoscience Canada Reprint Series 4, pp 227-251.
- Hoagland, K.D. and Peterson, C G., 1990 Effects of light and wave disturbance on vertical zonation of attached microalgae in a large reservoir. *J. Phycol.*, 26 450-457
- Hoyle, B and Beveridge, T.J , 1983 Binding of metallic ions to the outer membrane of *Escherichia coli* *Appl Environ Microbiol* , 46 749-752
- Huang, P M., 1991. Ionic factors affecting the formation of short-range ordered aluminosilicates. *Soil Sci. Soc. Am. J.*, 55 1172-1180
- Jordan, C.F., 1985. Soils of the Amazon rainforest. In: G.T. Prance and T.E. Lovely (Editors), *Amazonia*. Pergamon Press, Oxford, pp. 83-94.
- Kaakinen, J.W., Jorden, R M , Lawasani, M H , and West, R.E., 1975 Trace element behavior in coal-fired power plant. *Environ Sci. Technol.*, 9:862-868
- Kastner, M., Keene, J B., and Gieskes, J.M., 1977. Diagenesis of siliceous oozes -- 1. Chemical controls on the rate of opal-A to opal-CT transformation--An experimental study *Geochim Cosmochim Acta*, 41 1041-1059.
- Katzer, F , 1897. Das Wasser des unteren Amazonas, Sitz bohm Ges. Wiss Math naturw , 17:1-38
- Kaufherr, N. and Lichtman, D., 1984. Comparison of micron and submicron fly ash particles using scanning electron microscopy and X-ray elemental analysis *Environ. Sci Technol* , 18:544-547
- Kingston, J C., Lowe, R.L , Stoermer, E F , and Ladewski, T B., 1983. Spatial and temporal distribution of benthic diatoms in northern Lake Michigan. *Ecology*, 64 1566-1580
- Klammer, G., 1984. The relief of the extra-Andean Amazon Basin. In: H. Sioli (Editor), *The Amazon*, Junk Publishers, Dordrecht, pp. 47-84.

- Klein, D H , Andren, A W , Carter, J A , Emery, J F , Feldman, C , Fulkerson, W , Lyon, W S , Ogle, J C , Talmi, Y , Van Hook, R I , and Bolton, N , 1975 Pathways of thirty-seven elements through coal-fired power plant Environ Sci Technol , 9 973-978
- Klinge, H , 1965 Podzol soils in the Amazon Basin, J Soil Science, 16 95-103
- Klinge, H , Furch, K , Irmiler, U, and Junk, W., 1981 Fundamental ecological parameters in Amazonia, in relation to the potential development of the region In R Lal and E W Russell (Editors), Tropical Agricultural Hydrology John Wiley and Sons, New York, pp 19-36.
- Kronberg, B I , Fyfe, W S , Leonardos, O H , and Santos, A M , 1979 The chemistry of some Brazilian soils. element mobility during intense weathering. Chem Geol , 24 211-229
- Kuyucak, N and Volesky, B., 1989 The mechanism of gold biosorption Biorecovery, 1 219-235
- Lacerda, L.D., Pfeiffer, W.C., Ott, A T , and Silveira, E G , 1989 Mercury contamination in the Madeira River, Amazon-Hg inputs to the environment Biotropica, 21:91-93.
- Lack, T J , 1971 Quantitative studies on the phytoplankton of the rivers Thames and Kennet at Reading. Freshwat. Biol., 1:213-224
- Lamar, W L , 1986 Evaluation of organic color and iron in natural surface waters U S Geol Surv Prof Paper 600-D, D24-D29
- Larocque, A., 1989. Trace element behaviour during weathering of till from eastern Ontario, with implications for geochemical exploration Ph D Thesis, University of Western Ontario, London, Ontario, 201 pp
- Leenheer, J A., 1980. Origin and nature of humic substances in the waters of the Amazon River Basin. Acta Amazonica, 10 513-526
- Leonardos, O H., Fyfe, W.S., and Kronberg, B I., 1987. The use of ground rocks in laterite systems An improvement to the use of conventional soluble fertilizers? Chem Geol 60 361-370.
- Leslie, A C D., 1981. Aerosol emissions from forest and grassland burnings in the southern Amazon Basin and Central Brazil Nucl Instr. and Meth., 181 345-351
- Lewin, J C , 1961 The dissolution from diatom walls Geochim. Cosmochim Acta, 21 182-198

- Lewin, J C and Guillard, R R L , 1963 Diatoms *Annu Rev Microbiol* , 17 373-414
- Lindquist, O and Rodhe, H , 1985 Atmospheric mercury, a review *Tellus*, 37 136-159
- Livingstone, D A , 1963 Chemical composition of rivers and lakes *U S Geol Surv Prof Pap* 440-G, pp 1-63.
- Lowenstam, H A , 1981 Minerals formed by organisms *Science*, 211 1126-1131
- Lowenstam, H A and Weiner, S , 1989 *On Mineralization* Oxford University Press, N Y , 324 pp
- Lyles, L and Tatarko, J., 1986. Wind erosion effects on soil texture and organic matter. *J. Soil and Water Cons* , 41.191-193
- Mallas, J and Bendicto, N , 1986 Mercury and goldmining in the Brazilian Amazon *Ambio*, 15 248-249
- Malm, O , Pfeiffer, W C., Souza, C M.M., and Reuther, R., 1990. Mercury pollution due to gold mining in the Madeira River Basin, Brazil. *Ambio*, 19:11-15.
- Mann, H , Fyfe, W S., and Kerrich, R , 1987. Geochemistry of thermal waters and thermophilic microorganisms, Yellowstone. In: Program with Abstracts, Annual meeting of the Geological Association of Canada, University of Saskatchewan, Saskatoon, pp 12 71.
- Mann, H , and Fyfe, W S., 1988 Biogeochemical cycling of the elements in some fresh water algae from gold and uranium mining districts. *Biorecovery*, 1:3-26.
- Mann, H , Fyfe, W S , Kerrich, R, and Wiseman, M , 1989 Retardation of toxic heavy metal dispersion from nickel-copper mine tailings, Sudbury District, Ontario. Role of acidophilic microorganisms I Biological pathway of metal retardation. *Biorecovery*, 1 155-172
- Mann, S , 1983 Mineralization in biological systems *Struct Bond* , 54 125-174.
- Mann, S , 1986 Biomineralization in lower plants and animals-chemical perspectives. In: B S C Leadbeater and R. Riding (Editors), *Biomineralization in Lower Plants and Animals* The Systematics Association. Special Volume NO. 30, Clarendon Press. Oxford, pp 39-54
- Marques, J , Santos, J M., Villa Nova, N A , and Salati, E , 1977 Precipitable water and water vapour flux between Belém and Manaus *Acta Amazonica*, 7:355-362

- Meade, R H , Nordin, Jr C F , Curtis, W F , Rodrigues, M C , Vale, C M , and Edmond, J M , 1979 Sediment loads in the Amazon River *Nature*, 278 161-163
- Mullen, M D , Wolf, D C , Ferris, F G , Beveridge, T J , Flemming, C A , and Baily, G.W , 1989. Bacterial sorption of heavy metals *Appl Environ Microbiol* , 55.3143-3149.
- O'Kelley, J C , 1974 Inorganic nutrients In W D P Stewart (Editor), *Algal Physiology and Biochemistry*. University of California Press, Berkely, pp 610-635
- Oltman, R E , 1965 Some observations of Amazon River hydrology. *South Carolina Engineer*, 16:6-12
- Pfeiffer, W C and Lacerda, L D , 1988. Mercury inputs to the Amazon Basin *Environ Technol. Lett.*, 9:325-330.
- Putzer, H , 1984 The geological evolution of the Amazon Basin and its mineral resources In H. Sioli (Editor), *The Amazon* Junk Publishers, Dordrecht, pp 15-46.
- Raimondi, A , 1884. *Agua Potable dei Perù*. F. Masias, Lima, pp. 127-134.
- Rashid, M.A., 1974 Absorption of metals on sedimentary and peat humic acids. *Chem Geol* , 13:115-123
- Reuter, J H and Perdue, E M , 1977 Importance of heavy metal-organic matter interactions in natural waters. *Geochim. Cosmochim Acta*, 41 325-334.
- Reynolds, C.S , 1986. Diatoms and the geochemical cycling of silicon, In B.S.C. Leadbeater and R. Riding (Editors), *Biominalization in Lower Plants and Animals Systematics Association Special Volume 30* Claredon Press, Oxford, pp. 269-289
- Salati, E. and Vose, P B., 1984 Amazon Basin A system in equilibrium *Science*, 225:129-138
- Schelske, C.L. and Stoermer, E.F., 1971 Eutrophication, silica depletion, and predicted changes in algal quality in Lake Michigan *Science*, 173 423-424
- Schlesinger, W.H and Melack, J.M., 1981 Transport of organic carbon in the world's rivers *Tellus*, 33 172-187.
- Seiler, W and Crutzen, P J , 1980 Estimates of gross and net fluxes of carbon between the biosphere and the atmosphere from biomass burning. *Climatic Change*, 2 207-247.
- Setzer, A W. and Pereira, M.C., 1991. Amazonia biomass burnings in 1987 and an estimate of their tropospheric emissions *Ambio*, 20:19-22

- Sigleo, A C , 1978 Organic geochemistry of silicified wood, Petrified Forest National Park, Arizona *Geochim Cosmochim Acta*, 42 1397-1405.
- Simkiss, K , 1986 The processes of biomineralization in lower plants and animals. In B S C Leadbeater and R Riding (Editors), *Biomineralization in Lower Plants and Animals The Systematics Association Special Volume NO. 30*, Clarendon Press. Oxford, pp 19-38
- Sioli, H., 1950. Das Wasser im Amazonasgebiet. *Forsch. Fortschr., Amazonasgebiet. Arch Hydrobiol* , 43:267-283
- Sioli, H., 1967 Studies in Amazonian waters. *Atos do Simposio sôbre a Biota Amazônica, Rio de Janeiro (Limnologia)*, 3:9-50.
- Sioli, H., 1968. Hydrochemistry and geology in the Brazilian Amazon Region. *Amazoniana*, 1:267-277.
- Sioli, H , 1975. Tropical rivers as expressions of their terrestrial environments. In: F.B. Golley and E Medina (Editors), *Tropical Ecological Systems. Trends in Terrestrial and Aquatic Research*. Springer Verlag, New York. pp. 275-288.
- Sioli, H., 1984. The Amazon and its main affluents: Hydrography, morphology of the river courses, and river types. In H. Sioli (Editor), *The Amazon*. W. Junk Publishers, Dordrecht. pp 127-166.
- Stallard, R.F , 1978 Amazon chemistry - Alpha Helix 1967-1977. *Eos*, 59:276.
- Stallard, R.F. and Edmond, J.M., 1981. Geochemistry of the Amazon 1: Precipitation chemistry and the marine contribution to the dissolved load at the time of peak discharge *J. Geophys. Res.*, 86:9844-9858.
- Stallard, R.F. and Edmond, J M , 1983. Geochemistry of the Amazon 2. The influence of geology and weathering environment on the dissolved load. *J. Geophys. Res.*, 88:9671-9688
- Steinhorn, I. and Gat, J.R., 1983. The Dead Sea. *Sci. Am.*, 249:102-109.
- Straughan, I R., Elseewi, A.A., Page, A.L., Kaplan, I.R., Hurst, R.W., and Davis, T.E., 1981. Fly ash-derived strontium as an index to monitor deposition from coal-fired power plants *Science*, 212:1267-1269
- Stumm, W and Morgan, J J , 1970 *Aquatic Chemistry*, Wiley-Interscience, New York, 583 pp.



- Sullivan, C W and Volcani, B E., 1981 Silicon in the cellular metabolism of diatoms. In T L Simpson and B E Volcani (Editors), *Silicon and Siliceous Structures in Biological Systems* Springer-Verlag, New York, pp 15-42
- Tassinari, C C G , Hirata, W.K , and Kawashita, K., 1982 Geologic evolution of the Serra dos Carajás, Pará, Brazil. *Revista Brasileira de Geociências*, 12:263-267
- Tazaki, K , Fyfe, W S , Sahu, K C , and Powell, M , 1989 Observations on the nature of fly ash particles. *Fuel*, 68:727-734.
- Victoria, R L., Martinelli, L A , Richey, J E , Devol, A.H., Forsberg, B.R., and Ribeiro, M.N.G , 1989. Spatial and temporal variations in soil chemistry on the Amazon floodplain. *GeoJournal*, 19:45-52.
- Volcani, B.E., 1983. Aspects of silicification in biological systems. In: P. Westbroek and E.W. de Jong (Editors), *Biom mineralization and Biological Metal Accumulation* D Reidel Pub Co pp 389-405.
- Wada, K , 1981. Amorphous clay minerals-Chemical composition, crystalline state, synthesis, and surface properties. In. H. van Olphen and F. Veniale (Editors), *Developments in Sedimentology, Vol. 35 Proceedings of the VII International Clay Conference*. Elsevier Scientific Pub , Amsterdam, pp. 385-398.
- Williams, L.A., Parks, G.A., and Crerar, D.A., 1985. Silica diagenesis, 1. Solubility controls *J. Sediment Petrol.*, 55:301-311.
- Wissmar, R.C., Richey, J.E , Stallard, R F., and Edmond, J.M., 1981. Plankton metabolism and carbon processes in the Amazon River, its tributaries, and floodplain waters, Peru-Brazil, May-June 1977. *Ecology*, 62:1622-1633.
- Wong, C S., 1978. Atmospheric input of carbon dioxide from burning wood. *Science*, 200:197-200
- Wu, C.T., 1986. Operation Manual for X-ray Fluorescence Analysis Department of Geology, University of Western Ontario, London, pp. 8.